Accuracy of Computer-Assisted Surgery in Segmental Mandibular Resection and Reconstruction

MSc Thesis Technical Medicine

Lisa Arkes

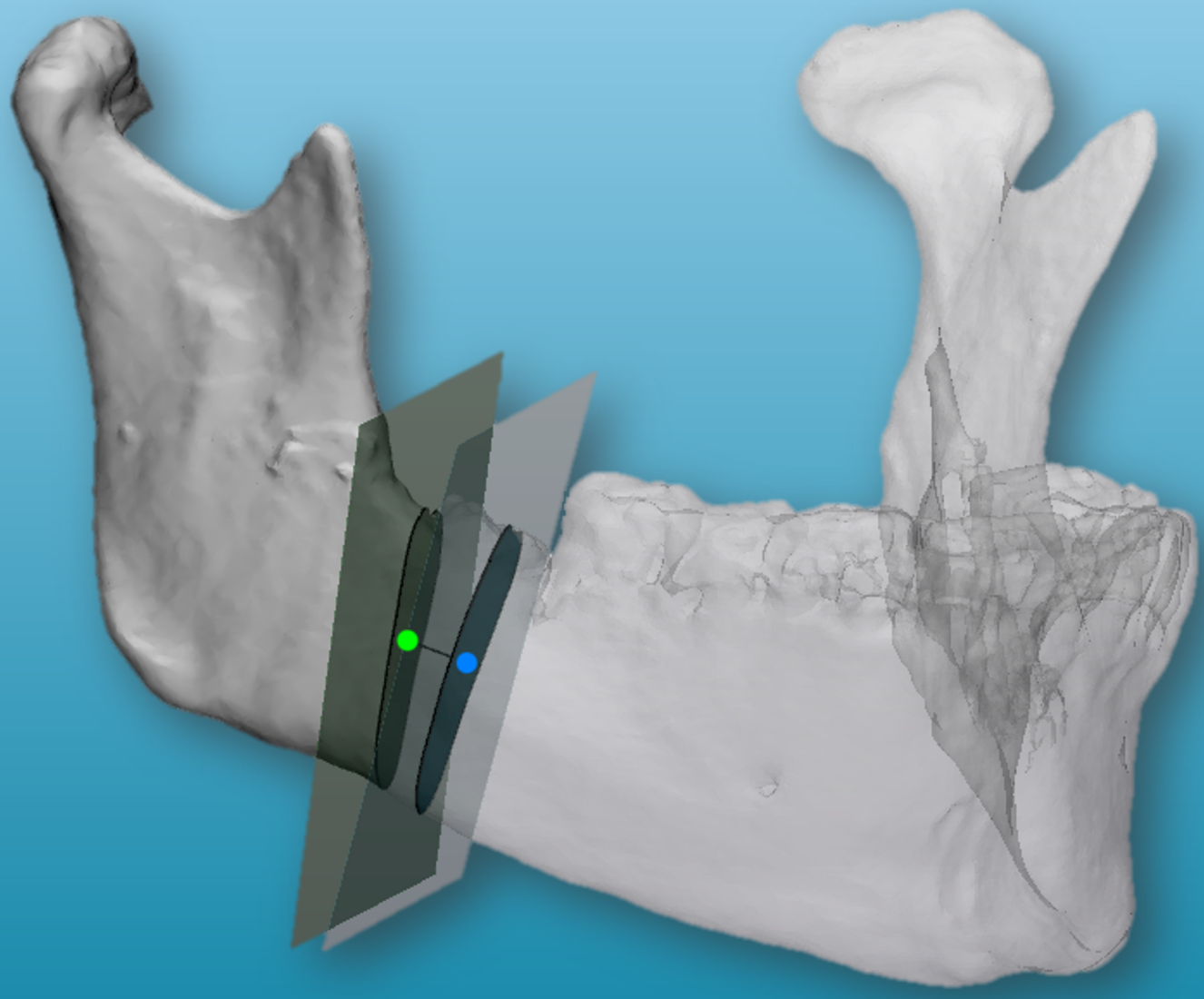

Universiteit Leiden

TU Delft Delft University of Technology

Erasmus Universiteit Rotterdam

Accuracy of Computer-Assisted Surgery in Segmental Mandibular Resection and Reconstruction

MSc Thesis Technical Medicine

by

Lisa Arkes

Student number: 4556216

Graduation date: 28th of May 2024

Thesis in partial fulfilment of the requirements for the joint degree of Master of Science in

Technical Medicine

Leiden University; Delft University of Technology; Erasmus University Rotterdam

Master thesis project (TM30004; 35 ECTS)
Dept. of Biomechanical Engineering, TUDELFT
01-11-2023 – 28-05-2024

Supervisors:

Technical supervisor:	Dr. RPJ. van den Ende	Technical physician
Medical supervisor:	Prof. Dr. T. Forouzanfar	Oral and maxillofacial surgeon
Daily supervisor:	MSc. L. Leeuwrik	PhD Student

Thesis committee members:

Prof. Dr. T. Forouzanfar	LUMC	Chair & Medical member
Dr. RPJ. van den Ende	LUMC	Technical member
Dr. B. Cornelissen	Erasmus MC	External member

Universiteit Leiden

TU Delft Delft University of Technology

Erasmus Universiteit Rotterdam

Preface

Nine months ago, I began my Master's thesis, and this document proves its successful completion! This achievement marks the final milestone in my studies in technical medicine at TU Delft, Erasmus University, and Leiden University.

During this project, I had the opportunity to conduct research on computer-assisted surgery. My interest in this topic emerged during the first year of the Master's program, during the course on Computer-Assisted Reconstructed Surgery in the last semester. In the second year, I further explored this interest during an internship at the maxillofacial department of the LUMC. This internship provided the start for my master's thesis, where I researched the accuracy of computer-assisted surgery in segmental mandibular resection and reconstruction.

I am grateful to my three supervisors, Tim Forouzanfar, Roy van den Ende, and Lars Leeuwrik, for their guidance throughout my thesis. Tim and Lars provided a clinical perspective on my work, ensuring its clinical relevance was never lost. A special thanks to Roy for his support and guidance. The biweekly sessions allowed me to delve deeper into my research. His encouragement to ask questions and make academic decisions strengthened both my research and my critical thinking skills.

Finally, I would like to thank my friends and family for supporting me throughout my thesis. A special thanks to my friend Irene. Eight years ago, we began our Bachelor of Technical Medicine together. Though you chose not to pursue a Master's in Technical Medicine, we managed to keep our timelines aligned. Starting our thesis together in September was the perfect way to conclude our studies.

Throughout this academic journey, I have not only deepened my understanding of the medical technology field but also developed a profound appreciation for it. I am eagerly looking forward to translating this knowledge into practical applications and making meaningful contributions to the ongoing innovation in healthcare.

Lisa Arkes
Rotterdam, May 2024

Summary

Introduction

Virtual surgical planning is often used to prepare mandibular segment resection with subsequent reconstruction. Patient-specific cutting guides translate the planned resection and reconstruction osteotomies to the surgery. The accuracy of computer-assisted surgery is currently evaluated by heterogeneous methodologies for post-operative imaging, segmentation, registration, and accuracy measurements.

Objective

This thesis aims to develop an objective, reproducible and insightful evaluation methodology. The evaluation methodology will compare planned osteotomies with actual osteotomies in segmental mandibular resection and reconstruction. The designed methodology will be applied in a retrospective study.

Method

Actual osteotomies were defined by a plane fitted through manually defined points on the post-operative imaging. The actual osteotomies were aligned to the pre-operative mandible or fibula model. Distance and angular deviation were measured between the planned and actual osteotomies. Resection osteotomy distance deviation was defined as the distance between the centre of mass of the actual and planned intersection of the pre-operative mandible model and the osteotomies. The maximum distance between the intersections was also measured. Reconstruction osteotomy distance deviation was defined as the length difference between the planned and actual fibula segments. Angular deviation of the resection and reconstruction osteotomies were defined by two angular differences based on the saw slot, i.e. the angle across the saw slot (x-axis) and the angle through the saw slot (y-axis).

Results

A semi-automatic novel methodology was developed. The intra-observer variation of the osteotomy localisation was ± 0.4 mm for distance deviation and ± 2.1° for the angular deviation. The inter-observer variation was ± 0.8 mm for the distance deviation and ± 2.4° for the angular deviation.
Sixteen patients were included in the retrospective study. For the resection osteotomies, the absolute average distance deviation was 2.1 ± 1.9 mm for the centre of mass and 3.1 ± 2.3 mm for the maximum distance. The fibular segments differed by 2.4 ± 2.5 mm in length. Angular deviations around the x-axis were 3.7 ± 3.4° for resection and 6.9 ± 7.1° for reconstruction osteotomies, and deviations around the y-axis were 5.7 ± 5.8°and 9.1 ± 11.4°, respectively.

Conclusion

The evaluation methodology provides guidelines for post-operative imaging, segmentation, osteotomy localisation, registration, and osteotomy comparison. The difference in distance deviated was within an absolute average of 3 mm. The angular deviation was significantly larger for the reconstruction osteotomies than for resection osteotomies, requiring further research.

Contents

Abbreviations

Abbreviation	Definition
3D	Three Dimensional
CAS	Computer Assisted Surgery
CBCT	Cone-beam Computed Tomography
COM	Center of Mass
CT	Computed Tomography
FFF	Free Fibula Flap
kVp	kilo Voltage peak
LCS	Local Coordinate System
MRI	Magnetic Resonance Imaging
PSC	Patient Specific Cutting Guide
WCS	World Coordinate System

1

Introduction

1.1. General introduction

Patients suffering from osteomyelitis, osteoradionecrosis, or tumours invading the mandible, require a segmental resection [1]. Ablative surgery removes the tumour and/or affected tissue, creating a bone- and soft-tissue defect in the oral cavity. The defect causes impairments in speech, swallowing, mastication, nutrition, and appearance [2].
The current golden standard for reconstructing large mandibular defects is a reconstruction with a microvascular free fibula transfer [3, 4]. The reconstruction restores the mandibular contour, the internal soft tissue and creates the foundation for dental rehabilitation [1, 5, 6].

For the segmental mandibular resection and reconstruction, the resection osteotomies need to be made accurately to ensure adequate tumour removal. While doing so, vital tissues like nerves and dentition should be preserved whenever possible. Additionally, the created mandibular gap should allow for a reconstruction that results in a proper neo-mandible contour and facilitates the placement of a fibular graft segment that is at least 1.5 cm long [7].

Computer-assisted surgery (CAS) is frequently used to optimize the complex procedure described above. Computer-assisted segmental mandible resection and reconstruction is a multi-step process, consisting of 1) Acquisition of pre-operative imaging data, 2) Computer-assisted planning, 3) 3-dimensional (3D) printing, 4) Surgery and 5) Evaluation. The workflow starts with acquiring high-quality CT and MRI scans of the craniomaxillofacial region and a CT angiography of the graft site, see Figure 1.1.A. These 2-dimensional images can be converted into 3D surface models using image segmentation, see Figure 1.1.B. The resection osteotomies are positioned based on oncological and functional considerations. The reconstruction segment is created by positioning the fibula (multiple times, for more segments) in the mandibular defect, see Figure 1.1.C.

The transition from virtual to physical in-patient osteotomies is enabled by 3D-printed patient-specific cutting guides (PSC). The PSC is made up of two main components: the slot or flange and the supporting surface. The slot or flange is designed to guide the saw in the direction of the planned osteotomy. The design of the slot/flange is dependent on the surgical approach, osteotomy location, and sterilization (determining the part thickness and slit dimension of the slots) [8]. The supporting surface needs to comply with the following design factors: 1) stable contact, which can be enhanced by fixating the guide with screws [8]; 2) facilitation of unique position and orientation for precise guide placement; and 3) non-interference with other tissues to prevent the spread of tumour cells. A connecting arc is often designed to connect the proximal and distal resection cutting guides, creating one cohesive unit, to increase its stability and uniqueness. Two guides are developed: a resection guide for the resection of the tumour and a reconstruction guide for creating the graft segment(s) for reconstruction, see Figure 1.1.D.

Lastly, reconstruction of the mandible is achieved by fixating the fibular segments and the remnant mandibular segments to each other.

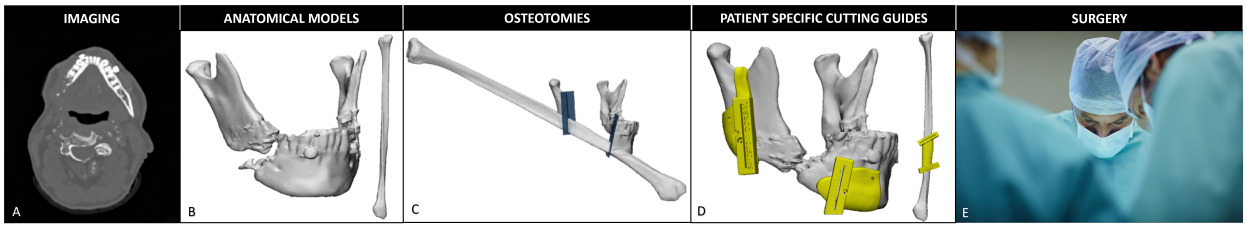

Figure 1.1: Overview computer-assisted surgery process
Figure 1.1.A shows the workflow for craniomaxillofacial reconstruction starts with obtaining high-quality CT and MRI scans of the craniomaxillofacial region along with a CT angiography of the graft site. **Figure 1.1.B**, using imaging segmentation, 3D models of the mandible and fibula are created. **Figure 1.1.C**, the resection osteotomies are positioned based on oncological and functional considerations. The reconstruction segment is created by positioning the fibula in the mandibular defect. **Figure 1.1.D**, the resection and reconstruction cutting guides are designed to translate the planned osteotomies to surgery. **Figure 1.1.E**, the resection and reconstruction osteotomies are executed, and the mandibular reconstruction is accomplished by fixating the fibular segment(s) to the remnant mandibular segments.

Inaccuracies between the planned and the actual in-patient reconstruction can arise by intentional and unintentional deviation. Intentional deviations occur if the computer-assisted planning is not (or no longer) assumed to be valid. The invalidity of the planning can, among other reasons, be caused by tumour growth due to the time between pre-operative imaging and the surgery [9]. Unintentional deviations, on the other hand, arise from errors such as misplacement of the PSC, incorrect saw orientation within the PSC saw-slot, or incorrect fixation of graft segments [10, 11]. These unintentional deviations can affect the adequacy of tumour margins and the preservation of vital structures. The intentional and unintentional deviation may result in suboptimal resection and reconstruction, leading to less favourable patient outcomes and prolonged surgical duration [12].

The inaccuracies caused by the aforementioned reasons should be evaluated as the last step of the CAS process. The literature reports deviations ranging between 0 mm and 12.5 mm and between 0.9° and 17.5°. However, the evaluation methods and, therefore, outcome parameters are heterogeneous, making comparison weak [13].

Baar et al. [14] introduced a guideline in 2019 aiming to standardize the evaluation method. However, a limitation of this guideline is the generality of the outcomes derived from the proposed evaluation method. The method compares the entire post-operative reconstruction to the pre-operatively planned reconstruction. It does so by calculating the deviation in the mandibular contour. The deviation in the final post-operative mandibular contour is, however, a summation of all the deviations that can occur during the CAS process, as explained above. The origin of these deviations cannot be retrieved at a later stage. This hampers identifying causes of the deviations and, thus, the ability for innovation and improvement.

Due to many factors influencing the post-operative accuracy, a focus is required. Translating the virtual to the physical osteotomies using the PSC is an important step for accurate reconstruction. The deviation caused in this step can be evaluated by comparing the planned osteotomies to the actual executed osteotomies.

As preliminary research, a comparative literature review was conducted [15] investigating the different methodologies used in the literature for comparing planned and actual osteotomies. The methodologies of twenty-four articles were assessed [11, 12, 16–37]. The articles used a wide variety of incomplete and poorly described methods for segmentation, osteotomy localisation, registration and accuracy assessment. It could be concluded that a standardized and well-described methodology for comparing planned and actual osteotomies is imperative.

1.2. Aim and objectives

This thesis aims to develop a methodology for assessing inaccuracies between the planned segmental mandibular resection and reconstruction and the actual post-operative result. It focuses on the deviation that occurs when translating planned osteotomies to surgery using a PSC. This evaluation is conducted by comparing the differences between the planned and actual osteotomies.

Objective 1: Methodology development

The first objective entails the development of a reproducible and objective accuracy assessment method, comparing the planned osteotomy with the actual osteotomy. The methodology will consist of two parts:

- Developing and/or describing the methodology for post-operative imaging, segmentation, localisation of the actual osteotomies, and registration.
- Developing a distance and angular deviation measurement to evaluate the accuracy between the planned and the actual resection and reconstruction osteotomies.

Objective 2: Retrospective study

The second objective is to retrospectively analyse the accuracy of CAS in segmental mandibular resection and reconstruction, using the novel method developed in objective one, for patients treated at the Leiden Medical University Centre.

2

Technical background

In CAS procedures, mathematics is used to understand and guide processes such as the virtual planning of mandibular resection and reconstruction. 3D virtual representations of the patient's anatomy are created to develop a virtual resection and reconstruction plan. A similar approach must be applied to evaluate the accuracy of the virtual surgery. Therefore, this introduction explains the principles needed to understand the developed methodology for evaluating the accuracy between planned osteotomies and actual osteotomies.

2.1. Imaging

The input for the 3D models are imaging scans like CT and CBCT. The quality of the scan affects the segmented 3D models [38] and the localisation of the actual osteotomies. The scan quality is determined by the acquisition technique and the used parameters like the kilo Voltage peak (kVp), slice thickness and pixel spacing. The optimal level of kVp is a trade-off between high energy (highly penetrating, low contrast) versus lower energy (less penetrating, higher contrast) X-rays [39]. The slice thickness determines the longitudinal sampling resolution [40]. A thinner slice thickness will improve the spatial resolution but at the cost of an increased radiation dose or image noise and scanning time [41]. The sampling resolution in the transaxial dimension depends on the selected field of view of the CT scanner and the imaging matrix (256x256 or 512x 512) yielding pixel spacing. The pixel space is a trade-off between spatial resolution (small pixel spacing) and the measurable signal affecting the signal-to-noise ratio [40].

2.2. Segmentation

Image segmentation is the grouping of pixels in an image according to specific properties. Segmentation is used to distinguish between regions that have homogenous characteristics, such as bone and soft tissue. [40, 42]. Accurate segmentation is essential as it forms the basis for CAS.

Many approaches can be used to create a segmentation. The initial approach is often thresholding, which groups pixels by intensity. An upper and lower threshold can be set, classifying pixels into groups [40]. The optimal threshold depends on the imaging modality, acquisition parameters, and the nature of the tissue being segmented [40].

Region growing is a segmentation approach that detects connected regions based on intensity and connectivity. In region growing, a seed point is manually selected and connected voxels with the correct intensity are included. There are three types of connectivities that can be used to identify connecting voxels: 6, 18, and 26. In 6 connectivity, all voxels with adjacent faces are included. In 18 connectivity, all voxels with adjacent edges are included and in 26 connectivity, all voxels with adjacent vertices are included [40]. The connected region is separated and manually labelled after the specific structure.

Advanced techniques, including interpolation approaches, automatic adjustments and the use of artificial intelligence, are used to enhance segmentation accuracy and decrease segmentation time and observer variability [43] [44].

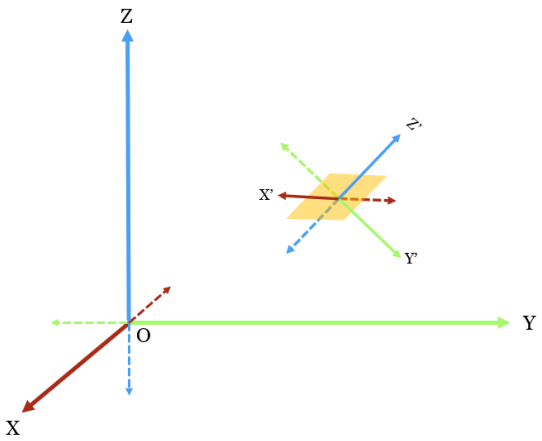

Figure 2.1: Global coordinate system (X, Y, Z) and a plane (yellow) with its local coordinate system (x', y', z')

2.3. 3D surface models

From segmentation, a 3D surface model is created using algorithms such as the marching cubes algorithm. The mesh defines a surface model, outlining the object's shape through a collection of polygons, typically triangles, composed of vertices, edges, and faces [45]. Vertices define the corners, edges are the lines between vertices, and faces represent flat surfaces.

2.4. Coordinate systems

The position and orientation of the created 3D models are defined in three-dimensional space. Within this space, a coordinate system describes a structured framework. This system centres around an origin point, from which three orthogonal axes emerge—the x-axis, y-axis, and z-axis. The direction of these axes follows the right-handed rule, defining it as a right-handed coordinate system. The axes, extending from the origin, designate positive values, while the opposing side represents negative values [46, 47].

In this three-dimensional space, any point p can be assigned coordinates $\mathbf{p} = (p_x, p_y, p_z)$, representing signed distances along the three axes from the origin [46].

The world coordinate system (WCS) is a universal reference, positioning objects and defining spatial relationships within a given environment. The WCS origin is situated at $[0, 0, 0]$, and orthonormal axes x,y,z are represented by $i = (1, 0, 0)$, $j = (0, 1, 0)$, and $k = (0, 0, 1)$ [46].

The location of an object can be expressed within the world coordinate system, but they can also have their own local coordinate system (LCS), see figure 2.1. LCSs have their own origin and three orthogonal axes. Each coordinate system can be expressed as a 4x4 matrix adhering to special constraints, positioning the LCS in a reference frame of another system, such as the WCS. Therefore, these matrices also facilitate coordinate system changes, allowing the expression of positions and orientations in a local coordinate system to be translated to the global coordinate system [47].

2.5. Spatial transformation

Spatial transformation refers to a rigid or deformable transformation of an object [40, 48]. Within the scope of this report, rigid translation and rotation will be further explained. The translation and rotation can be combined in a single 4x4 rigid transformation matrix, see Matrix (2.1).

$$M = \begin{bmatrix} R_{xx} & R_{yx} & R_{zx} & T_x \\ R_{xy} & R_{yy} & R_{zy} & T_y \\ R_{xz} & R_{yz} & R_{zz} & T_z \\ 0 & 0 & 0 & 1 \end{bmatrix} \tag{2.1}$$

The top-left 3x3 sub-matrix of the matrix shown above, represents a rotation transform, while the last column represents a translation. This matrix can also be interpreted as a coordinate system. The position is

represented in the last column, and the orientation in space is represented in the top-left 3×3 matrix. The last row of the matrix is always $(0, 0, 0, 1)$, ensuring a uniform 4x4 structure. This uniformity enables the representation of both translation and rotation operations in a single transformation matrix through matrix multiplication, facilitating efficient geometric transformations [47].

2.5.1. Translation

A translation matrix can move an object along one or more of the three axes. The basic form of a transformation matrix that solely shows translations is as follows:

$$M = \begin{bmatrix} 1 & 0 & 0 & t_x \\ 0 & 1 & 0 & t_y \\ 0 & 0 & 1 & t_z \\ 0 & 0 & 0 & 1 \end{bmatrix} \tag{2.2}$$

When a translation matrix is applied to a point v, it can be shown that Mv only produces translation (shift) by adding the translation vectors tx, ty, and tz to the components of v (vx, vy, and vz):

$$Mv = \begin{bmatrix} 1 & 0 & 0 & t_x \\ 0 & 1 & 0 & t_y \\ 0 & 0 & 1 & t_z \\ 0 & 0 & 0 & 1 \end{bmatrix} \begin{bmatrix} v_x \\ v_y \\ v_z \\ 1 \end{bmatrix} = \begin{bmatrix} v_x + t_x \\ v_y + t_y \\ v_z + t_z \\ 1 \end{bmatrix}$$

2.5.2. Rotation

An object can be rotated around one or more of the three axes by a rotation matrix. The rotation matrix is formed by the 3x3 top-left section. The matrices RX, RY, and RZ represent transformations that rotate points by the angle θ in radians around the origin of the WCS [48].
The transformation matrix for rotation around the x-axis by an angle θ:

$$R_x(\theta) = \begin{bmatrix} 1 & 0 & 0 & 0 \\ 0 & \cos(\theta) & -\sin(\theta) & 0 \\ 0 & \sin(\theta) & \cos(\theta) & 0 \\ 0 & 0 & 0 & 1 \end{bmatrix}$$

The transformation matrix for rotation around the y-axis by an angle θ:

$$R_y(\theta) = \begin{bmatrix} \cos(\theta) & 0 & \sin(\theta) & 0 \\ 0 & 1 & 0 & 0 \\ -\sin(\theta) & 0 & \cos(\theta) & 0 \\ 0 & 0 & 0 & 1 \end{bmatrix}$$

The transformation matrix for rotation around the z-axis by an angle θ:

$$R_z(\theta) = \begin{bmatrix} \cos(\theta) & -\sin(\theta) & 0 & 0 \\ \sin(\theta) & \cos(\theta) & 0 & 0 \\ 0 & 0 & 1 & 0 \\ 0 & 0 & 0 & 1 \end{bmatrix}$$

The total rotation is a multiplication of the three rotation matrices in a specific order. To go from the total rotation matrix to intuitive values, the rotation matrix should be converted into Euler angles [48]. Euler angles express the rotation around one of three perpendicular axes (the x, y, and z axes), in degrees (°). Due to the non-commutative nature of matrix multiplication for rotation matrices, the order of multiplication affects the result [49]. In the methodology in Section 3.1.5, rotation is first applied around the z-axis, then the x-axis and finally the y-axis.

2.5.3. Registration

Registration is the spatial alignment of two datasets (e.g. images or surface models). Different methods for registration can be used. In the methodology proposed in Chapter 3, landmark registration is used as an initial registration, globally aligning the objects. An iterative closest point registration will later facilitate precise alignment. Both registration methods are explained below. The spatial alignment of landmark registration is based on a limited set of identified points (landmarks). Landmark-based registration mostly performs rigid transformations. A disadvantage is that the landmarks are often picked manually. The optimization process of landmark-based registration is relatively fast as the input data (the set of landmarks) is sparse compared to the original image/model content [50].

After landmark registration, iterative closest point registration is performed for optimisation. Iterative closest point registration tries to find the closest point pairs using rigid transformations and iterates until the error metric is minimal and stable. The error metric is typically the sum of the squared differences between the coordinates of the matched pairs [51].

3

Accuracy guideline

This chapter outlines a methodology to evaluate the accuracy of computer-assisted segmental mandible resection and reconstruction. It focuses on comparing planned osteotomies with actual ones using a mathematical approach to ensure objectivity and reproducibility.

All measurements are conducted on virtual representations of the anatomical structures and osteotomies. All models that are created for the planning will be referred to as *planned*. All the models representing the post-operative result will be referred to as *actual*. The osteotomies can be categorised into resection and reconstruction osteotomies. The *resection osteotomies* remove the affected tissue from the mandible and create the mandibular gap. The *reconstruction osteotomies* are made in the fibula to create fibula segment(s) for the reconstruction of the mandible.

An overview of the methodology is shown in Figure 3.1. The methodology begins with the collection or creation of the virtual representation of the planned and actual models and osteotomies, see Figure 3.1.A. The virtual representation of the planning is derived from the computer-assisted pre-operative plan. A virtual representation of the actual result is generated from the post-operative imaging. The neo-mandible is segmented from this imaging to create 3D models of the actual remnant mandible and fibula segments. The actual osteotomies are also determined based on the post-operative imaging. To compare the actual osteotomies with the planned ones, the actual osteotomies are registered to the pre-operative mandible or fibula.

The osteotomies are compared by measuring distance and angular deviation, see Figure 3.1.B. The calculation of distance deviation differs between resection and reconstruction osteotomies. For the angular deviation, an identical methodology is used. Additionally, a more clinical value is determined by assessing the maximum distance deviation of the resection osteotomies. The value is important in the context of the preservation of adequate tumour margins and the avoidance of vital structures.

The first part of the methodology is executed in Mimics and 3-Matic (Materialise NV, Leuven, Belgium) [52, 53]. A Python script is developed to perform the final calculations.

This methodology is intended to provide guidance on different steps of the evaluation process, including:

Pre-processing:

1. Planned data collection
2. Actual data generation
   2.1. Post-operative imaging
   2.2. Segmentation
   2.3. Localisation of the osteotomies
3. Registration

Osteotomy comparison:

1. Distance deviations
   1.1. Resection osteotomies
      - Maximum distance
      - Distance direction
   1.2. Reconstruction osteotomies
2. Angular deviations
   2.1. Resection osteotomies
   2.2. Reconstruction osteotomies

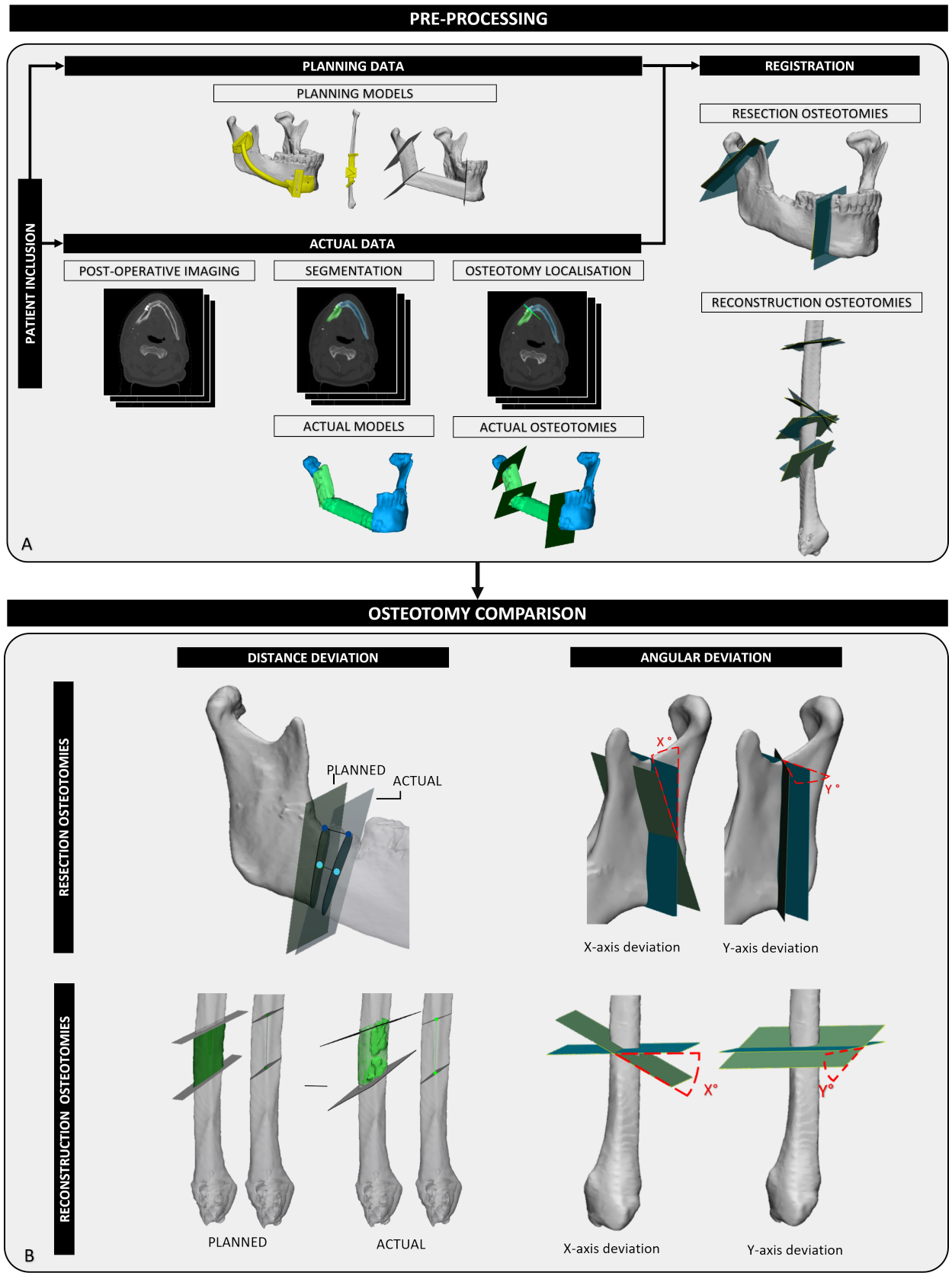

Figure 3.1: Methodology overview

Figure 3.1.A shows the preprocessing steps, where the data is prepared for osteotomy comparison. The planned data is collected from the pre-operative planning, while the actual data is based on the post-operative imaging. 3D models are created through segmentation, and the actual osteotomies are defined on the post-operative imaging. Lastly, the actual osteotomies are aligned with the pre-operative mandible/fibula. **Figure 3.1.B** shows the osteotomy comparison, consisting of measuring a distance and angular deviation.

3.1. Accuracy methodology

Pre-processing

3.1.1. Planned input data

The planned input data is collected from the pre-operative planning. This includes models of the pre-operative mandible and fibula. Additionally, models of the planned resection and reconstruction are necessary. These models entail the remnant mandible, fibula segments, and the resection and reconstruction osteotomies. Lastly, models of the resection and reconstruction PSCs should be gathered.

3.1.2. Actual input data

Imaging

Post-operative imaging is used to create the actual 3D models of the mandibular reconstruction and locate the actual osteotomies. The evaluation accuracy depends on the CT imaging quality, requiring optimization and uniformity. The quality of the post-operative imaging is dependent on the study type. For prospective research, the acquisition parameters and scanner model should be uniform. A maximum slice thickness of 1.25 mm is recommended [38]. To minimize the impact of bone healing and resorption [54], post-operative imaging must be conducted as soon as possible after surgery. Retrospective research must present the acquisition parameters, including imaging modality, slice thickness, pixel spacing, kVp, manufacturer, and model name for both pre-operative and post-operative imaging. Additionally, the time interval between surgery and post-operative imaging must be presented.

Segmentation

3D surface models of the actual reconstructed mandible must be created by image segmentation in Mimics (Materialise NV, Leuven, Belgium) [52]. The created models include the left and right remnant mandible and the fibular segments. Segmentation functions used include thresholding, region growing, smart fill, split mask and edit mask (manual editing).

Osteotomy localisation

The next step is the localisation of the actual osteotomy. The osteotomies must be located on the post-operative CT or CBCT imaging in Mimics (Materialise NV, Leuven, Belgium) [52]. The osteotomies are located on the ends of the remnant mandible and fibula segments. The natural shape of the structure is disrupted here, which is seen as an abrupt and unexpected change in contrast. The resection and the reconstruction osteotomies are localised using the same protocol. However, before localising the resection osteotomies, the PSC design must be examined. The saw slot or flange of the PSC does not always cover the full cross-section of the mandible, see Figure 3.2.A. Especially osteotomies crossing the ramus or dentition. If the PSC partially guides the osteotomy, the assessment of the actual osteotomy is only valid on the guided part. Therefore, the PSC should be aligned with post-operative imaging to determine the proper location for assessing the actual osteotomy. The transformation necessary for this alignment is established by aligning the planned remnant mandible with the actual one [Figure 3.2.B]. Subsequently, the resection PSC is registered using the same transformation [Figure 3.2.C]. The alignment is executed in 3-Matic (Materialise NV, Leuven, Belgium) [53]. Importing the aligned PSC in Mimics (Materialise NV, Leuven, Belgium) [52] will present the PSC in a proper position on the post-operative imaging [Figure 3.2.D].

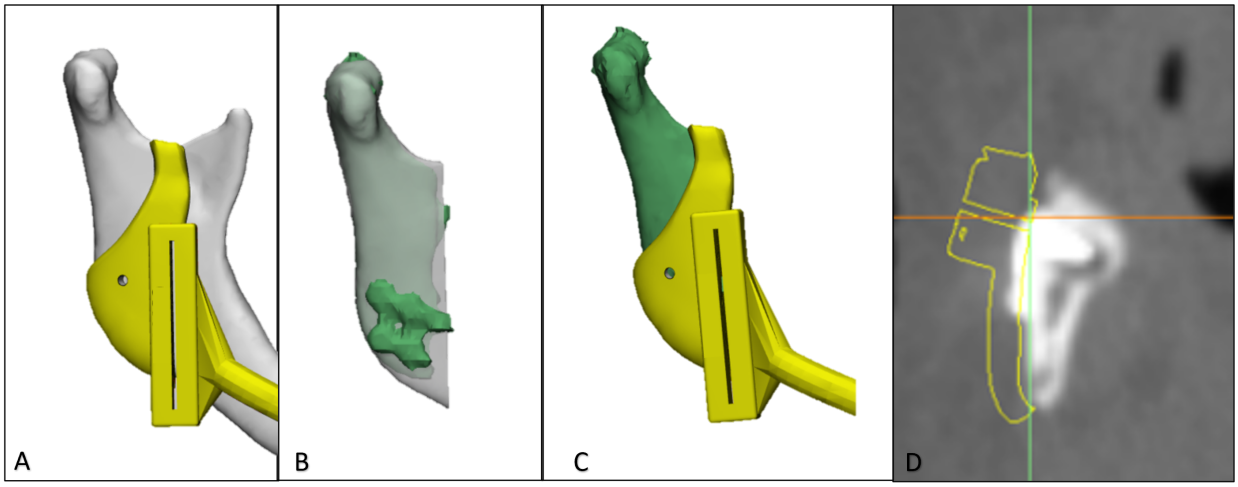

Figure 3.2: Registration resection cutting guide
Figure 3.2.A Pre-operative mandible with the designed PSC. The PSC slot only guides the saw on the caudal part of the osteotomy across the ramus. **Figure 3.2.B** shows the registration of the planned remnant mandible (grey) to the actual remnant mandible (green). **Figure 3.2.c** shows the PSC aligned with the actual remnant mandible. **Figure 3.2.D** shows the PSC aligned with the post-operative imaging.

The osteotomy must be localised by placing points at the end of the sawn bone segments on post-operative imaging in Mimics (Materialise NV, Leuven, Belgium) [52]. These points should be positioned next to the outermost edge of the bone segment. Starting from one side of the bone cut, points must be placed every couple of slices towards the opposite side. The points must only be positioned in slices where the bone contour is clearly visible, as some regions are affected by artefacts from fixation material. The points will together form a point cloud. A plane that represents the actual osteotomy will be fitted through the point cloud in 3-Matic (Materialise NV, Leuven, Belgium) [53].

3.1.3. Registration

Resection osteotomies

To analyse the deviation between a planned and actual resection osteotomy, the actual osteotomy must be aligned to the pre-operative mandible. The registration is performed by aligning the actual remnant mandible to the planned remnant mandible. The actual osteotomy must then undergo an identical transformation. The registrations must be performed initially using landmark registration, followed by optimization using surface registration. Through this alignment, the new position of the actual osteotomy becomes relative to the pre-operative mandible model, enabling comparison to the planned osteotomy.

Reconstruction osteotomies

The fibula bone has a uniform shape, making it difficult to accurately determine the longitudinal position of the actual segment. Therefore, it is not feasible to align the fibular segments with just the pre-operative fibula bone. To register the actual fibular segments with their associated osteotomies, they must be aligned with the planned fibular segment at the location of the pre-operative fibula. An initial registration must again be performed using landmark registration, followed by iterative closest point registration. Manual alignment is performed when necessary due to the homogeneous shape of the fibula and segmentation errors in the actual fibular segments.

Registration is performed in 3-Matic (Materialise NV, Leuven, Belgium) [53].

Osteotomy comparison

3.1.4. Distance deviation

Resection osteotomies

To determine the distance deviation of the resection osteotomy, the positional difference between two reference points representing the planned and actual osteotomies must be measured. The reference points are located at the centre of mass (COM) of the intersection between the osteotomy and the pre-operative

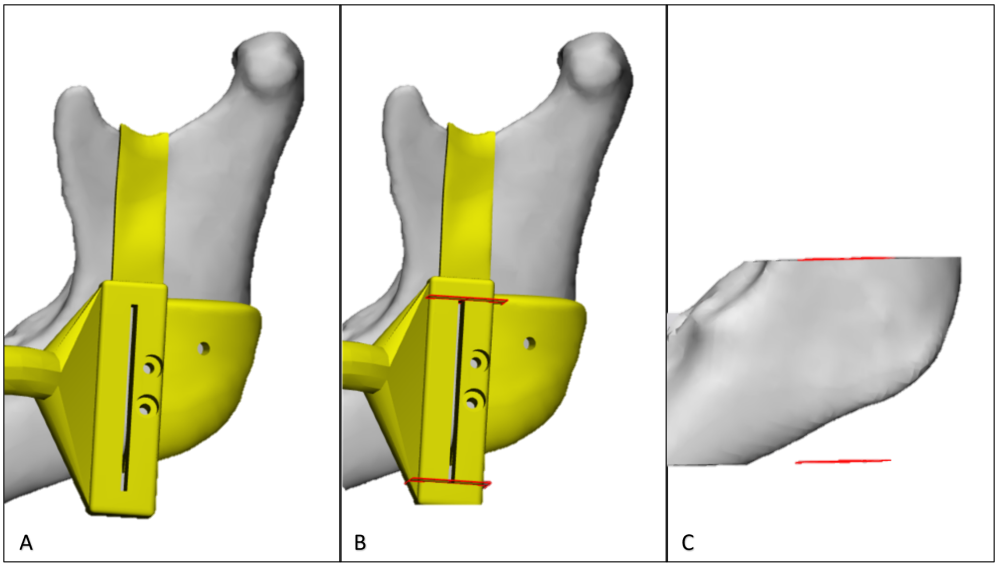

Figure 3.3: Definition of the accurate cut mandible.
Figure 3.3.A shows that the PSC only partially guides the osteotomy. **Figure 3.3.B** shows that the mandible is cut based the PSC. **Figure 3.3.C** shows the accurate mandible which is relevant for the osteotomy comparison.

mandibular model. The intersection must be created by performing a boolean intersection of the osteotomy (actual and planned) with the pre-operative mandible model in 3-Matic (Materialise NV, Leuven, Belgium) [53]. Similarly to the localisation of the actual osteotomy, described in Section 3.1.2, the intersection is limited to the part of the osteotomy where the saw is guided by the PSC. If the osteotomy is only partly guided by the saw, then the pre-operative mandible model is cut based on the length of the slot or flange PSC, see Figure 3.3. The cut pre-operative mandible model is used to perform the boolean intersection with the planned and actual osteotomy.

The intersections must be saved and will be loaded into the Python script. In this script, the COM of the intersection is calculated. The distance between the planned COM and the actual COM is calculated by the Euclidean distance using Formula (3.1). Figure 3.4 shows the measurement of the distance deviation.

$$\text{Euclidean Distance} = \sqrt{(x_2 - x_1)^2 + (y_2 - y_1)^2 + (z_2 - z_1)^2} \tag{3.1}$$

Maximum distance

The maximum distance between the actual and planned intersection is calculated in the Python script. The maximum distance is defined as the maximum perpendicular distances between the planned and actual intersection [55]. The vertices of the actual intersection are used to convert the intersection STL model into a point cloud. The perpendicular distances are measured from all points of the actual point cloud to the planned intersection. The maximum of these absolute distances defines the maximum distance between the intersections, see Figure 3.5.A.

Tumour margin deviation

The resection osteotomies are planned with a specific tumour margin. Based on the position of the actual osteotomy relative to the planned osteotomy and the tumour, the tumour margins can increase or decrease. This gives the COM and the maximum distance deviation a direction. Negative values represent deviations where less mandibular tissue is removed, placing the actual osteotomy closer to the tumour. Positive values represent deviations where more mandibular tissue is removed, moving the actual osteotomy further away from the tumour. The direction is determined by manually selecting a point within the resection gap representing the tumour. The distance between the tumour reference point and the COM of the planned and actual intersection is measured in the Python script, see Figure 3.6. If the distance between the tumour and the COM of the actual intersection is smaller than the distance from the tumour to the planned intersection of the actual intersection, the direction of the deviation is negative, indicating the actual COM lies closer to the tumour. A similar measurement is performed for the maximum distance.

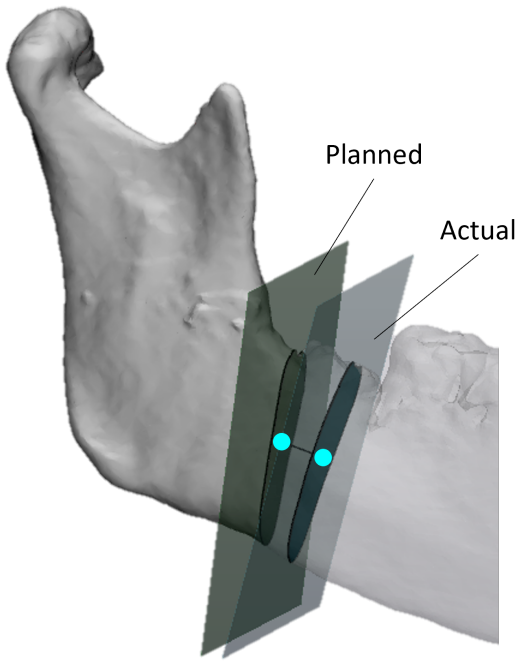

Figure 3.4: Resection osteotomy distance deviation.
The distance deviation is measured by first creating an intersection between the osteotomies (planned and actual) and the pre-operative mandible. The COM of the intersections is then calculated. The distance deviation is defined as the distance between the planned COM and the actual COM

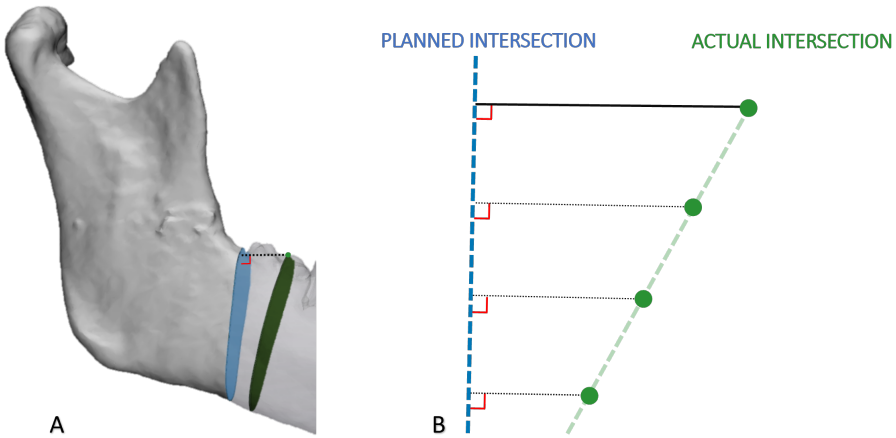

Figure 3.5: Maximum distance deviation
Figure 3.5.A shows the 3D presentation of the maximum distance between the planned (blue) and actual (green) intersection. **Figure 3.5.B** is a schematic representation of the maximum distance measurement. The blue dotted line represents the planned intersection. The green point represents the point cloud of the actual intersection. The distance from each point in the actual point cloud is measured perpendicularly to the planned intersection (black lines). The maximum distance between the actual and planned intersections is the largest absolute distance measurement (thick black line).

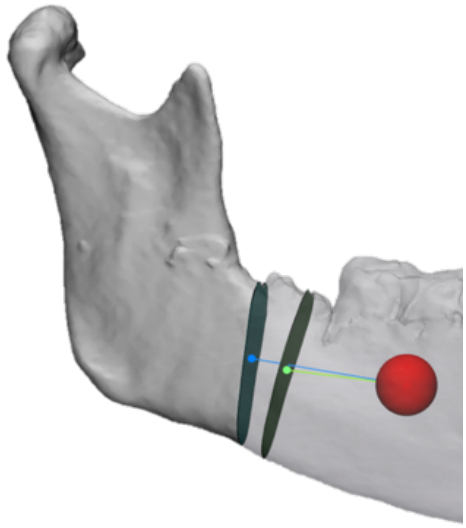

Figure 3.6: Direction of distance deviation
The direction of the distance deviation is based on the distance between the reference point of the tumour (red) and a reference point on the actual (green) and planned (blue) intersection. The reference points can be the COMs of the intersections or the points on the intersection associated with the maximum distance. In this figure, the direction measurement of the COM is displayed. The green line (tumour to COM of the actual intersection) is shorter than the blue line (tumour to the COM of the planned intersection), indicating the actual COM lies closer to the tumour, making the COM deviation a negative value.

Reconstruction osteotomies

As explained in Section 3.1.3, the longitudinal alignment of the fibular segments is not accurate enough. This prohibits the distance deviation to be measured per osteotomy (one planned and actual pair), as the method of the resection osteotomies. A measurement is employed that is not influenced by this longitudinal position of the fibula segment. The assessment of distance deviation in reconstruction osteotomy must be measured by comparing the planned and actual lengths of the fibular segment. Boolean intersections must be computed between the pre-operative fibular model and the two pairs of reconstruction osteotomies creating the planned and actual fibular segment. The intersection is again created in 3-Matic (Materialise NV, Leuven, Belgium) [53]. The intersections must be saved and will be loaded into the Python script. The COM is calculated for each of the four intersections. The length of the planned and actual segment is measured by the distance between the COM of the intersections. The difference in length is determined by subtracting the actual fibular segment length from the planned length, see Figure 3.7. The fibular segment length difference is determined for all fibular segments in the reconstruction.

3.1.5. Angular deviation

The calculation of the angular deviation is identical for the resection and reconstruction osteotomies. The angular deviation of the actual osteotomy is determined in reference to the planned osteotomy. The angular deviation must be measured by the difference in orientation of the LCS of the osteotomies. The x and y axes of this local coordinate system must be defined in-plane while the z-axis is pointing outwards, determined by the right-hand rule. The direction of the x- and y-axis of the planned osteotomy is determined by the saw slot/flange, see Figure 3.8A1/B1. The saw slot/flange is designed to guide the saw through the bone in one specific direction, identical to the planned osteotomy, see Figure 3.8.C1. The x-axis of the local coordinate system is presented by the height of the slot/flange. The difference in this angle defines the deviation of the saw across the saw slot/flange, see Figure 3.8A2/B2/C2. The y-axis of the local coordinate system is defined by the length of the PSC slot/flange. This deviation defines the angle of the saw going through the saw slot, see Figure 3.8A3/B3/C3. The angular deviation along the z-axis does not yield clinically valuable information and will thus be irrelevant.

For the LCS of the actual osteotomy, the x and y direction are roughly determined. The direction must represent the same direction as the LCS of the planned osteotomy, but cannot be determined exactly. In a later step, a rotation around the z-axis will move the x-y axes of the actual osteotomy to the correct position.

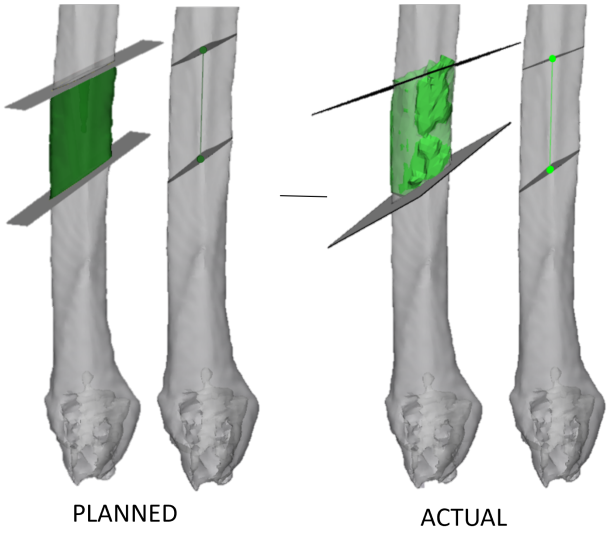

Figure 3.7: Reconstruction osteotomy distance deviation
The distance deviation for the reconstruction osteotomies is defined as the difference in length between the planned and actual fibula segment. The length is determined by the distance between the intersections of the upper and lower osteotomies of each segment, with the fibula.

The LCS of the planned and actual osteotomy must be saved and will be loaded into the Python script.

To determine the angular deviation, the rotation matrix that transforms the LCS of the planned osteotomy to the LCS of the actual osteotomy is calculated. This calculation involves first translating both the actual and planned LCS to the centre of rotation, which is located at the origin [0,0,0]. Next, the inverse of the planned LCS is determined. The inverse of an LCS rotates the LCS to the WCS. By multiplying the inverse of the planned LCS with the actual LCS, the deviation matrix is obtained, see Formula (3.2).

$$R = R_{\text{actual}} \cdot R_{\text{planned}} - 1 \tag{3.2}$$

Finally, Euler angles are computed from the rotation matrix to facilitate easy interpretation. The order of rotation is Z, X, Y. First, a rotation around the z-axis is performed to position the x and y axes of the LCS correctly, as described before. This angular information itself is not clinically relevant. Subsequent rotations around the x and y axes are determined in degrees.

3.1.6. How to use this evaluation guideline

Appendix A, B and C provide a step-by-step guide for the execution of the methodology. The input for this methodology is the pre-operative plan in 3D models and the post-operative imaging. The first steps of the evaluation are done in Mimics and 3-Matic (Materialise NV, Leuven, Belgium) [52, 53], for which a license must be available. A Python script is developed, performing the final calculations and exporting the results into an Excel sheet (Mircosoft, Redmond, Washington, USA). Python (python software foundation, Wilmington, Delaware, USA) installation is necessary to execute the script, which can be run using a Python interpreter.

3.2. Evaluation of the methodology

Assessment of observer variability is a required step in developing a new measurement methodology [56]. The developed method consists of a combination of manual and automatic steps, each with its own variability risk. The analysis evaluated the intra- and inter-variability, focusing on the localisation of the actual osteotomies. The variability test involved two observers; the first observer conducted the intra-observer variability. This observer performed the measurements twice on an identical set of samples. The initial measurement served as the reference, which was then compared to the second measurement for variability assessment. The inter-observer variability involved comparing the reference measurement (first

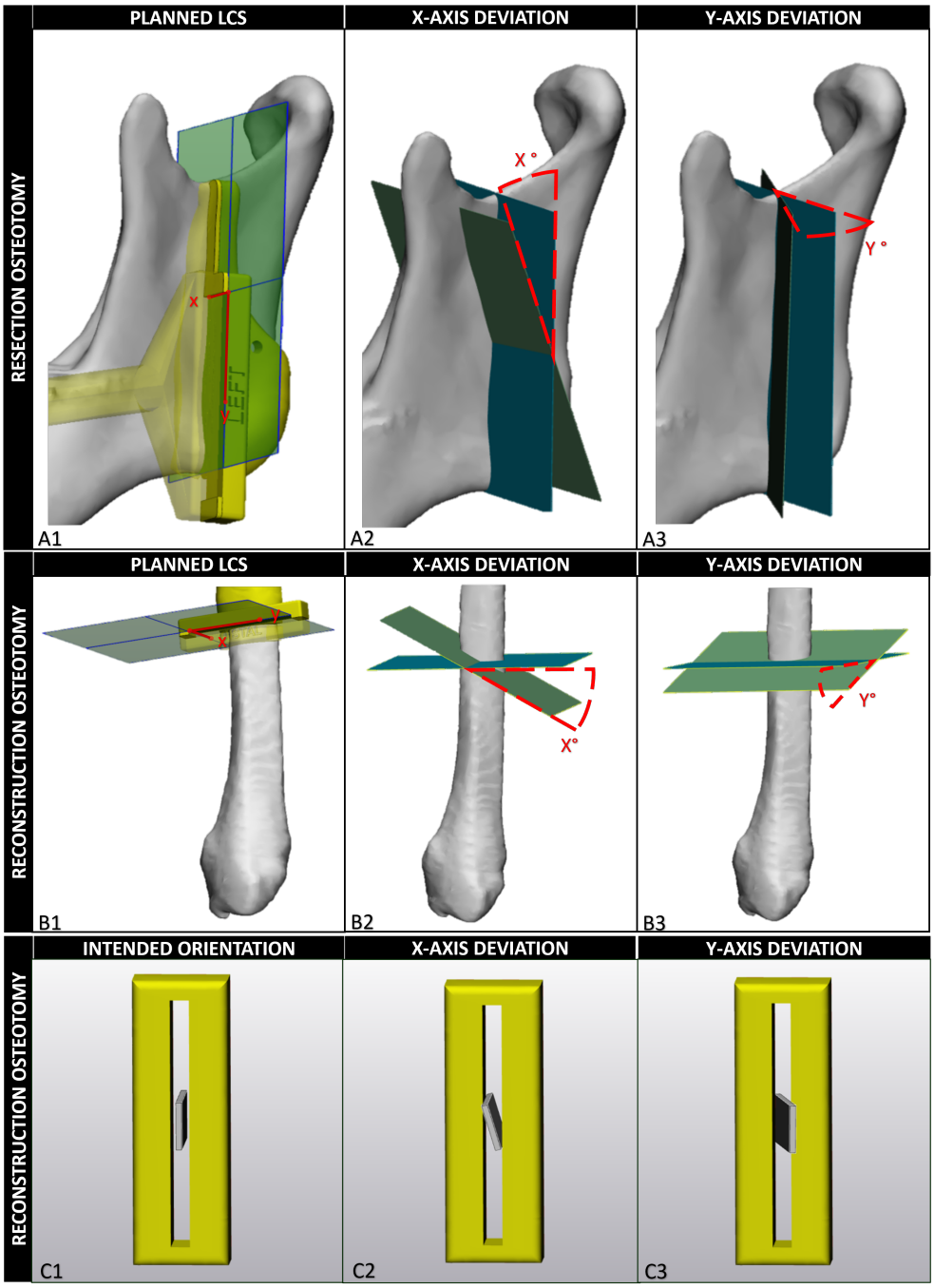

Figure 3.8: Angular deviation

The angular deviation is determined using the same method for both resection and reconstruction osteotomies. **Figures 3.8.A1** and **3.8.B1** show how the direction of the angular deviation is determined based on the PSC. The x-axis is defined by the height of the PSC slot, and the y-axis is defined by the length of the PSC slot. **Figures 3.8.A2** and **3.8.B2** provide an example of deviation around the x-axis, resembling the angular deviation across the saw slot. Similarly, **Figures 3.8.A3** and **3.8.B3** show the deviation around the y-axis, resembling the angular deviation through the saw slot. **Figure 3.8.C** show the PSC with the saw orientation as intended (1), with a deviation around the x-axis (2), and with a deviation around the y-axis (3)

Table 3.1: Variability osteotomy localisation (absolute average difference)

	Distance deviation						Angular deviation			
	COM [mm]		**Max [mm]**		**Fibula length [mm]**		**X axis [°]**		**Y axis [°]**	
	Average	STD	Average	STD	Average	STD	Average	STD	Average	STD
Intra	0.3	0.5	0.4	0.5	0.4	0.6	1.9	2.7	2.2	3.1
Inter	0.8	1.2	1.2	1.8	0.8	1.1	2.0	2.5	2.8	3.7

Table 3.2: Variability osteotomy localisation (intraclass correlation coefficient)

	Intra Observer			Inter Observer		
	ICC	**P**	**CI95%**	**ICC**	**P**	**CI95%**
COM Distance	0.99	<0.01	[0.96-1.00]	0.96	<0.01	[0.85 - 0.99]
Max Distance	0.99	<0.01	[0.96-1.00]	0.93	<0.01	[0.73 - 0.98]
Fib Length Actual	1.00	<0.01	[1.00 - 1.00]	0.95	<0.01	[0.79 - 0.99]
Rotation X axis	0.87	<0.01	[0.75 - 0.94]	0.94	<0.01	[0.88 - 0.97]
Rotation Y axis	0.98	<0.01	[0.96 - 0.99]	0.97	<0.01	[0.94 - 0.99]

Abbreviations: IC: confidence interval, ICC: intraclass correlation coefficient

measurement by the first observer) with a measurement taken by the second observer on the same set of samples. Five samples were used for the variability analysis and were randomly selected from the included patients of Chapter 4. The observers were guided by a step-by-step guide (see Appendix A.4) on localising post-operative osteotomies. The first observer executed the remaining steps of the designed method to minimize the deviations in the following steps. The disparities in the final outcomes (distance and angular deviation between planned and actual osteotomies) were compared. Furthermore, the intra-class correlation (ICC) was determined to assess the inter- and intra- agreement.

Observer variability

For the intra-observer variability, the absolute average difference was 0.3 (± 0.5) mm for the COM distance, 0.4 (± 0.5) mm for the maximum distance and 0.4 (± 0.6) mm for the fibula length. The absolute average angular deviation was 1.9 (± 2.7)° for the x-axis and 2.2 (± 3.1)° for the y-axis. The ICC of the intra-observer variability was 0.99 [95% CI 0.98 - 0.99]. Table 3.2 shows the ICC values with the confidence interval per deviation outcome.

For the inter-observer variability, the absolute average difference was 0.8 (± 1.2) mm for the COM distance, 1.2 (± 1.8) mm for the maximum distance and 0.8 (± 1.1) mm for the fibula length. The absolute average angular deviation was 2.0 (± 2.5)° for the x-axis and 2.8 (± 3.7)° for the y-axis. The ICC of the inter-observer variability was 0.99 [95% CI 0.98 - 0.99]. Table 3.2 shows the ICC values with the confidence interval per deviation outcome.

3.3. Discussion

A novel method for assessing the accuracy of computer-assisted surgery in segmental mandibular resection and reconstruction is developed. The method compares the planned osteotomies with the actual osteotomies. Actual osteotomies should be defined by a plane fitted through manually defined points on the post-operative imaging. The resection and reconstruction osteotomies must be evaluated separately by comparing the distance and angular deviation. Resection osteotomy distance deviation should be defined as the distance between the COM of the planned and actual intersection of the pre-operative mandible model and the osteotomies. Additionally, the maximum distance between the intersection and the direction of the distance must be calculated to provide a clinically valuable measurement. The distance direction indicates if the deviation reduces or increases the planned tumour margin. Reconstruction osteotomy distance deviation should be measured as the length difference between the planned and actual fibula segments. Angular deviation of the resection and reconstruction osteotomies must be defined by two angular differences based on the saw slot, i.e. the angle across the saw slot (x-axis) and the angle through the saw slot (y-axis).

3.3.1. Literature comparison

The novel method is the first guideline on computer-assisted osteotomy accuracy evaluation in segmental mandibular resection and reconstruction. It provides a detailed step-by-step guide of a semi-automatic methodology to ensure reproducible, objective and quantitative accuracy evaluations. Systematic use of the accuracy evaluation guidelines reduces heterogeneity in the literature. Homogeneity is important for multi-centre comparison and the establishment of an acceptable deviation range. The developed method evaluates the inaccuracy between the planned osteotomies and the actual performed osteotomies. Assessing osteotomy accuracy focuses on the deviation caused by translating the virtual osteotomies to actual osteotomies. Therefore, excluding other origins of deviation such as the fixation method and the postoperative mandibular position relative to the cranium and maxilla.
Baar et al. [14, 57] developed a post-operative evaluation guideline for mandibular reconstruction using CAS. A comparison is made between the total planned mandibular reconstruction and the total actual mandibular reconstruction, measured by axial, coronal, and sagittal mandibular angles. The angles are calculated based on four bony landmarks (the condyle superior, condyle posterior, vertical corner and horizontal corner) and the midsagittal line. Comparing the actual and planned reconstruction results is a valid clinical outcome evaluation as it measures the total deviation. However, when measuring the total deviation, it is not possible to determine the cause of the deviation. For example, the sagittal mandibular angles are calculated between the lines from the condyle posterior to the vertical corner and the lines from the vertical of the mandible. In the simplest case, this angle consisted of a remnant mandibular segment and one fibula segment. The deviation of this angle is, however, caused by at least the accuracy of two osteotomies (mandible and fibula) and the fixation of these segments together. If two fibula segments are used to reconstruct this sagittal angle, the deviation factors even double (four osteotomies, two times fixation). The deviation's origin cannot be determined from this measurement alone, making further improvements hard.

Osteotomy localisation

The osteotomy localisation is performed on the post-operative imaging by manually setting points. A plane is automatically fit through these points, representing the actual osteotomy. A similar approach is used by Weijs et al. [34]. They determined the actual osteotomy from the 2D axial slices. The osteotomy plane was indicated using 25 landmarks, which were used to calculate the resection plane with the least-square fitting principle. Other studies mostly determined the osteotomy based on the post-operative 3D models instead of the post-operative imaging [12, 16, 18, 21, 25, 30]. When establishing the osteotomy on 3D models, segmentation errors can influence the result. Consequently, determining the osteotomy plane directly from 2D slices may yield a more reliable result.
Brouwer de Koning et al. [12] performed a more automatic approach for point selection. One point was manually selected on the 3D resection surface, for which the outward-facing normal vector was calculated. All adjacent points were considered part of the resection surface if their normal vectors differed by no more than 10 degrees. The method may reduce the risk of manual errors but might again be highly influenced by segmentation errors.
Instead of automatically fitting a plane through selected points, Modabber et al. and Pu et al. [21, 25, 30] manually aligned a plane. The osteotomies are planned as a straight plane. During surgery the osteotomy is manually sawn, making it impossible to create a perfectly straight line. Thus, determining the actual osteotomy requires reaching a consensus. While Modabber et al. and Pu et al. [21, 25, 30] achieve this consensus manually, in this study, the consensus is automatically reached.

Distance deviation

The distance deviation of the resection osteotomies is measured by comparing the COMs of the actual and planned intersections. The intersections are taken between the pre-operative mandible model and the osteotomies. Assessing the osteotomy translation by comparing the deviation in the COM of the intersection, takes an average measurement. This is a proper approach when summarising a complex transformation into a distance deviation. Brouwer de Koning et al. [12], Schepers et al. [32] and yang et al. [35] also compared the distance deviation by the distance between the midpoint of the resection osteotomies.
To still maintain clinically valuable outcomes, the max distance is measured. This measurement combines an angular deviation with a distance deviation and is important when planning the resection osteotomies at a specific margin. Similar measurements were conducted by de Maesschalck et al. and Roser et al. [19, 31]. To our knowledge, no article in the literature presented the methodology used for assigning the direction of the osteotomy deviation in perspective to the tumour.

Due to the fibula bone's homogeneous shape and lack of landmarks, a different approach was necessary, compared to the distance deviation of the resection osteotomies. Since aligning the actual segment (with osteotomies) to the full pre-operative fibula bone was unfeasible, alignment was performed between the actual segment and the planned segment. However, this alignment is limited in determining the correct longitudinal position of the segment on the fibula. Therefore, the distance deviation of the reconstruction osteotomies is defined as the difference in fibular segment length. Most studies in the literature also measure the distance deviation of the reconstruction osteotomy by assessing the difference in fibular length [11, 26, 37].

These longitudinal displacements in the alignment will not affect the segment length difference and, therefore, will not influence the results. However, during surgery, the reconstruction PSC placement is often adjusted based on the perforator's location. As a result, the PSC can be positioned more proximally or distally along the fibula's length, creating a longitudinal deviation. While this deviation will not impact the segment length, these deviations are interesting factors for future research.

Angular deviation

Angular deviation of the resection osteotomies must be defined by two angular differences based on the saw slot, i.e. the angle across the saw slot (x-axis) and the angle through the saw slot (y-axis). These angles are both relevant when assessing the accuracy of angular deviation. In literature, most articles only present a singular angular deviation for the resection osteotomies [18, 23, 26, 34, 35]. Only Hanken et al. [23] and Moe et al. [26] clarified the method of the angle calculation, which can be compared to the x-axis deviation of this methodology [Chapter 3.1.5]. Brouwer de Koning et al. [12] and Bernstein et al.[16] calculated two angular measurements, but assessed the deviation in reference to anatomical axes. These anatomical axes are static while the osteotomy can vary in location and position throughout the mandible. Measuring the angle using this method will not provide a uniform deviation result. The result depends on the location of the osteotomy in relation to the static anatomical axis. In the developed method of this study, the angular deviation is determined in reference to the PSC slot/flange design (i.e. the orientation of the planned osteotomy).

The angular deviations of the reconstruction osteotomies are determined in an identical way to the angular deviation of the resection osteotomies. In the literature, the angle deviations are again mostly measured in one angle [11, 20, 23, 28, 29], resulting in similar limitations as for the resection osteotomies. Through registration, as proposed in the methodology, is the actual segment aligned to the planned segment, positioned in the pre-operative fibula model. The registration methodology is important for measuring the full deviation in the angular measurement. Goormans et al. [11] aligned the actual segment to the planned reconstruction, while other articles did not mention the specific registration methodologies used [20, 35].

3.3.2. Strengths, limitations and future research

Repeatability

To evaluate reproducibility, the observer variability of the actual osteotomy localisation was determined. The distance and angular deviation differed by an average of 0.3 mm and ≤2.2° for the intra-observer variability. The inter-observer variability was larger, with a distance deviation difference of 0.8 mm and an angular deviation of < 2.8°. As also indicated by ICC, the inter- and intra-observer agreement was excellent (> 0.87). However, when comparing the observer variations with the order of magnitude of distance and angular deviations, these variations are still of influence and even better reproducibility should be pursued.

Usability

The developed method remains time-consuming due to a series of manual steps. Further automation within the analysis would enhance user-friendliness and decrease the likelihood of manual errors. The challenge in enhancing automation primarily arises from the patient-specific nature of the 3D planning. The placement of osteotomy and the design of PSC are tailored and refined according to each patient's unique requirements. As a result, evaluation data varies due to patient-specific choices.
The registration algorithms in 3-Matic (Materialise NV, Leuven, Belgium) [53] demonstrate high quality and user-friendliness, ensuring the reliability and convenience of the registration process. While implementing similar functionalities in Python (python software foundation, Wilmington, Delaware, USA) is feasible, it must adhere to the same standards of quality and usability.

Outcome comprehensiveness

This evaluation guide focuses on the accuracy between planned and actual osteotomies in segmental mandible resection and reconstruction. The methodology measures inaccuracies arising during the translation from the virtual osteotomies to the actual osteotomies. The outcome measure cannot differentiate between errors caused by PSC misplacement or deviations caused by the direction of the saw through the slot or along the flange. Brouwer de Koning et al. [12] conducted an intra-operative CT scan to determine the position of the PSC, enabling differentiation between these two sources of deviation. Furthermore, an additional methodology should be developed to evaluate the deviation errors caused by fixating the segments.

3.4. Conclusion

The evaluation methodology offers complete guidelines for evaluating the accuracy of computer-assisted segmental mandibular resection and reconstruction by comparing the planned and actual osteotomies. It provides guides for gathering and creating the input data and conducting the osteotomy comparison.

4

Accuracy of computer-assisted surgery in segmental mandibular resection and reconstruction: Results of a single-center series

Abstract

Background Mandibular segment resection with subsequent reconstruction is often prepared using virtual surgical planning. Patient-specific cutting guides translate the planned resection and reconstruction of osteotomies into surgery. This study evaluates the accuracy of computer-assisted mandibular segment resection with fibular free flap reconstruction by comparing planned and actual osteotomies.

Method Sixteen patients were retrospectively included. Actual osteotomies were defined by a plane fitted through manually defined points on the post-operative imaging. The actual osteotomies were aligned to the pre-operative mandible or fibula model. Distance and angular deviation were measured between the planned and actual osteotomies. Resection osteotomy distance deviation was defined as the distance between the centre of mass of the actual and planned intersection of the pre-operative mandible model and the osteotomies. The maximum distance between the intersections was also measured. Reconstruction osteotomy distance deviation was defined as the length difference between the planned and actual fibula segments. Angular deviation of the resection and reconstruction osteotomies were defined by two angular differences based on the saw slot, i.e. the angle across the saw slot (x-axis) and the angle through the saw slot (y-axis).

Results For the resection osteotomies, the absolute average deviation was 2.1± 1.9 mm for the centre of mass and 3.1 ± 2.3 mm for the maximum distance. The fibular segments differed by 2.4 ± 2.5 mm in length. Angular deviations around the x-axis were 3.7 ± 3.4° for resection and 6.9 ± 7.1° for reconstruction osteotomies, and deviations around the y-axis were 5.7 ± 5.8°and 9.1 ± 11.4°, respectively.

Conclusion The difference in distance deviated was within an absolute average of 3 mm. The angular deviation was significantly larger for the reconstruction osteotomies compared to resection osteotomies, requiring further research.

4.1. Introduction

Patients who suffer from conditions such as osteomyelitis, osteoradionecrosis, or tumours affecting the mandibular bone may require a segmental mandibular resection as treatment. The surgical removal of the affected bone of resection leaves a discontinuity in the mandible, which requires reconstruction to restore functionality and aesthetics. Microvascular free fibula transfer (FFF) is a common method of reconstruction [3, 4]. This treatment remains one of the most challenging operations in head and neck surgery. Surgical accuracy, morphological results, and patient outcomes have significantly improved with the introduction of

computer-assisted surgery (CAS), compared to conventional methods [58–60]. CAS involves several steps, including analyzing pre-operative imaging data [61], creating 3D models, determining the location and orientation of the resection and reconstruction osteotomies, and designing patient-specific cutting guides (PSC). The PSC is used to transfer the virtual osteotomies to the actual surgery [61–63].

The accuracy of CAS is evaluated by comparing the planned resection and reconstruction to the post-operative results. The inaccuracies arise at different stages in the CAS process; the preoperative imaging, image segmentation, additive manufacturing, the surgery, and the evaluation of postoperative results [13]. These inaccuracies can be categorized into intentional and unintentional deviations. Intentional deviations may occur, if the tumour has grown significantly since the initial planning [9]. Unintentional deviations, on the other hand, arise from errors such as misplacement of the PSC, incorrect saw orientation within the PSC saw-slot, or imprecise fixation of graft segments, thereby deviating from the virtual surgical plan [64]. These unintentional deviations can affect the adequacy of tumour margins and the preservation of vital structures such as nerves. This may result in suboptimal reconstruction, leading to less favourable patient outcomes and prolonged surgical duration [12]. The literature reports deviations ranging between 0 mm and 12.5 mm and between 0.9° and 17.5° [13]. However, the heterogeneity in assessment methodologies across studies withholds inter-study comparisons and meta-analysis.

Chapter 3 introduces a novel methodology for reproducible and comprehensive accuracy analysis of CAS in segmental mandibular resection and reconstruction. This methodology depicts the assessment of distance and angular deviations between the planned and the actual executed osteotomies. Focusing on osteotomy deviation, the methodology offers the advantage of identifying deviations that arise during the translation of the virtual osteotomies to the actual surgery using the PSCs.

This study will retrospectively analyse the accuracy of CAS in segmental mandibular resection and reconstruction, by comparing the location and orientation of the planned osteotomy planes with the actual osteotomies using the novel method of Chapter 3.

4.2. Method

4.2.1. Patients

Patients who underwent a segmental mandibular resection with subsequent reconstruction between May 2020 and January 2024 at the Leiden University Medical Center, were retrospectively included. Inclusion criteria were: 1) The use of an in-house developed virtual surgical plan; 2) Availability of post-operative CT imaging on which the complete remnant mandible and reconstruction are depicted; 3) Reconstruction using a FFF approach.

All patients underwent a preoperative CT scan and MRI scan of the head and neck region along with a preoperative CT angiography (CTA) exam of the pelvic and legs. The same technical physician performed all virtual surgical plans. The preoperative scans were imported for segmentation in the medical 3D image-based engineering software program Mimics (Materialise NV, Leuven, Belgium) [52]. The resection osteotomies were determined in consultation with the oncology surgeon, taking into account oncological and functional considerations. Based on the resulting bone defect, the number of fibula segments and their respective length and orientation were determined. Subsequently, a resection PSC for the mandible, a reconstruction PSC for the fibula, and a reconstructed mandible model were designed. The PSCs directed the saw with either slots (6 mm height, 1 mm width, n=25) to cut through or with flanges to cut along (6 mm height, n=6). The osteotomies were made using a reciprocating or oscillating saw blade (3 - 5 mm blade width and 0.3 blade thickness) (B Braun Medical B.v., Melsungen, Germany). The planning and the design were performed using 3DSMax (Autodesk, San Rafael, California, USA) [65], Blender (Blender, Amsterdam, The Netherlands) [66] and 3-Matic (Materialise NV, Leuven, Belgium) [53] software. The PSCs were printed using Selective Laser Sintering technology with Polyamide 12 by the external company Oceanz (Oceanz, Ede, The Netherlands) [67]. During the operation, small fixation plates were manually bent according to the 3D-printed model of the reconstructed mandible.

4.2.2. Postoperative accuracy measurement

The methodology developed in Chapter 3 was used to evaluate the deviation between the virtually planned osteotomies and the actual performed osteotomies. Postoperative CT imaging was used to create 3D models of the postoperative reconstruction in Mimics (Materialise NV, Leuven, Belgium) [52] (Section 3.1.2).

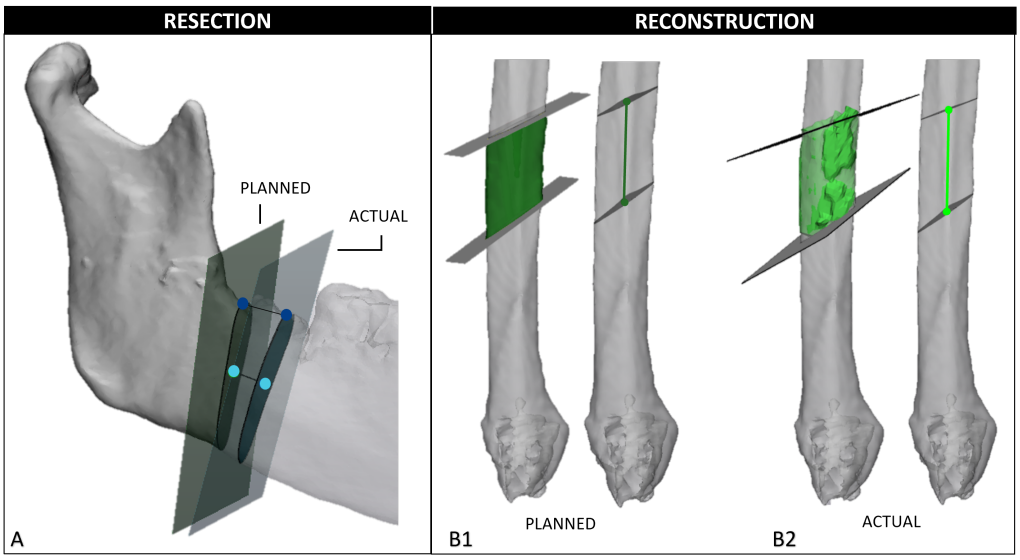

Figure 4.1: Distance deviation
Figure 4.1.A shows the distance deviation of the resection osteotomies. The figure shows the preoperatively planned resection plane of the right mandible and the actual resection plane of the right mandible in relation to the pre-operative mandible. The position of the actual osteotomy planes is determined by the registration of the actual right remnant mandible with the planned right remnant mandible. Intersections of both osteotomy planes (planned & actual) with the original mandible are taken. In light blue, the Euclidean distance between the centre of mass of these intersections is presented. In dark blue, the maximum distance is shown. **Figure 4.1.B** The distance deviation for the reconstruction osteotomies. The figure shows the preoperative fibula model with the planned fibula segment and osteotomies in 4.1.B1 and the aligned actual fibula segment with osteotomies in 4.1.B2 illustrates the measurements of the fibula segment length. Intersections are determined between the fibula model and the osteotomy planes. The Euclidean distance is defined between the centre of mass of the intersections. The actual fibula length is subtracted from the planned fibula length to obtain the length deviation.

A minimum threshold of 267 HU for CT and 400 for CBCT images was used for the segmentation of the neo-mandible. Individual models for the different fibula segments and remnant mandible were created and defined as the actual models. A plane is automatically fit through manually placed points adjacent to the ends of the bone segments on the post-operative imaging, representing the actual osteotomy (Section 3.1.2). For analysis, the actual models are aligned with the planned models (Section 3.1.3).

The accuracy of the resection osteotomy planes was determined by comparing the planned osteotomy with the actual osteotomy made in the mandible. To measure accuracy, the following parameters were computed: the distance between the COMs, the maximum distance (Section 3.1.4) and the angular deviation (Section 3.1.5). The COM and the maximum distance are measured on intersections created between the planned/actual osteotomy and the pre-operative mandible model, see Figure 4.1.A. Angular deviation of the resection and reconstruction osteotomies were defined by two angular differences based on the saw slot or flange (Section 3.1.5), i.e. the angle across the saw slot (x-axis) and the angle through the saw slot (y-axis), see Figure 4.2a.A.

The accuracy of the reconstruction osteotomy planes was determined by comparing the planned osteotomy with the actual osteotomy made in the fibula. Translation of the osteotomy was measured by comparing the planned and actual fibular segment length (Section 3.1.4), see Figure 4.1.B. The angular deviation (Section 3.1.5) was defined by similar angles as for the resection osteotomies, see Figure 4.2b.

4.2.3. Statistics

The deviation between planned and actual osteotomies was statistically evaluated. The averages and standard deviations were calculated from all measurements. Outcomes were subdivided into comparison groups. The effect of resection osteotomy location was analysed based on the deviation difference between anterior and posterior osteotomies. Furthermore, the influence of PSC types (flanges vs. slots) was examined per osteotomy. Lastly, the angular deviations between resection and reconstruction osteotomies were compared. The normality of the data was determined using the Shapiro-Wilk test. Depending on the outcome, an independent two-sample t-test was used for parametric data and the Mann-Whitney U test

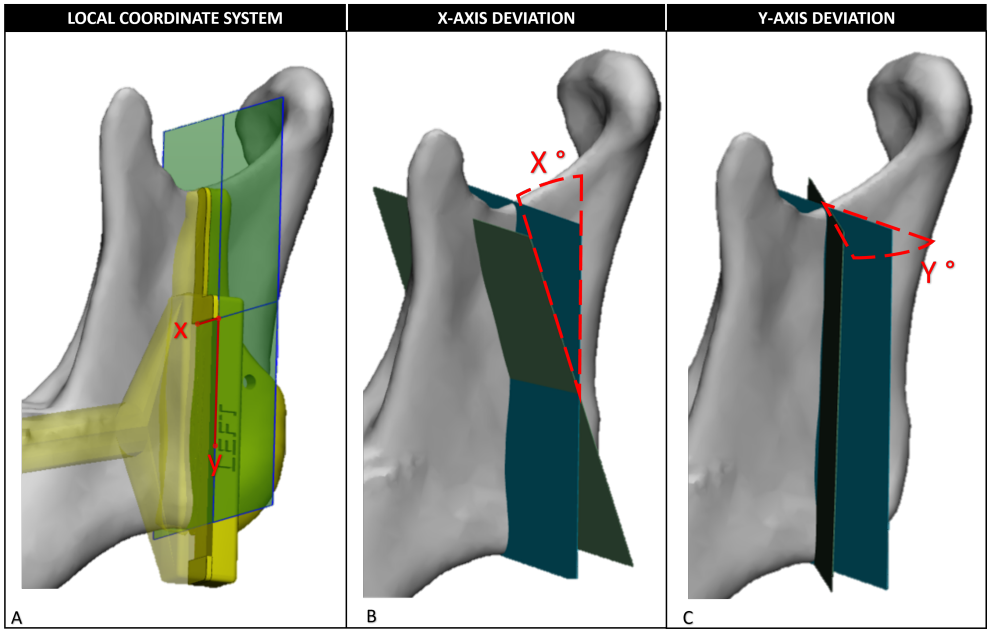

(a) Angular difference resection osteotomy

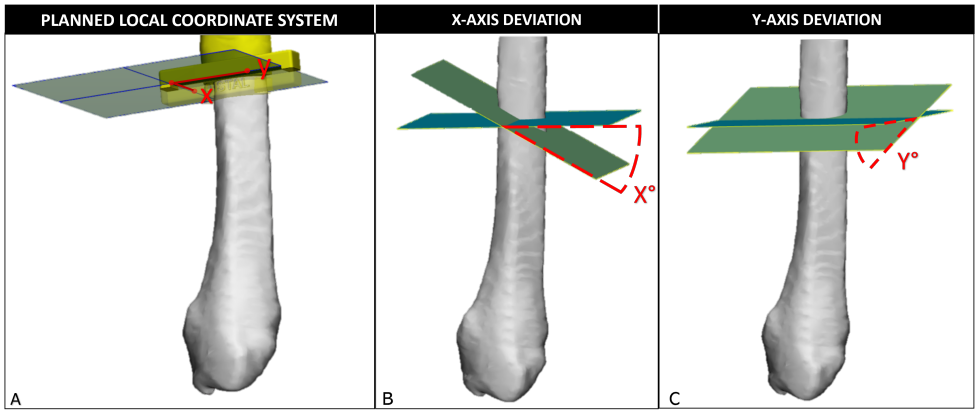

(b) Angular difference reconstruction osteotomy

Figure 4.2: Angular measurement
The angular deviation is determined using the same method for both resection and reconstruction osteotomies. **Figures 4.2a.A** and **4.2b.A** show how the direction of the angular deviation is determined based on the PSC. The x-axis is defined by the height of the PSC slot, and the y-axis is defined by the length of the PSC slot. **Figures 4.2a.B** and **4.2b.B** provide an example of deviation around the x-axis, resembling the angular deviation across the saw slot. Similarly,**Figures 4.2a.C** and **4.2b.C** show the deviation around the y-axis, resembling the angular deviation through the saw slot.

Table 4.1: Patient characteristics

Patient ID	Age	Sex	Indication for surgery	Staging	Resected side	Reconstruction type*	Donor side	# Fib segments	Condyle preservation	Resection guide type	Reconstruction guide type
Pt001	76	M	SCC	pT4aN1M0	Left	Class IV	Left	2	Yes	Slots	Slots
Pt002	53	F	SCC	pT4aN0M1	Left	Class II	Right	2	Yes	Slots	Slots
Pt003	51	M	SCC	T4bN2bM0	Right	Class I	Left	2	Yes	Slots	Slots
Pt004	61	F	SCC	T4N2bM0	Both	Class IV	Right	3	Yes	Slots	Slots
Pt005	22	M	AC	Unknow	Right	Class IV	Left	2	No	slots	Slots
Pt006	67	F	SCC	T4N0M0	Right	Class IV	Left	2	Yes	Slots	Slots
Pt007	60	M	SCC	T4bN2bM0	Right	Class I	Right	2	Yes	Flanges (R) & Slot (L)	Slots
Pt008	71	M	PF	n/a	Right	Class I	Left	1	Yes	Slots	Slots
Pt009	67	M	ERS	T4aN0M0	Both	Class IV	Left	3	Yes	Slots	Slots
Pt010	77	M	AC	Unknow	Right	Class II	Left	2	Yes	Slots	Slots
Pt011	37	M	SCC	T4aN0M0	Right	Class II	Left	2	yes	Flanges	Slots
Pt012	57	M	SCC	pT1N0M0	Right	Class I	Left	1	Yes	Slots	Slots
Pt013	63	M	SCC	cT4aN0M0	Left	Class III	Right	2	Yes	Slots	Slots
Pt014	66	F	SCC	cT4bN0M0	Left	Class II	Right	2	Yes	Flanges (L) & Slot (R)	Slots
Pt015	63	M	SCC	cT4aN0M0	Left	Class I	Right	1	Yes	Slots	Slots
Pt016	58	M	SCC	T4aN0M0	Right	Class I	Left	1	Yes	Flanges	Slots

* The type of reconstruction was determined using the Brown et al. classification system [68].
Abbreviations: AB: Ameloblastoma, ERS: Epithelioid rhabdomyosarcoma, L: Left, PF: Pathological Fracture, R: Right, SCC: Squamous Cell Carcinoma.

was conducted for non-parametric data. For each test statistical significance was set at $P < 0.05$.

4.3. Results

A total of 17 cases involving segmental mandibular resection with reconstruction were included. One patient was later excluded as no reliable actual osteotomies could be localised on the post-operative imaging, which may be due to the long time interval between the operation and the scan (1104 days).

Patient characteristics are shown in Table 4.1. The male/female distribution is 12/4, and the average age at reconstruction is 59 years (range, 22 – 77 years). The primary indication for reconstruction was tumour resection (n = 16); the other indication was a pathological fracture caused by osteoradionecrosis (n=1). The reconstruction types were class I (n=6), class II (n=4), class III (n=1), and class IV (N=5). The pre-operative CT scans were acquired on a Siemens Somatom Drive (slice thickness 1.0 mm, pixel spacing 0.74–0.77mm × 0.74–0.77mm, 70-100 kVp), a Canon Medical Systems Aquilion One (slice thickness 0.5-1.0 mm, pixel spacing 0.43–0.93mm × 0.43–0.93mm, 100-120 kVp) or a Planmeca Promax (slice thickness 0.4 mm, pixel spacing 0.40-0.40mm × 0.40-0.40mm, 96 kVp). The post-operative imaging characteristics are presented in Table 4.2. The post-operative scans CT scans (n=13) were acquired on a Canon Medical Systems Aquilion One (slice thickness 0.5-1.0 mm, pixel spacing 0.53–0.63 mm × 0.53–0.6 3mm, 120 kVp), a Philips Vereos PET/CT (slice thickness 1.0 mm, pixel spacing 0.63-0.66 mm × 0.63-0.66 mm, 120 kVp) or a Philips Brilliance Big Bore (slice thickness 2.0 mm, pixel spacing 1.0-1.08 mm × 1.0-1.08 mm, 120 kVp). The post-operative scans CBCT scans (n=13) were acquired on a Planmeca ProMax (slice thickness 0.4 mm, pixel spacing 0.40 mm x 0.40 mm, 96 kVp). The average time interval between operation and postoperative imaging was 134 days (range, 8 – 386 days).

4.3.1. Post operative accuracy

An overview of all results is shown in Table 4.3.

Distance Deviation

The average deviation of the COM of the resection planes was 2.1 $\pm$ 1.9 mm (range, 0.1 - 8.3 mm). The maximum deviation was 3.1 $\pm$ 2.3 mm (range, 0.2 - 12.2 mm). In 13/31 (41.9%) resection osteotomies, less mandibular bone was resected, decreasing the planned tumour margin. Figure 4.3a shows a box plot of the deviation in the resection osteotomies' centre of mass (COM) and maximum deviations. Negative values represent deviations where less mandible tissue is resected, placing the osteotomy closer to the tumour. Positive values represent deviations where more mandible tissue is resected, moving the osteotomy further away from the tumour. One notable outlier was observed, with a COM deviation of -8.3 mm and a maximum deviation of -12.2 mm. Appendix E.1 presents a table with the distance deviations of the resec-

Table 4.2: Post-operative imaging characteristics

Patient ID	Time till post-op imaging (days)	Post-op Imaging Modality	Slice Thickness [mm]	Pixel spacing [mm]	kVp	Manufacturer	Model name
Pt001	308	CT	0.5	0.53/0.53	120	Canon Medical Systems	Aquilion One
Pt002	174	CT	1.0	0.63/0.63	120	Canon Medical Systems	Aquilion One
Pt003	386	CBCT	0.4	0.40/0.40	96	Planmeca	ProMax
Pt004	9	CTA	0.5	0.60/0.60	120	Canon Medical Systems	Aquilion One
Pt005	8	CT	0.5	0.52/0.52	120	Canon Medical Systems	Aquilion One
Pt006	134	CT	1.0	0.66/ 0.66	120	Philips	Vereos PET/CT
Pt007	33	CT	2.0	1.08/1.08	120	Philips	Brilliance Big Bore
Pt008	8	CBCT	0.4	0.40/0.40	96	Planmeca	ProMax
Pt009	49	CT	2.0	1.14/1.14	120	Philips	Brilliance Big Bore
Pt010	42	CBCT	0.4	0.40/0.40	96	Planmeca	ProMax
Pt011	36	CT	2.0	1.02/1.02	120	Philips	Brilliance Big Bore
Pt012	261	CT	0.5	0.63/0.63	120	Canon Medical Systems	Aquilion One
Pt013	383	CT	2.0	1.03/1.03	120	Philips	Brilliance Big Bore
Pt014	35	CT	2.0	1.0/1.0	120	Philips	Brilliance Big Bore
Pt015	36	CT	0.2	0.63/0.63	120	Canon Medical Systems	Aquilion One
Pt016	236	CT	1.0	0.63/0.63	120	Philips	Vereos PET/CT

Abbreviations: CBCT: cone-beam computed tomography, CT: computed tomography, kVp: Kilovoltage peak

Table 4.3: General results

	Distance			Angle			
	Resection		Reconstruction	Resection		Reconstruction	
	COM (mm)	Max (mm)	Seg Length (mm)	x-Axis °	y-Axis °	x-Axis °	y-Axis °
Absolute Average	2.1	3.1	2.4	3.7	5.7	6.8	9.1
STD	1.9	2.3	2.5	3.4	5.8	7.1	11.4
Absolute Min	0.1	0.3	0.4	0.1	0.3	0.0	0.6
Absolute Max	8.3	12.2	12.0	17.5	24.5	38.2	52.9

Abbreviations: COM: centre of Mass, Max: Maximum, Min: Minimum, Seg: Segments

tion osteotomies per patient.
Thirty fibular segments were evaluated, ranging between 1, 2, or 3 segments per reconstruction, see Table 4.1. The absolute average deviation in fibular segment length was 2.4 $\pm$ 2.5 mm (range, -9.6 - 12.0 mm). Twelve of the thirty (40%) segments were shorter than planned. The data is shown in the box plot of Figure 4.3b. The two outliers came from two different patients. The first outlier showed an actual segment that is 12.0 mm shorter than the planned segment. The other segment of this reconstruction is in line with the average, with a deviation of -1.1 mm. The other outlier shows a segment which was 9.6 mm longer than planned. The deviations of the other segments of this reconstruction were -2.4 mm and -3.6 mm. Appendix E.2 presents a table with the distance deviations of the reconstruction osteotomies per patient.

Angular deviation

The average angular deviation of the resection osteotomy was 3.7 ± 3.4° (range, 0.1-17.5°) for the x-axis and 5.7 ± 5.8° (range, 0.3 - 24.5°) for the y-axis. For the reconstruction osteotomy, the deviation was 6.8 ± 7.1°(range, 0.0 - 38.2°) for the x-axis and 9.1 ± 11.5° (range,0.6 - 52.9°) for the y-axis. All data was non-parametric. A significant difference was observed between the resection and reconstruction deviation in the x direction (p= 0.02); however, this was not observed in the y direction (p= 0.19). A box plot of the data can be seen in Figure 4.3c. The reconstruction angular deviation outcomes have larger values and more outliers than the resection angular deviation. Appendices E.3 and E.4 present a table with the angular deviations per patient.

Anterior and posterior resection osteotomies

The deviations in the COM distance for anterior and posterior osteotomies were 2.2 ± 2.1 and 1.9 ± 1.7 mm, respectively. The deviation in the maximum distance for anterior and posterior osteotomies were 3.4 ± 2.8 and 2.8 ± 1.9 mm, respectively. The angular deviation around the x-axis was 3.9 ± 3.9° for the anterior osteotomies and 3.4 ± 2.8° for the posterior osteotomies. The angular deviation around the y-axis was 5.5 ± 6.3° for the anterior osteotomies and 5.9 ± 5.4° for the posterior osteotomies. All data was non-parametric. No significant difference was observed between the anterior and posterior osteotomies in all four measurements.

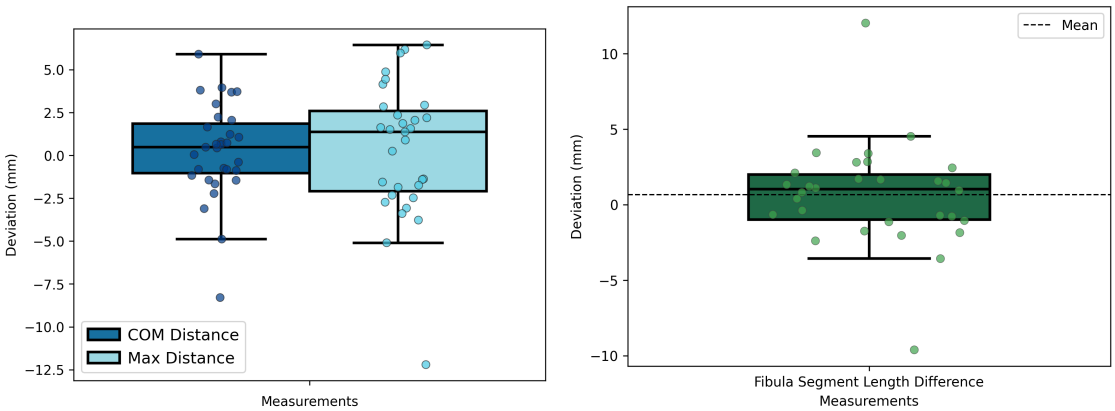

(a) Deviation in COM and MAX

(b) Difference in fibula segment length

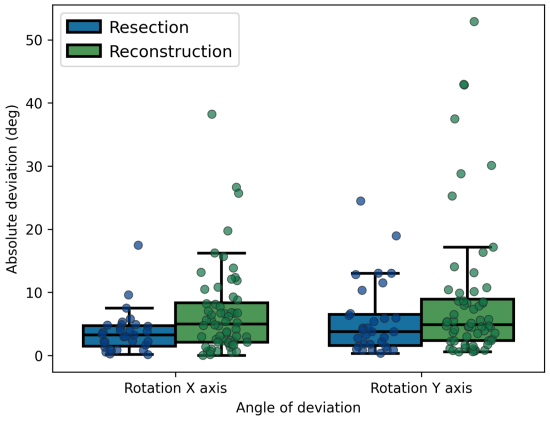

(c) Angular deviation (°) in the x and y axis

Figure 4.3: Boxplots

Figure 4.3a shows the distance deviation between the centre of mass of the intersections in light blue. The maximum distance deviation is presented in dark blue. The values are positive(+)/negative(-) representing more/less mandible resected compared to the planning. **Figure 4.3b** shows the difference in length between the planned fibula segment and the actual fibula segment. Negative values represent the segments that are actually shorter than planned, and positive values represent segments that are longer than planned. **Figure 4.3c** shows the difference in orientation between the planned and the actual osteotomy plane in the X and Y axis for the resection and reconstruction osteotomy.

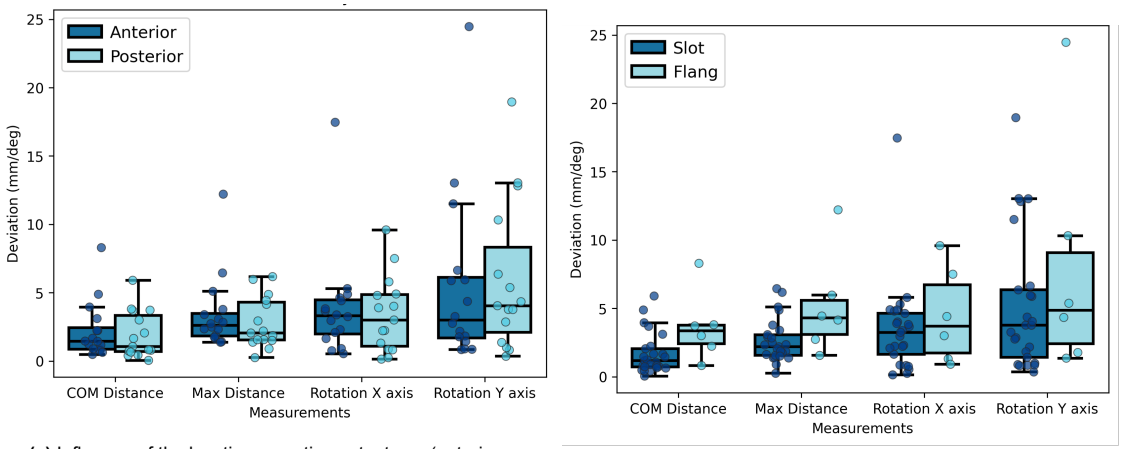

(a) Influence of the location resection osteotomy (anterior vs posterior)

(b) Influence of the resection guide design

Figure 4.4: Boxplots

Figure 4.4a shows the difference in all measurements subcategorised into the anterior and posterior osteotomy location. **Figure 4.4b** shows the difference in all measurements subcategorised into the type of resection PSC. The difference is made between saw slots and flanges.

Cutting guide design

The discrepancies in the absolute average of COM distance for slots and flanges resection guides were 1.7 ± 1.5 and 3.6 ± 2.5 mm, respectively. For the maximum distance, the absolute average for slots was 2.6 ± 1.6 mm and for flanges 5.2 ± 3.8 mm. Similar to the distance deviation, is the angular accuracy of the flanges lower. An angular deviation in the x-axis for the slots and flanges being 3.5 ± 3.4° and 4.5 ± 3.5°, and a deviation in the y-axis being 5.2 ± 4.9° and 7.9 ± 8.7°, respectively. The sample size of the flanges was too small (n=6) to perform a statistical analysis.

4.4. Discussion

This study performed a novel accuracy assessment method to evaluate the deviation between planned osteotomies and actually executed osteotomies in segmental mandibular resection and reconstruction. The methodology focuses on distance and angular deviations between planned and actual osteotomies. The study showed an absolute average deviation of 2.1 ± 1.9 mm for the COM and 3.1 ± 2.3 mm for the maximum distance for resection osteotomies. Additionally, the deviation in fibular segment length was 2.4 ± 2.5 mm. The average angular deviations around the y-axis were 5.7 ± 5.8° for resection and 9.1 ± 11.4° for reconstruction osteotomies. Deviations around the x-axis were 3.7 ± 3.4° and 6.9 ± 7.1°, respectively. There is a lack of standardization within the evaluation of CAS, resulting in various methods used in the literature. Consequently, a comparison between this study and the literature is only limitedly possible.

Distance deviation

The COM distance of the reconstruction osteotomies deviated with an absolute average of 2.1 ± 1.9 mm. The deviation was larger than the 1 mm width of the slot of the PSCs. The distance deviation is, therefore, also caused by other factors like misplacement of the PSC or incorrect angulation of the saw during osteotomy creation. Brouwer de Koning et al. [12], Scherpers et al. [32] and yang et al. [35] measured resection distance deviation with a similar methodology by calculating the distance between a midpoint of the intersections. They measured the following deviations: 1.3 ± 0.9 mm [12], 2.0 ± 1.3 mm [32] and 3.2 ± 1.3 mm [35], respectively. These results are in line with the results measured in this study.

The results showed a maximum absolute average deviation of 3.1 ± 2.3 mm, cutting into the margins. High accuracy is important in mandibular resection to avoid vital structures like nerves and ensure complete tumour removal with an adequate margin. A general margin of at least 10 mm is used to plan the resection osteotomies. The patient with the largest maximum deviation of -12.02 mm was the only patient whose tumour margin was completely exceeded. For this particular patient, two virtual plans were created pre-operatively. The first plan involved a smaller resection, but the frozen section pathology performed intra-operatively showed a positive anterior margin. As a result, the second plan for a larger resection was carried out, for which the margin was clean. During the post-operative evaluation, it was discovered that while using the resection guides from the second plan; the resection osteotomy was still positioned as close to the tumour as planned in the first plan. The design of the PSC may have contributed to this deviation. The PSC was designed with flanges without a connecting arch. The absence of a connecting arch halves the total support surface of the PSC, thereby diminishing the uniqueness and stability of the PSC fit. Furthermore, a flange was used instead of a slot. The flange only guides the saw on one side, potentially leading to larger deviations as saw position and tilting are unrestricted, see Figure 4.5.A/B. De Maesschalck et al. [19] and Roser et al. [31] measured the maximum distance between the planned resection osteotomy and the actual remnant model. They measured a maximum deviation of 2.3 ± 1.0 mm and 2.0 ± 1.12 mm. As indicated in Section 3.3, this measuring method can be influenced by segmentation errors.

The segment length deviation was 2.3 ± 2.6 mm (range, -9.6 - 12.0 mm). Goormans et al. [11] measured the fibula segment length deviation based on three anatomical measurements: the outer upper margin, the outer lower margin, and the inner median margin deviations. The average segment length deviation was 1.74 mm (range, 0.02 – 6.10 mm). Hanken et al. [23] performed a similar methodology to Goormans et al. [11] and measured an average length difference of −0.12 mm (95 %CI (−0.89 – 0.65 mm)).

Angular deviation

The average angular deviation along the x-axis was 3.7 ± 3.4° (range, 0.1 - 17.5°) for the resection osteotomies and 6.8 ± 7.1° (range, 0.0 - 38.2°) for the reconstruction osteotomies. The average angular deviation along the y-axis was 5.7 ± 5.8° (range, 0.3 - 24.5°) for the resection osteotomies and 9.1 ± 11.5°

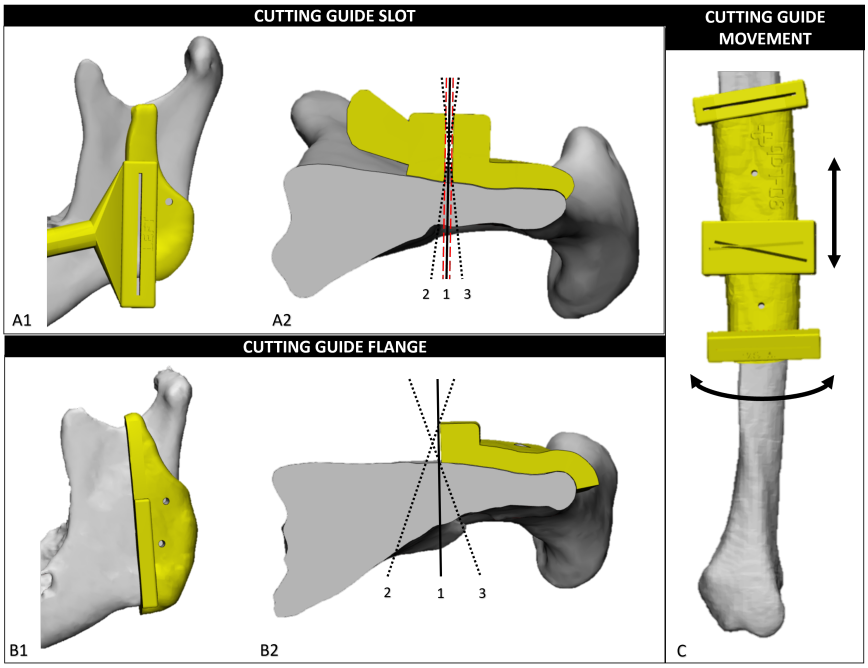

Figure 4.5: Deviation caused by the cutting guide
Figure 4.5.A/B Shows a PSC design with a slot and flange, respectively. Line 1 represents the ideal cutting line designed in the virtual surgery, line 2 and 3 represent the maximum possible angular deviation in the x-axis. More angular deviation is possible when using a flange. The red line shows the maximum distance deviation for the slot design. **Figure 4.5.C** illustrates the movement possibilities of the resection PSC. The fibula has a cylindrical shape, resulting in possible errors in positioning the guide by placing it either too distal, too proximal or circumferentially around the fibula. Similarly, some degree of positional errors can also be observed with the resection guide.

(range, 0.6 - 52.9°) for the reconstruction osteotomies. Angular deviation arising from saw orientation in the PSC slot depends on the width of the saw blade for the x-axis deviation and the thickness of the saw blade for the y-axis deviation. In this study, a minimum saw blade width of 3 mm was used, yielding a maximum x-axis angular deviation of 13.7° in a slot with a 1 mm width. The thickness of the saw blade was 0.3 mm, resulting in a maximum y-axis angular deviation of 6.5° for a slot with a 1 mm width and a 6 mm height. The results did contain values that were larger than these maximum values. This may be caused by the saw cutting through the material of the PSC or by misplacement of the PSC. These maximum values do not apply for PSCs designed with a flange for reasons similar to those stated above.

Brouwer de Koning et al. [12] measured the angular deviation of the resection osteotomies in two angles: the angle along the cranial-caudal axis (yaw) and the angle along the lateral-medial axis (pitch). With this methodology, the orientation and location of the osteotomies influence the results. Osteotomies that are located medial and in a straight line with the cranial-caudal and lateral-medial axes, resembled the outcomes from this research. The pitch will be comparable to the x-axis deviation, and the yaw will be comparable to the y-axis deviation. The pitch deviation found was 3.1 ± 1.5°, and the yaw deviation found was 7.0 ± 6.4°, which are both in line with the resection angular deviation found in this study.

A significant difference was observed between the resection and reconstruction angular deviation, possibly due to the accuracy of positioning a PSC on the fibula compared to the mandible. The mandible is a distinct structure where accurate positioning and orientation of the resection guide are important. While reconstruction osteotomies do not require consideration of tumour removal or avoidance of vital structures, surgeons must adjust the placement of the PSC to the position of the perforator. Consequently, the PSC may be positioned more proximal or distal along the length of the fibula. The PSC can also be placed in a different circumferential position due to the cylindrical shape of the bone, as illustrated in Figure 4.5.C. Although the changes in PSC position will not impact the length of the fibula segment, it will cause the osteotomy to be oriented differently compared to the fibula and, thus, the planned reconstruction osteotomies. This results in a different cross-section of the fibular segment end, leading to sub-optimal reconstruction.

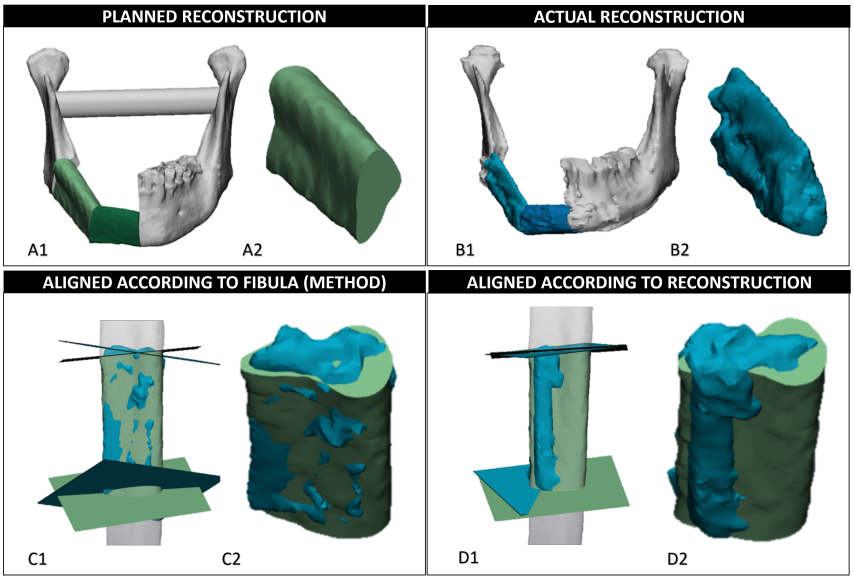

Figure 4.6: Segment rotation along the length of the fibula
The Figure shows the effect of a circumferential rotation of reconstruction PSC. The planned fibular segments and osteotomies are presented in green, and the actual fibular segments and osteotomies are in blue. **Figure 4.6.A** shows the planned reconstruction with the planned bone-cut surface of the right fibular segment in A2. **Figure 4.6.B** shows the actual reconstruction with the actual bone-cut surface of the right fibular segment in B2. Based on the fibula shape, it can be concluded that the right fibular segment is rotated around its longitudinal axis. **Figure 4.6.C** shows the osteotomy deviation according to the method employed in this study, where the actual fibula segment (blue) is aligned based on its shape, see C2. In **Figure 4.6.D**, the alignment is based on the position of the actual fibula segment in the reconstruction. Although there is no match between the shape of the planned and actual fibula segment, the osteotomy angular deviation is smaller. This suggests that there may have been some rotation of the reconstructive PSC.

These PSC positional deviations could account for the outliers in reconstruction data of angular deviation, especially when considering the methodology employed. According to accuracy assessment methodology [Section: 3.1.5], the fibular osteotomy angle deviation was measured based on the planned position of the reconstructive PSC on the pre-operative fibula model. For the measurement, the actual fibula segment was aligned to the pre-operative fibula based on its shape, see Figure 4.6.C. A difference in circumferential position will result in a (large) deviation of the angles, mainly unrelated to the saw deviation within the PSC slot. If angular measurements of the fibula segments were taken in the context of its position in post-operative reconstruction, deviation of the PSC position in the circumferential position is neglected, see Figure 4.6.B. This leads to smaller angular deviations but an incomplete measurement of osteotomy accuracy, see Figure 4.6.D. The circumferential position of the PSC on the fibula is important as the specific fibular bone-cut intersection surfaces are used in the planning for optimal surface alignment between segments. The accuracy assessment method used in this study offers a comprehensive analysis of osteotomies, aligning with the study's objectives. The results, however, should be interpreted with care as large angular deviations in fibula segments may not directly affect the final reconstruction outcomes to the same degree. Goormans et al. [11] calculated the osteotomy angle deviation for each fibula segment by comparing an angular measurement taken on the planned and actual segment. The angular measurement was obtained by measuring the angle between a plane on the lateral side and a plane on the outer side (the cut side). The average angular deviation of osteotomy planes was 1.98° (range 0.04 – 5.86°). This measurement is most comparable to the y-axis results of this study, which was 9.1 ± 11.4°. Reasons for this difference might correspond to the different assessment methodology used by Goormans et al. [11]. It measured the angular deviation based on the position of the fibular segment in the final reconstruction, as explained above. Hanken et al. [23] measured the angular deviation of the angular deviation of the resection osteotomies by an angle defined in a plane orthogonal to the planned intersection direction. This outcome is most comparable with the x-axis angular deviation. The method of registration was undefined. A deviation of 10.81° (95% CI (9.44°–12.17°)) was measured. These results were slightly larger than the x-axis angular deviation of the resection osteotomies of 6.8 ± 7.1°, measured in this study.

Anterior and posterior resection osteotomies

When comparing anterior and posterior resection osteotomies, a higher deviation was observed in the anterior osteotomies for both the COM and maximum distances. The outcomes did not differ significantly. This result was unexpected as a greater deviation in more posterior osteotomies was anticipated due to reduced surgical freedom when deeper into the patient's anatomy. Brouwer de Koning et al. [12], however, showed a difference of 0.9 ± 0.5 mm anterior compared to 2.0 ± 1.0 mm posterior.

4.4.1. Strengths and weaknesses

The methodology used in this study is designed to produce comprehensive and reproducible results. By analysing the deviation between planned and actual osteotomies, a more focused analysis of specific deviations within osteotomies can be achieved. Enabling a deeper understanding of their origins. To ensure clinical relevance, the assessment included measuring the maximum distance to integrate both distance and angular aspects. This parameter is essential for tumour margin planning and protecting vital structures such as nerves.

This retrospective study has several limitations. Firstly, the results should be interpreted cautiously, as the sample size of 16 patients was relatively small. Secondly, CT and CBCT are both included as post-operative imaging modalities. A CBCT is more sensitive to metal materials, causing image artefacts. These artefacts influence the segmentation, which is important for model registration. Manually altering is used to improve inaccurate segmentation, which maintains the quality of the results. Thicker slices can also influence the segmentation and actual osteotomy localisation. There was a large variation in the time interval of the post-operative imaging after surgery (8-386 days). Over time, the chance of bone segment shifting, consolidation, and resorption increases [54]. Due to the retrospective nature of this study, consolidation and resorption may influence the determination of the actual osteotomies.

Lastly, the fit and the surgical compliance to the PSC are highly important for identifying the reasons for inaccuracy, specifically in outliers. Due to the retrospective nature of this study, information about the intra-operative usage of the PSC depends on the comprehensiveness of the post-surgical reports. Specific details on the usage of the PSC were only provided in limited patient cases.

4.4.2. Future research

Future comparative studies with the proposed standardized methodology of Chapter 3 must be performed to facilitate valid comparisons and strengthen the scientific conclusions of the results. In addition to researching the accuracy of osteotomy planes, researchers should investigate other factors that may cause inaccuracies, such as the positional relationship between segments after fixation of the reconstruction. An overview analysis would be of value to draw relations and provide a total evaluation of the accuracy. Furthermore, prospective comparative studies could diminish current limitations by creating an objective study outline. The prospective approach facilitates further clarification of the underlying cause of the observed errors. This will enhance the understanding of intra-operative execution of the virtual plan by expanding the surgical report on the usages of the PSC and the creation of the osteotomies. Brouwer de Koning et al. [12] conducted intraoperative CT scans to research the position of the PSC to be able to differentiate between positional PSC and saw errors. Lastly, to our knowledge, no studies have yet been performed evaluating the required level of accuracy, which would still affect patient outcomes. The level of sufficient accuracy is currently constituted by outcomes of other studies performed with different methods and logical reasoning. A scientifically grounded understanding of the requisite accuracy level is necessary to guide innovation and evaluate institutional accuracy outcomes properly.

4.5. Conclusion

Deviations were found between the location and orientation of the planned and actual osteotomy planes. The difference in distance deviation was within an absolute average of 3 mm. Both the distance and angular deviation measurements surpassed the maximum deviation constrained by the PSC slot, indicating that inaccuracies also arise from other origins. The angular deviation was significantly larger for the reconstruction osteotomies compared to the resection osteotomies, requiring further research.

References

[1] Batchu Pavan Kumar et al. “Mandibular reconstruction: overview”. In: *Journal of maxillofacial and oral surgery* 15 (2016), pp. 425–441.

[2] SN Rogers et al. “Health-related quality of life and clinical function after primary surgery for oral cancer”. In: *British Journal of Oral and Maxillofacial Surgery* 40.1 (2002), pp. 11–18.

[3] Devin Okay et al. “Worldwide 10-year systematic review of treatment trends in fibula free flap for mandibular reconstruction”. In: *Journal of Oral and Maxillofacial Surgery* 74.12 (2016), pp. 2526–2531.

[4] Richard E Hayden, David P Mullin, and Andrew K Patel. “Reconstruction of the segmental mandibular defect: current state of the art”. In: *Current opinion in otolaryngology & head and neck surgery* 20.4 (2012), pp. 231–236.

[5] Arun Chandu, Andrew C.H. Smith, and Simon N. Rogers. “Health-Related Quality of Life in Oral Cancer: A Review”. In: *Journal of Oral and Maxillofacial Surgery* 64.3 (2006), pp. 495–502. ISSN: 0278-2391. DOI: https://doi.org/10.1016/j.joms.2005.11.028. URL: https://www.sciencedirect.com/science/article/pii/S0278239105018355.

[6] Haye H Glas, Nathalie Vosselman, and Sebastiaan AHJ de Visscher. “The use of 3D virtual surgical planning and computer aided design in reconstruction of maxillary surgical defects”. In: *Current opinion in otolaryngology & head and neck surgery* 28.2 (2020), pp. 122–128.

[7] Wolfgang Bähr. “Blood supply of small fibula segments: An experimental study on human cadavers”. In: *Journal of Cranio-Maxillofacial Surgery* 26.3 (1998), pp. 148–152.

[8] Frank Wilde et al. “Multicenter study on the use of patient-specific CAD/CAM reconstruction plates for mandibular reconstruction”. In: *International journal of computer assisted radiology and surgery* 10 (2015), pp. 2035–2051.

[9] Hongyang Ma et al. “Adherence to computer-assisted surgical planning in 136 maxillofacial reconstructions”. In: *Frontiers in Oncology* 11 (2021), p. 713606.

[10] Omar Suhaym, Loren Moles, and Nicholas Callahan. “Cutting guides in mandibular tumor ablation: Are we as accurate as we think?” In: *The Saudi Dental Journal* 36.2 (2024), pp. 340–346.

[11] Femke Goormans et al. “Accuracy of computer-assisted mandibular reconstructions with free fibula flap: Results of a single-center series”. In: *Oral oncology* 97 (2019), pp. 69–75.

[12] SG Brouwer de Koning et al. “Evaluating the accuracy of resection planes in mandibular surgery using a preoperative, intraoperative, and postoperative approach”. In: *International Journal of Oral and Maxillofacial Surgery* 50.3 (2021), pp. 287–293.

[13] Gustaaf JC van Baar et al. “Accuracy of computer-assisted surgery in mandibular reconstruction: a systematic review”. In: *Oral oncology* 84 (2018), pp. 52–60.

[14] Gustaaf J.C. van Baar et al. “Accuracy of computer-assisted surgery in mandibular reconstruction: A postoperative evaluation guideline”. In: *Oral Oncology* 88 (2019), pp. 1–8. DOI: https://doi.org/10.1016/j.oraloncology.2018.11.013. URL: https://www.sciencedirect.com/science/article/pii/S1368837518304226.

[15] Lisa Arkes et al. “Methodology for Assessing Osteotomy Accuracy in Computer-Assisted Mandible and Maxilla Resection and Reconstruction: A Comparative Review”. In: (2023).

[16] Jonathan M Bernstein et al. “Accuracy and reproducibility of virtual cutting guides and 3D-navigation for osteotomies of the mandible and maxilla”. In: *PLoS One* 12.3 (2017), e0173111.

[17] Albert H Chao et al. “Pre-programmed robotic osteotomies for fibula free flap mandible reconstruction: a preclinical investigation”. In: *Microsurgery* 36.3 (2016), pp. 246–249.

[18] Jie Chen et al. “Deviation analyses of computer-assisted, template-guided mandibular reconstruction with combined osteotomy and reconstruction pre-shaped plate position technology: a comparative study”. In: *Frontiers in Oncology* 11 (2021), p. 719466.

[19] Thibault De Maesschalck, Delphine S Courvoisier, and Paolo Scolozzi. “Computer-assisted versus traditional freehand technique in fibular free flap mandibular reconstruction: a morphological comparative study”. In: *European Archives of Oto-Rhino-Laryngology* 274 (2017), pp. 517–526.

[20] Marie de Boutray et al. “Robot-guided osteotomy in fibula free flap mandibular reconstruction: a preclinical study”. In: *International Journal of Oral and Maxillofacial Surgery* (2023).

[21] Yan Guo et al. “Design and implementation of a surgical planning system for robotic assisted mandible reconstruction with fibula free flap”. In: *International Journal of Computer Assisted Radiology and Surgery* 17.12 (2022), pp. 2291–2303.

[22] Matthew M Hanasono and Roman J Skoracki. “Computer-assisted design and rapid prototype modeling in microvascular mandible reconstruction”. In: *The laryngoscope* 123.3 (2013), pp. 597–604.

[23] Henning Hanken et al. “Virtual planning of complex head and neck reconstruction results in satisfactory match between real outcomes and virtual models”. In: *Clinical oral investigations* 19 (2015), pp. 647–656.

[24] Mingming Lv et al. “Sequential application of novel guiding plate system for accurate transoral mandibular reconstruction”. In: *Oral Oncology* 111 (2020), p. 104846.

[25] Ali Modabber et al. “Comparison of augmented reality and cutting guide technology in assisted harvesting of iliac crest grafts–A cadaver study”. In: *Annals of Anatomy-Anatomischer Anzeiger* 239 (2022), p. 151834.

[26] Justine Moe et al. “An in-house computer-aided design and computer-aided manufacturing workflow for maxillofacial free flap reconstruction is associated with a low cost and high accuracy”. In: *Journal of Oral and Maxillofacial Surgery* 79.1 (2021), pp. 227–236.

[27] Toshiaki Numajiri et al. “Low-cost design and manufacturing of surgical guides for mandibular reconstruction using a fibula”. In: *Plastic and Reconstructive Surgery Global Open* 4.7 (2016).

[28] Piotr Pietruski et al. “Navigation-guided fibula free flap for mandibular reconstruction: A proof of concept study”. In: *Journal of Plastic, Reconstructive & Aesthetic Surgery* 72.4 (2019), pp. 572–580.

[29] Piotr Pietruski et al. “Supporting fibula free flap harvest with augmented reality: a proof-of-concept study”. In: *The Laryngoscope* 130.5 (2020), pp. 1173–1179.

[30] Jingya Jane Pu et al. “A Comparative Study on a Novel Fibula Malleolus Cap to Increase the Accuracy of Oncologic Jaw Reconstruction”. In: *Frontiers in Oncology* 11 (2022), p. 743389.

[31] Steven M Roser et al. “The accuracy of virtual surgical planning in free fibula mandibular reconstruction: comparison of planned and final results”. In: *Journal of oral and maxillofacial surgery* 68.11 (2010), pp. 2824–2832.

[32] Rutger H Schepers et al. “Accuracy of fibula reconstruction using patient-specific CAD/CAM reconstruction plates and dental implants: a new modality for functional reconstruction of mandibular defects”. In: *Journal of Cranio-Maxillofacial Surgery* 43.5 (2015), pp. 649–657.

[33] Da-long Shu et al. “Accuracy of using computer-aided rapid prototyping templates for mandible reconstruction with an iliac crest graft”. In: *World journal of surgical oncology* 12.1 (2014), pp. 1–9.

[34] Willem LJ Weijs et al. “Accuracy of virtually 3D planned resection templates in mandibular reconstruction”. In: *Journal of Cranio-Maxillofacial Surgery* 44.11 (2016), pp. 1828–1832.

[35] Wei-fa Yang et al. “Three-dimensionally printed patient-specific surgical plates increase accuracy of oncologic head and neck reconstruction versus conventional surgical plates: a comparative study”. In: *Annals of Surgical Oncology* 28 (2021), pp. 363–375.

[36] Wen-Bo Zhang et al. “Improving the accuracy of mandibular reconstruction with vascularized iliac crest flap: Role of computer-assisted techniques”. In: *Journal of Cranio-Maxillofacial Surgery* 44.11 (2016), pp. 1819–1827.

[37] Ruiqi Zhao et al. “Augmented reality guided in reconstruction of mandibular defect with fibular flap: A cadaver study”. In: *Journal of Stomatology, Oral and Maxillofacial Surgery* 124.2 (2023), p. 101318.

[38] Jonathan M Ford and Summer J Decker. “Computed tomography slice thickness and its effects on three-dimensional reconstruction of anatomical structures”. In: *Journal of Forensic Radiology and Imaging* 4 (2016), pp. 43–46.

[39] DR Dance et al. “Diagnostic radiology physics: A handbook for teachers and students. endorsed by: American association of physicists in medicine, asia-oceania federation of organizations for medical physics, european federation of organisations for medical physics”. In: (2014).

[40] Terry S Yoo. *Insight into images: principles and practice for segmentation, registration, and image analysis*. AK Peters Ltd, 2004.

[41] Pascal Monnin et al. “Optimal slice thickness for object detection with longitudinal partial volume effects in computed tomography”. In: *Journal of applied clinical medical physics* 18.1 (2017), pp. 251–259.

[42] Anil K Jain, M Narasimha Murty, and Patrick J Flynn. “Data clustering: a review”. In: *ACM computing surveys (CSUR)* 31.3 (1999), pp. 264–323.

[43] Trevor J Huff, Parker E Ludwig, and Jorge M Zuniga. “The potential for machine learning algorithms to improve and reduce the cost of 3-dimensional printing for surgical planning”. In: *Expert review of medical devices* 15.5 (2018), pp. 349–356.

[44] Bingjiang Qiu et al. “Automatic segmentation of mandible from conventional methods to deep learning—a review”. In: *Journal of personalized medicine* 11.7 (2021), p. 629.

[45] Mario Botsch et al. *Polygon mesh processing*. CRC press, 2010.

[46] James Stewart. *Calculus: early transcendentals*. Cengage Learning, 2012.

[47] Rainer. `https://www.brainvoyager.com/bv/doc/UsersGuide/CoordsAndTransforms/CoordinateSystems.html`.

[48] Rainer. `https://www.brainvoyager.com/bv/doc/UsersGuide/CoordsAndTransforms/SpatialTransformationMatrices.html`.

[49] Gregory G. Slabaugh. “Computing Euler angles from a rotation matrix”. In: (2011).

[50] JB Antoine Maintz and Max A Viergever. “A survey of medical image registration”. In: *Medical image analysis* 2.1 (1998), pp. 1–36.

[51] Michel A Audette, Frank P Ferrie, and Terry M Peters. “An algorithmic overview of surface registration techniques for medical imaging”. In: *Medical image analysis* 4.3 (2000), pp. 201–217.

[52] *Materialise Mimics: 3D medical image segmentation software*. `https://www.materialise.com/en/healthcare/mimics-innovation-suite/mimics`. Version 25.0.0.

[53] *Materialise 3-matic: Design optimization software*. `https://www.materialise.com/en/industrial/software/3-matic`. Version 17.0.0.

[54] Tuija M Yla-Kotola et al. “Union and bone resorption of free fibular flaps in mandibular reconstruction”. In: *Journal of reconstructive microsurgery* (2013), pp. 427–432.

[55] Reymus Marcel, Hickel Reinhard, and Keßler Andreas. “Accuracy of CAD/CAM-fabricated bite splints: milling vs 3D printing”. In: *Clinical oral investigations* 24 (2020), pp. 4607–4615.

[56] Zoran B Popović and James D Thomas. “Assessing observer variability: a user’s guide”. In: *Cardiovascular diagnosis and therapy* 7.3 (2017), p. 317.

[57] Gustaaf JC van Baar et al. “A postoperative evaluation guideline for computer-assisted reconstruction of the mandible”. In: *JoVE (Journal of Visualized Experiments)* 155 (2020), e60363.

[58] Rene D Largo and Patrick B Garvey. “Updates in head and neck reconstruction”. In: *Plastic and reconstructive surgery* 141.2 (2018), 271e–285e.

[59] Achille Tarsitano et al. “Morphological results of customized microvascular mandibular reconstruction: a comparative study”. In: *Journal of Cranio-Maxillofacial Surgery* 44.6 (2016), pp. 697–702.

[60] Lei Zhang et al. “Evaluation of computer-assisted mandibular reconstruction with vascularized fibular flap compared to conventional surgery”. In: *Oral surgery, oral medicine, oral pathology and oral radiology* 121.2 (2016), pp. 139–148.

[61] Dennis Rohner et al. “Importance of patient-specific intraoperative guides in complex maxillofacial reconstruction”. In: *Journal of Cranio-Maxillofacial Surgery* 41.5 (2013), pp. 382–390.

[62] You-yuan Wang et al. “Virtual surgical planning in precise maxillary reconstruction with vascularized fibular graft after tumor ablation”. In: *Journal of Oral and Maxillofacial Surgery* 74.6 (2016), pp. 1255–1264.

[63] Francesco Mazzola et al. “Time and cost-analysis of virtual surgical planning for head and neck reconstruction: a matched pair analysis”. In: *Oral Oncology* 100 (2020), p. 104491.

[64] Donald J Annino Jr et al. “Virtual planning and 3D-printed guides for mandibular reconstruction: Factors impacting accuracy”. In: *Laryngoscope Investigative Otolaryngology* 7.6 (2022), pp. 1798–1807.

[65] *Mastering Autodesk 3ds Max 2013*. `https:https://www.autodesk.nl/products/3ds-max`. 2012.

[66] *Blender - a 3D modelling and rendering package*. Blender Institute, Amsterdam: Blender Foundation. URL: `http://www.blender.org`.

[67] Oceanz. *Oceanz. Online 3D printing professional. Medisch*. URL: `https://www.oceanz.eu/materialen/oceanz-pa11/`.

[68] James S Brown et al. “A new classification for mandibular defects after oncological resection”. In: *The Lancet Oncology* 17.1 (2016), e23–e30.

A

User guide: Preprocessing data

To evaluate the accuracy of computer-assisted surgery in mandibular segment resection and reconstruction, the planned osteotomies are compared to the actual executed osteotomies. The comparison is conducted on virtual representations of the anatomical structures and osteotomies. The virtual representation of the planning can be derived from the computer-assisted pre-operative plan. The virtual representation of the actual post-operative result is created from the post-operative imaging. All models that are created in the planning will be referred to as *planned*. All the models representing the post-operative result will referred to as *actual*.

In this manual, you will gather the required planned models and use Mimics [52] and 3-Matic [53] (Materialise NV, Leuven, Belgium) to create 3D models of the actual reconstruction. These models are 1) the remnant mandible (left and right), 2) the fibula segment(s), and 3) the resection and reconstruction osteotomies. This manual is intended to provide guidance through the following sections:

Planned models:

1. Loading planning data

Actual models:

2. Post-operative imaging
3. Segmentation
   (a) Threshold-based segmentation
   (b) Editing of segmentation
   (c) Part creation
4. Osteotomy localisation
   (a) Identification of the osteotomy
   (b) Point measurement
   (c) Fit plane and verification

A.1. Loading planning data

The first part of the analysis will be performed in 3-Matic (Materialise NV, Leuven, Belgium). The planned and actual 3D models need to be imported into a new 3-Matic project per each patient. The planned models have already been created for the planning and will be loaded into 3-Matic as the first step in this manual.

1. Start *3-Matic* and *open* a new file by clicking **New Project** from the *File* menu toolbar.
2. Save the file under a standardized name by using **Save As** from the *File* menu toolbar. Example *{StudyNumber_Measurement}*.
3. Import the following STL models from the planning file.
   (a) Anatomy
      i. Mandible
      ii. Fibula used for reconstruction (left or right)
      iii. Optional: Corresponding Artery and Tibia
   (b) Planning
      i. Remnant Mandible Left
      ii. Remnant Mandible Right
      iii. Fibula segment(s)
      iv. Resection osteotomies
      v. Reconstruction osteotomies
   (c) Guides
      i. Resection cutting guide
      ii. Reconstruction cutting guide
      iii. Optional: Reconstruction model

   An overview of the models is shown in figure A.1

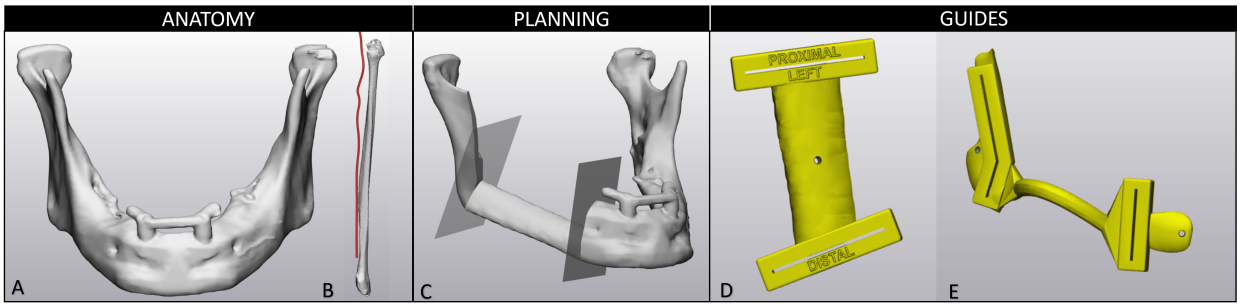

Figure A.1: Input models from the planning
A)/B) The original anatomy, including the mandible and fibula. C) The reconstructed mandible consists of separate models of the remnant mandible (left/right), fibula segment, and osteotomies. D)/E) The resection and reconstruction patient-specific cutting guides

4. Rename all models according to abbreviations in Table A.1.
5. For organisational purposes, group all the models loaded above in a group called *Pre-operative models* and create the subgroup *Anatomy, Planning and Guides* according to the list above. A group is created by right-clicking on a selection of specific models in the *project management tab*. Select **Create Group**.
6. The Mandible and Fibula model [Figure A.1.a] will later be used in a *Boolean Intersection operation*. Therefore, these models must be solid. If this is not the case, hole-filling editing should be performed. This can be done in the original file of the mask segmentation in Mimics [52] (Materialise NV, Leuven, Belgium).

Table A.1: Abbreviations planned models

Models	**Abbreviation**
Left Remnant Mandible	Man_L_P
Left Remnant Mandible	Man_R_P
Left Fibula segment	Fib_L_P
Right Fibula segment	Fib_R_P
Guides	
Reconstruction guide	-
Resection Guide	-
Reconstruction Model	-
Osteotomy	
Left Resection Osteotomy	Man_L_Osteo_P
Right Resection Osteotomy	Man_R_Osteo_P
Left Reconstruction Osteotomy Left segment	Fib_L_Osteo_L_P
Right Reconstruction Osteotomy Left segment	Fib_L_Osteo_R_P
Left Reconstruction Osteotomy Right segment	Fib_R_Osteo_L_P
Right Reconstruction Osteotomy Right segment	Fib_R_Osteo_R_P

L: Left, R; Right, P: Planned, Osteo: Osteotomy

A.2. Post-operative imaging

Post-operative imaging is the input for the creation of the actual 3D models. The imaging quality plays an important role in the precision of generating 3D models, consequently influencing the accuracy of the osteotomy analysis results. Key considerations should be given to imaging parameters, movement errors, comprehensive capture of relevant structures, slice thickness, kilovoltage (kV), and milliampere seconds (mAs). These parameters collectively impact the quality of the imaging data, ultimately shaping the reliability and robustness of the analyses.

A.3. Segmentation

In this section, the actual 3D Models are created from post-operative imaging using multiple segmentation techniques.

7. **Open** the post-operative CT imaging in *Mimics* [FigureA.2].

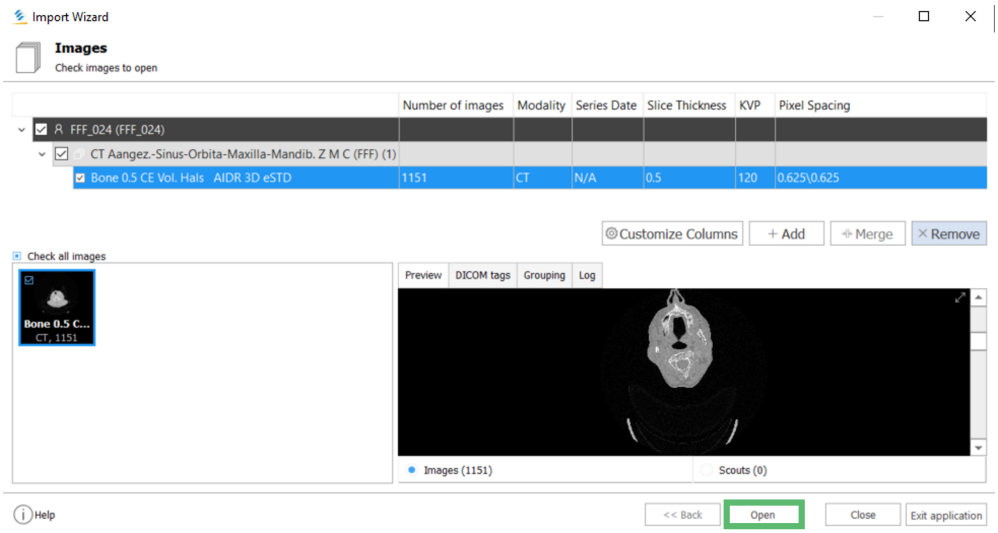

Figure A.2: Loading post-operative imaging in Mimics [52]

8. Save the file under a standardized name by using **Save As** from the *File* menu toolbar. E.g. *{StudyNumber_Segmentation_Osteotomy}*

Threshold-based segmentation

9. Create an initial segmentation by activating **New Mask** from the *Segment* Menu Toolbar [FigureA.3]. Apply a minimum threshold of 267 HU* for CT imaging and 400 HU for CBCT imaging to create a mask of the bone. Crop the included threshold area in the different image views to the region of interest.

   *The set threshold depends on imaging parameters and can be altered if needed. To find an appropriate initial threshold, the function **Draw Profile Line** can be used.

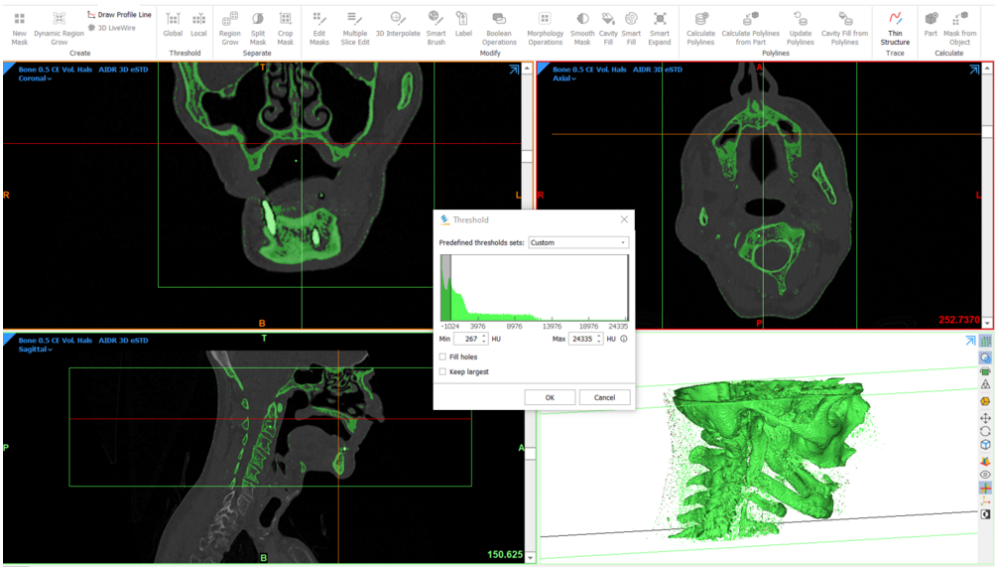

Figure A.3: Create new mask using threshold segmentation

Editing segmentation

10. To separate the target bone from any additional structures and noise, activate **Region Growing** from the *Segment* Menu Toolbar. Click on the reconstructed mandible. Check the box *Multiple layers* and *6-connectivity*. In the initial segmentation, the reconstructed mandible may still be connected to different bone structures, but these will be separated later.
11. Rename the Mask *Bone_segmenation* by double clicking on the mask in the *Project Management* Masks tab.
12. View the created mask in the different *Slices viewers* and in the *3D Viewport*. To visualise a mask in the 3D Viewport, activate **Mask 3D Preview** and select the mask in *Project Management* Masks tab. [Figure A.4]

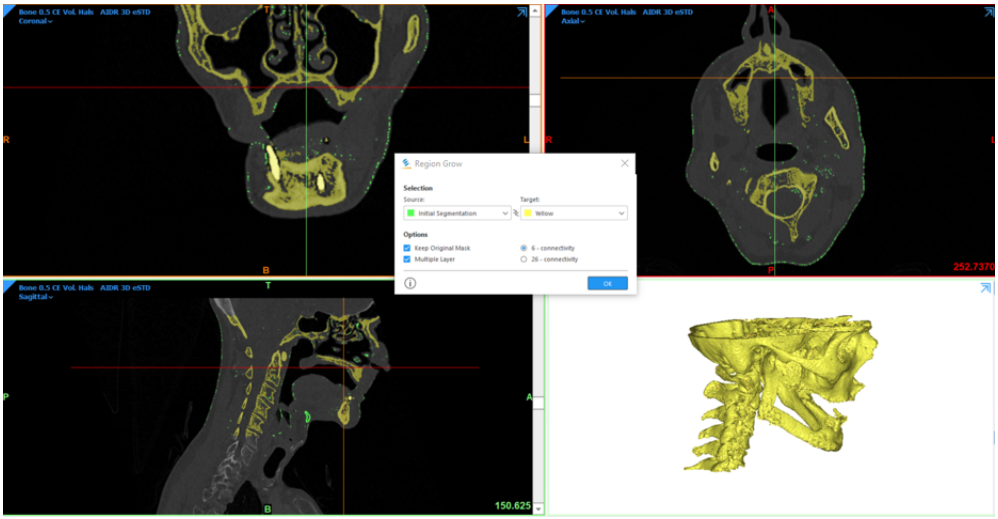

Figure A.4: Initial bone segmentation after region growing

The created segmentation is a combination of different bones. The reconstructed mandible must be separated and split into the remnant mandible (left and right), and the fibula segment(s) to achieve the desired 3D models. This is done by manually editing the mask using functions like Region Grown, Split Mask and Edit Mask. The **Region Grown** function will separate selected structures from other floating pixels or structures. The **Split mask** function allows for the separation of connected structures.

13. Selected the Mask *Bone_segmenation*
14. The mandible is an unconnected structure from the skull. However, with initial segmentation it can become connected, often in the cranial parts. Analyse the Mask *Bone_segmenation* and remove any connected parts of the mandible to the skull with **Edit Mask** function.
15. Activate **Region Grown** to split the reconstructed mandible from the *Bone_segmenation* and name this Mask *Mandible_A**.
    *The A stands for Actual and will later be useful if you have both Planned and Actual models.
16. Activate the **Split Mask** tool in the *Segment* Menu Toolbar to separate the Reconstructed Mandible from the Skull. To effectively use the Split Mask Tool, it is crucial to mark each structure in all three slice directions. The level of precision in marking depends on the complexity of the splitting task.
17. Create a region for every segment in the reconstructed mandible. In the example below this would be 3 regions: remnant mandible left, remnant mandible right and one fibula segment. Name the regions accordingly and split the mask.
    - Remnant Mandible Left: Man_L_A
    - Remnant Mandible Right: Man_R_A
    - Fibula segment: Fib_A
18. Identify any falsely categorized areas in the created result. If necessary, redo the previous step in more detail. Small adjustments can be fixed using the **Edit Mask** function.
19. Use the **Smart Fill** function to fix any holes that are present in the masks.

    The **Smart Fill** tool is a function that fills up cavities and gaps in a mask, using both a global and local approach. The parameter **Hole Closing Distance** will determine the size of the holes that will be filled. Be aware, when using a large **Hole Closing Distance** the mask can be smoothed. The Smart Fill tool also provides the option of **Local Hole Filling**. In this mode, the cursor has two circles: an inner circle (solid) and an outer circle (dotted). The inner circle will add precise pixels to the mask, while the outer circle will only add the pixels necessary to close the hole before filling it.

Part Creation

20. Calculate parts of the mask of the reconstructed mandible and the separate parts (mandible Left, Right and fibula segments). Select the mask and right click, select **Calculated parts**. In the calculate part window, check if all the right masks are selected and use the optimal quality to generate the parts.
21. The parts are now located in the object window. For organisation purposes, group the parts by selecting them all. Right-click on the selection and select the function **Group**. A shortcut for this function is *Ctrl-G.* Name the group as *Models*.
22. Next, the models are exported from Mimics and imported in 3-Matic. Selected the models that need to be exported (mandible left, mandible right, fibula segments and the reconstructed mandible) and copy them to the clipboard by pressing **Ctrl + c**. *Open* the 3-Matic files of the patient (this is the same file as the planning models were loaded in). Paste the models (**Ctrl + v**) in the 3-Matic file and group them as *Actual models*.
23. The last step is wrapping the models. The **Wrapping Tool** filters out minor inclusions or closes small holes by generating a wrapping surface around the chosen models. Set the **Closing Gap** to 0.5, this parameter determines the maximum size of the gaps that will be filtered away. Set the **Smallest Detail** to 1.0; this parameter determines the size of the triangles on the new surface.

You have now completed the segmentation part of this manual. As a result, you have multiple objects: the remnant mandible (left & right), the fibula segments and the post-operative reconstructed mandible.

A.4. Osteotomy localisation

The next step is to localise the osteotomy made during the surgery. The osteotomies are located on the ends of the remnant mandible and fibula segments. The natural shape of the structure is disrupted here, which is seen as an abrupt and unexpected change in the contrast. The same protocol is used for localisation of the resection and the reconstruction osteotomies. However, prior to the determination of the resection osteotomies, an examination of the cutting guide design must be performed. The PSC translates the planned osteotomy from the virtual environment to the operation room. The designed saw slot of the guide does not always cover the full cross-section of the mandible. Especially osteotomies, which cross the ramus or dentition. The distal part of these osteotomies requires high accuracy for the tumour margin and reconstruction. The proximal part can be done free-handed. It is important to review the PSC design and evaluate where the osteotomy is made according to the planning.

The osteotomy location is used to differentiate between osteotomies within one subject (see Figure A.5). These locations are abbreviated for more user-friendliness, as shown in Table A.2. This table illustrates the names of osteotomies for mandible reconstruction with multiple fibula segments.

Table A.2: Abbreviations

Osteotomy location	**Abbreviations**
Left resection osteotomy	Man_L_Osteo
Right resection osteotomy	Man_R_Osteo
Left osteotomy of the left fibula segment	Fib_L_Osteo_L
Right osteotomy of the left fibula segment	Fib_L_Osteo_R
Left osteotomy of right fibula segment	Fib_R_Osteo_L
Right osteotomy of right fibula segment	Fib_R_Osteo_R

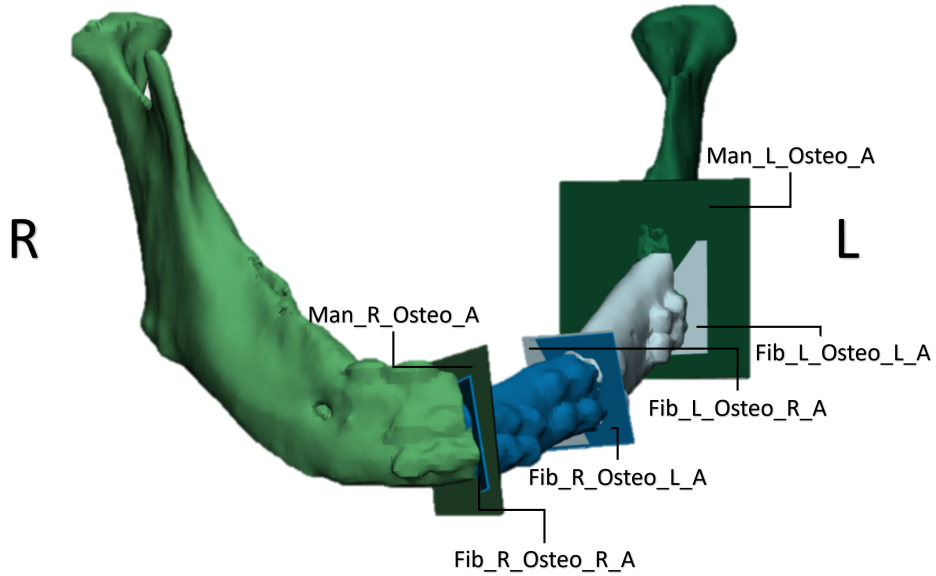

Figure A.5: Abbreviations osteotomies based on the location

24. Open the 3-Matic file of the evaluated patient, which has been created in the previous steps of this manual.
25. Create a *new group* called *Actual osteotomies* and create a subgroup for each osteotomy. Including two for the resection osteotomies (Man_L and Man_R) and two per fibula segment (Fib_X_L Fib_X_R).

The following part is only for resection osteotomies. If you are assessing reconstruction osteotomies, go to step 31 to continue.

26. Start with one of the resection osteotomies: Man_L or Man_R
27. View the resection guide on the pre-operative mandible in *3-Matic*. [A.6.a.b]
28. Inspect and verify if the cutting guide fully or partly covers the osteotomy surface. If it fully covers the bone surface, go to step 31. If not, continue with the next steps.

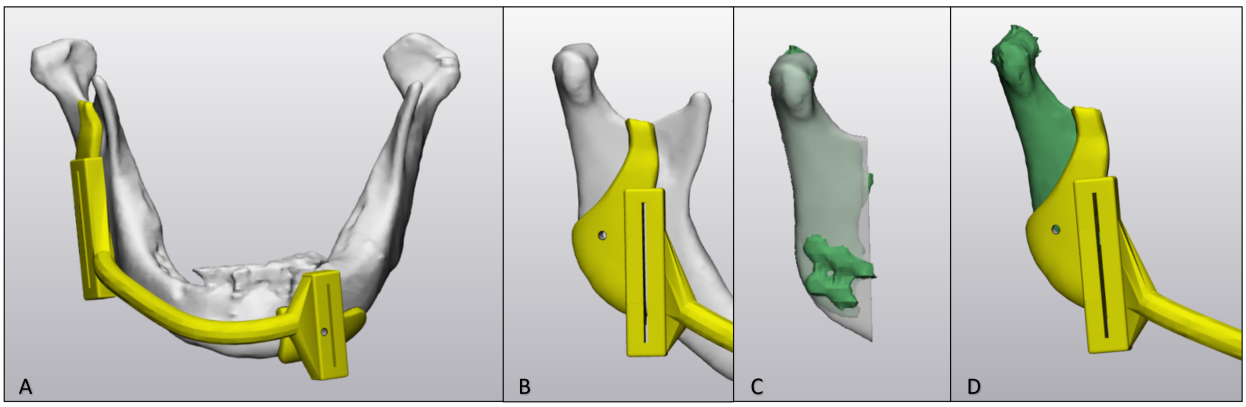

Figure A.6: Analyse resection cutting guide
A) and B) Overview of models delineating the precision area for osteotomy, including the resection cutting guide and the pre-operative mandible. C) Registration of the planned remnant mandible to the actual remnant mandible. D) Cutting guide aligned with the actual remnant mandible.

The osteotomy is partially guided by the PSC. The assessment of the actual osteotomy is only valid for

the guided part. Therefore, the PSC must be aligned with the post-operative imaging to properly consider where to assess the post-operative osteotomy. To register the PSC to the post-operative images, the planned remnant mandible of the evaluated side needs to be aligned to the actual remnant model [A.6.c], moving the resection PSC [A.6.d] with the same transformation.

29. To *align* the resection guide with the post-operative imaging; you must align the planned remnant mandible (left or right) to the actual remnant mandible, moving along the resection guide.
    1. First use **n-point registration**
    2. Later use **global registration**
30. Copy the transposed resection guide by selecting the object and pressing **Ctrl + c**. Paste the resection guide in Mimics **Ctrl + V**.

Point measurement

The osteotomy is determined by systematically setting points at the end of the sawn bone segments. These will form a point cloud through which a plane can be fitted. A point cloud will be created for each osteotomy. The following steps will guide you through the point measurements:

31. Start with one osteotomy that you want to determine. In this example, the right mandible resection osteotomy will be analysed.
    - If you are analysing a resection osteotomy you need to verify which part of the osteotomy is made according to the PSC.
    - Visualise the PSC in the 2D image viewer by making the object and its contours visible in the object tree [Figure A.7].
    - Analyse the PSC slot of the guide and set the points within that range.

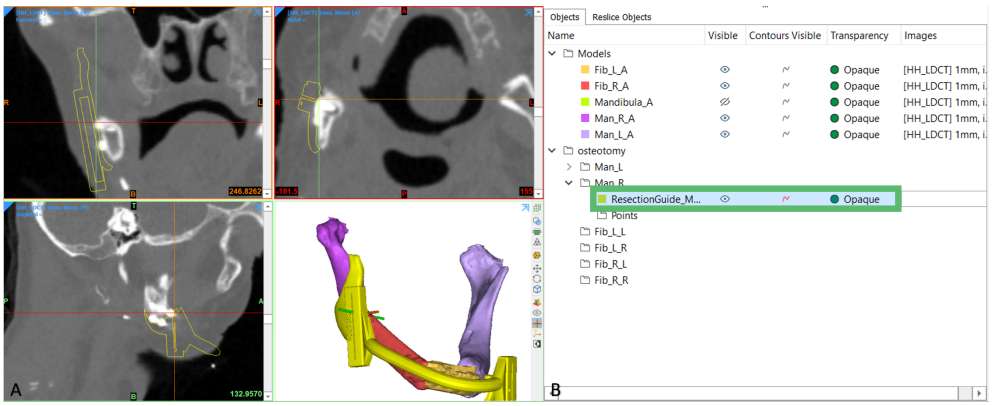

Figure A.7: A) The contour of the cutting guide on the post-operative imaging and the PSC on the post-operative mandible reconstruction. B) Visualize the resection guide in the 2D and 3D viewer.

32. To create a point measurement, activate **Point** in the *analyze menu* Toolbar.
33. Scroll through the axial, sagittal, and coronal slices and identify in which view the bone cut is seen the most clearly.
34. Begin by positioning a point on one side of the bone cut. Progress through the slices towards the opposite side of the bone cut, marking two points on every couple of slices adjacent to the outermost edge of the bone segment. Ensure that the points are placed only in areas that are clearly visible. Be aware that certain regions are hard to assess due to artefacts from the fixation material. [A.8].
35. The mask of the segmented parts may be used for orientation but must be turned off when setting the points to prevent bias.

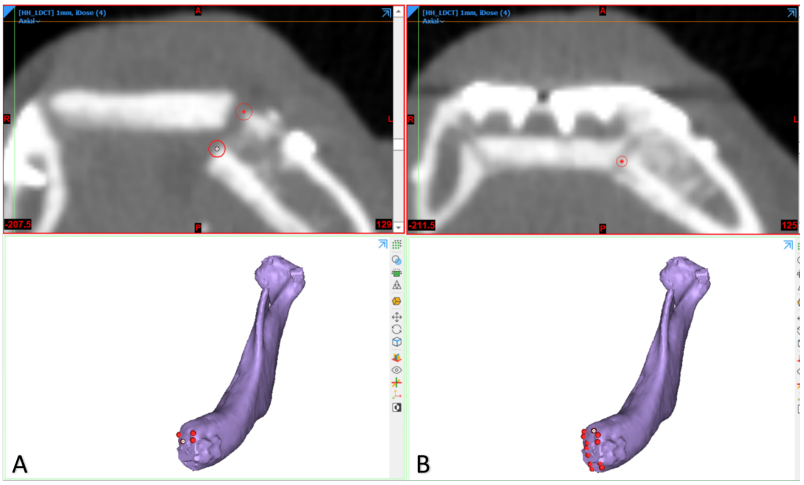

Figure A.8: Setting points.
A) Two points on the outermost edge of the bone segment. B) Only one point is set due to a scattered view caused by artefacts from fixation material

36. Complete the points for one osteotomy.
37. Confirm the points on the three different views (axial, coronal, sagittal) and adjust if necessary.
38. The created points will together form a point cloud. Select all the points and **group** them in a group named after the osteotomy location.
39. Select all the points again and *export* them as STL files by right-clicking and selecting **STL+** [Figure A.9].
40. In the *STL+* window press **Add** to add the points to *Objects to be converted*. Change the output directory by selecting the **File Icon**. Navigate to the analysed subject, load the files in a folder named after the assessed osteotomy and press **Finish**.

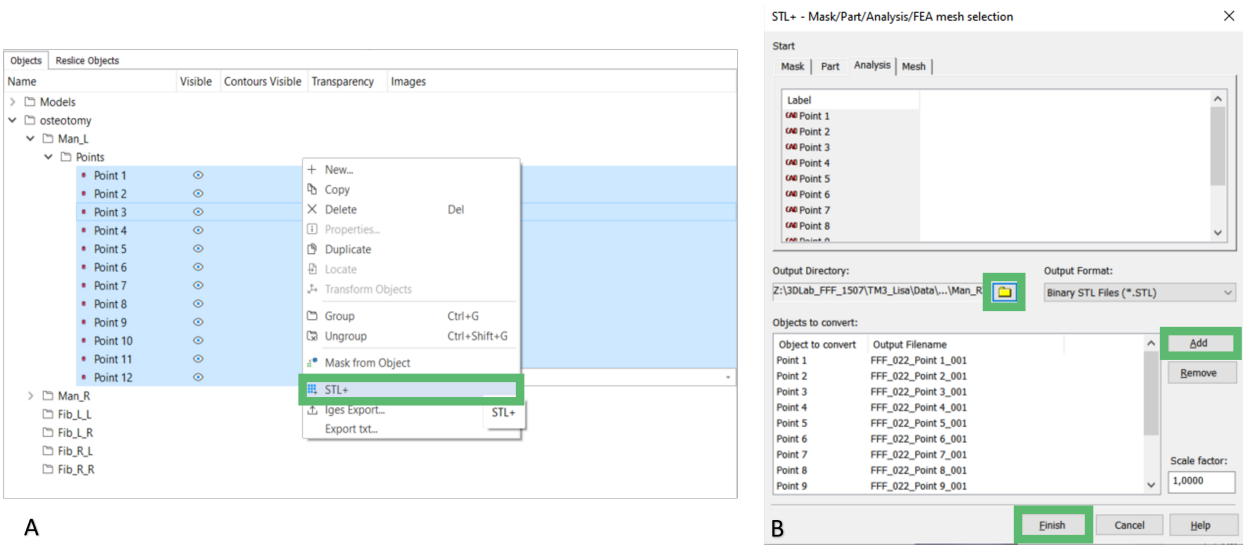

Figure A.9: Export point as STL

Fit plane

For the next step, the generated point cloud is imported into 3-Matic, and a datum plane is fitted through.

41. **Open** the 3-Matic file of the patient you are analysing.

42. Import the point cloud by clicking on **Import Part** from the File menu toolbar and import all the points.
43. Group all the points to a group named after the assessed osteotomy.
44. To fit a plane through the point cloud, navigate to the *Design* Toolbar, select *Analytical* and choose **Datum plane**.
45. The *Create a Datum plane* tab will open in the *Operation* section. Selected **Fit Plane** as *Method* and add the *points cloud* as *Fitting entities*. Press apply [Figure A.10].

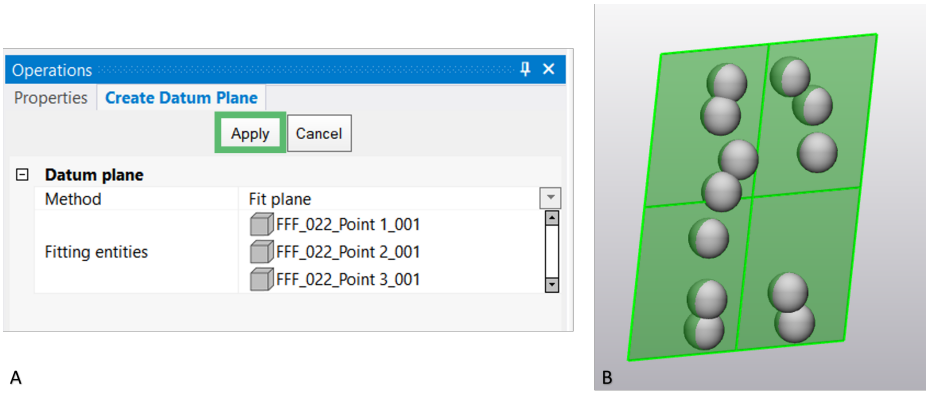

Figure A.10: A) Operational window *Create Datum Plane*. B) Fitted datum plane through points

46. Create an STL model from the datum plane by pressing **Analytical to Part** in the *Design* toolbar.
47. Rename the create plane; according to Table A.2
48. Transfer back to Mimics by **Copying** the plane in 3-Matic and **Pasting** it in Mimics.
49. Verify the location of the created osteotomy on the images in the axial, coronal and sagittal view. If the osteotomy is positioned incorrectly, check the placed points and adjust where necessary [Figure A.11].
50. Repeat steps 31 to 49 until you are satisfied with the result.

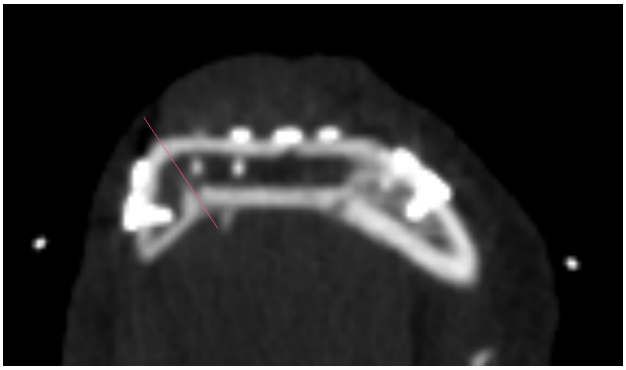

Figure A.11: Verification osteotomy post-operative images

51. Perform steps 31 to 49 for all the osteotomies of the patient.

Saving results

52. **Save** the Mimics and 3-Matic file.
53. Repeat the manual for all subjects.

B

User guide: Osteotomy accuracy

In user guide A, the actual models and osteotomies are created from the post-operative imaging. In this user guide, you will use 3-Matic (Materialise NV, Leuven, Belgium) and run the Python script to measure the distance and angular deviation between the planned and actual osteotomies. This user guide provides a detailed step-by-step guide for each part of the process. The parts include:

1. Resection osteotomies
   (a) Registration
   (b) Distance deviation
   (c) Angular deviation
2. Reconstruction osteotomies
   (a) Registration
   (b) Distance deviation
   (c) Angular deviation
3. Run Python script

Input for this guide are the planned and actual models. Table B.1 presents the abbreviations used for the different objects that will be used in this user guide.

After completing all the steps in 3-Matic (Materialise NV, Leuven, Belgium), the following objects and matrices are created:

1. Planned and Actual intersection of all osteotomies
2. Planned and Actual local coordinate systems
3. Reference point of the tumour

The outputs stated above will be the inputs of the Python script. This script will perform the distance and angular measurements between the osteotomies and provide the results in an Excel sheet.

B.1. Loading data

The analysis will be performed in Materialise 3-Matic (Materialise NV, Leuven, Belgium). When correctly followed user guide A. All the needed models are already located in the patient 3-Matic file.

1. Start *3-Matic* and *open* the patient file that will be analysed. Example *{StudyNumber_Measurement}*.

B.2. Resection osteotomies

In this section, you will create all the necessary parts to evaluate the resection osteotomies. The models used as input are listed below and shown in Figure B.1.

- Pre-operative mandible model
- PSC in reference to the planned reconstructive mandible.
- Planned remnant mandible (left and right)
- Actual remnant mandible (left and right)
- Planned and actual resection osteotomies

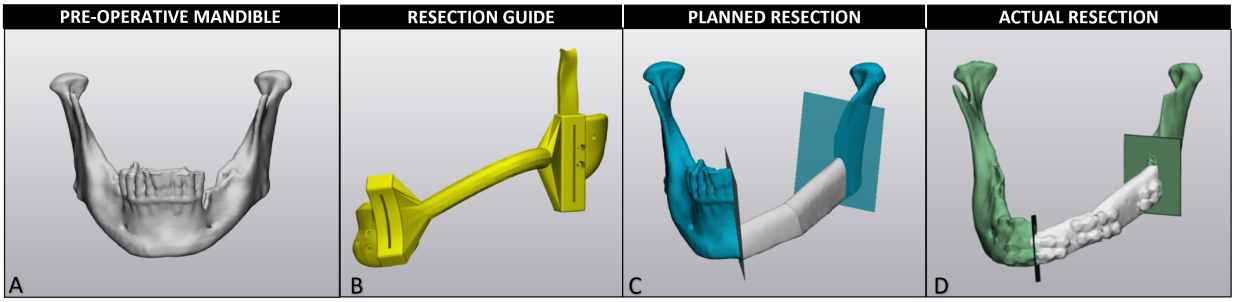

Figure B.1: Input models for the resection osteotomy analysis
A) The mandible before surgery. B) The cutting guide is used to execute the planned resection of osteotomies. C) The planned resection with the remnant mandible parts (left and right) in blue with associated resection osteotomies. D) The actual resection with the remnant mandible parts (left and right) in green, with associated reconstruction osteotomies.

2. Verify if all needed models (listed above) are present in the opened file.

B.2.1. Registration

The first step is to align the actual osteotomy to the pre-operative mandible model to establish the proper baseline for the deviation measurements. The actual remnant mandible will be aligned to the planned remnant mandible, the actual osteotomies are transformed using the same transformation.

3. Start with one of the two resection osteotomies. In this example, the left mandible resection osteotomy is analysed.
4. Create a **Duplicate** of the actual remnant model, the planned remnant model and the actual osteotomy (e.g. Man_L_P, Man_L_A and Man_L_Osteo_A).
5. Align the actual remnant model to the planned remnant model moving along the actual osteotomy by first roughly aligning them followed by a surface registration algorithm.
   (a) Selected **Align** from the *Menu Toolbar* and activate **N Points Registration**. The planned remnant mandible is the **Fixed Entity**, the actual remnant mandible is the **Moving Entity** and the actual osteotomy is the **Moving along entities**, see Figure B.2.A.
   (b) Selected a minimum of three *triangle nodes* on each model. Make sure to pick specific landmarks that are easily recognised on both models and press **Apply** to perform the transformation, see Figure B.2.B/C. Close the operation by pressing **Cancel**

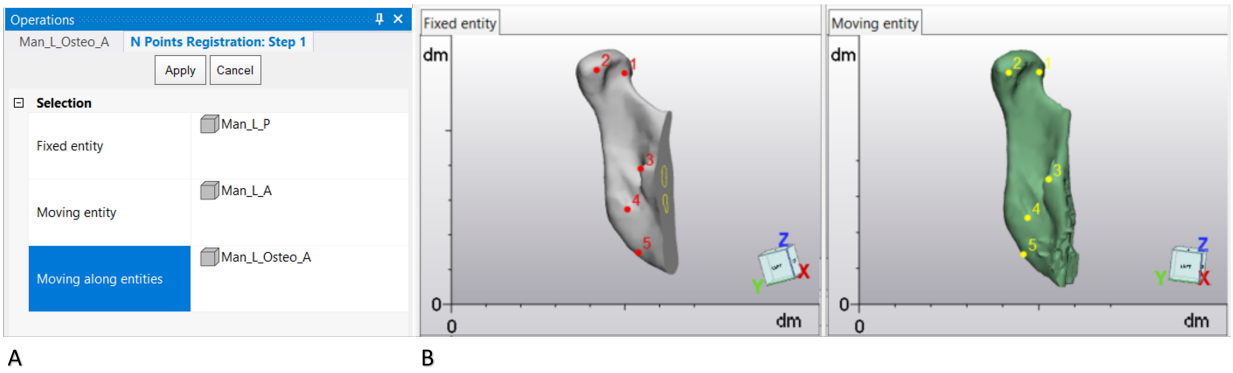

Figure B.2: Landmark registration
A) The operation window with the chosen entities. B) The landmarks on the planned remnant mandible. C) The landmarks on the actual remnant mandible in the same position.

(c) Activate the **Global Registration** from the **Align** toolbar and selected similar **Fixed**, **Moving** and **Moving along** entities, see Figure B.3.A.

(d) The **Distance Threshold** parameter be set on automatic. The number of iterations should be set to min 1000.

(e) **Apply** the global registration and evaluate the *average distance error* in in the *logger*. Press **Apply** again until you are satisfied with the results and the average distance error has stabilized, see Figure B.3.C.

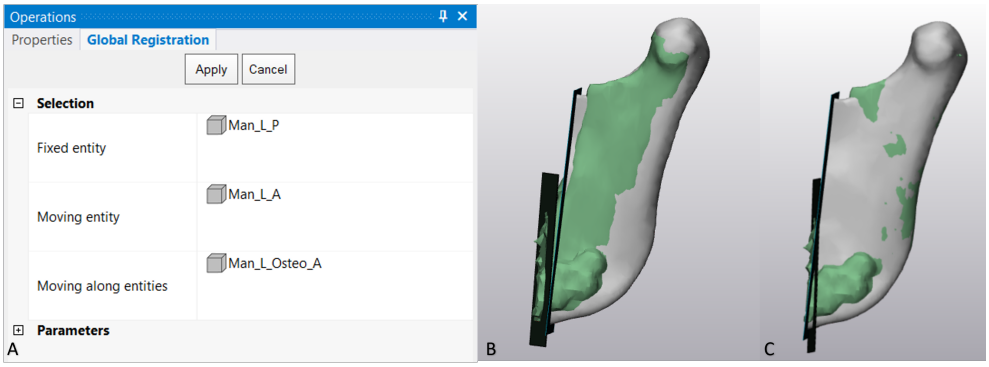

Figure B.3: Global registration
A) The operation window with the chosen entities. B) The starting position of the models. C) The end position of the models

(f) Create a new group called *Measurements*. With a subgroup named after the location of the evaluated osteotomy (e.g. Man_L). Group the aligned models in a new subgroup called *Aligned models*, and story this subgroup in the designated group (e.g. Man_L).

6. Add the planned osteotomy (e.g. Man_L_Osteo_P) to the newly created group of the aligned models.

B.2.2. Distance deviation

7. Activate **Update OCS** of the *align* menu toolbar. Selected the planned osteotomy (e.g. Man_L_Osteo_P) as an entity and *inertia axis* as method and press **Apply**. This function will update the coordinate system of the Man_L_Ostoe_P to its inertia axes.
8. Selected **Mesh** form the *Design* menu toolbar, and activate **Box**. Create a box around the osteotomy. The box should have a thickness of 0.2. The height and the weight should be set so the box covers the whole cross-section of the pre-operative mandible model, see Figure B.4.A. Rename the box to the location and if it was actual or planned (e.g. Box_L_P and Box_L_A), see Figure B.4.B.

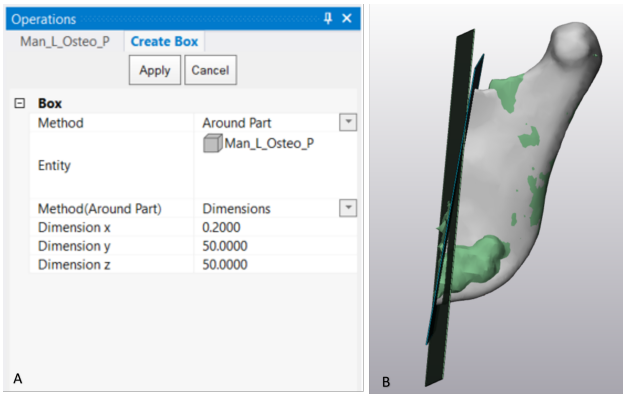

Figure B.4: Create Box
A) The operations window; make sure the thickness of the box is 0.2 mm. B) The created Planned and Actual Box

9. Hide all objects except the pre-operative mandible and the PSC. Inspect which area of the mandible is cut according to the guide, see Figure B.5.A. If the guide only partly guides the saw across the osteotomy; the relevant part of the mandibular should be evaluated.
   (a) Activate **Analytical** from the *Design* menu toolbar. Create two **Datum planes** one at the top part of the PSC and one at the bottom part, see Figure B.5.B. A datum plane is an endless plane.
   (b) The *datum plane* is created using **3 points** as *method*. The first point is the origin of the datum plane. The second point defines the x-axis together with point one. The third point defines the y-axis together with point one. Make sure that the datum plane is in line with the top/bottom of the PSC.
   (c) Duplicate the pre-operative mandible model (make sure the model is completely filled).
   (d) Activate **Cut** from the *Design* menu toolbar. Selected the duplicated mandible model as entities and the datum planes aligned at the top of the PSC as cutting entities. Press **apply**.
   (e) The mandible will be cut into separate parts.
   (f) Perform the cut operation again. Select the bottom part of the mandible as the entity and the bottom datum plane as the cutting entity.
   (g) The results will be the part of the mandible for which the osteotomy is translated accurately from the planning to the surgery, see Figure B.5.C. Rename this part to *Man_{side}_accurate*, e.g. *Man_L_accurate*

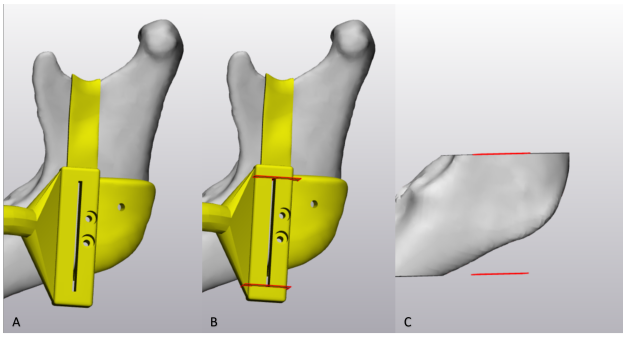

Figure B.5: Part of the mandible accurately cut by cutting guide guidance
A) The cutting guide only partially guides the osteotomy. B) Two datum planes are created on the top and bottom of the cutting guide. C) The mandible is cut according to the design of the cutting guide.

Create a **Boolean intersection** with the pre-operative mandible model or the just created *Man_{side}_accurate*. A boolean intersection results in a new volume that includes only the common volume of the selected parts.

10. Hide all objects except the two boxes around the osteotomies created in step 8 and the pre-operative mandible model / *Man_{side}_accurate*
11. Start with the planned osteotomy. Duplicate the box and the pre-operative mandible model *Man_{side}_accurate*.
12. Activate **Boolean Intersect** from the *Design* menu toolbar. Selected the box of the planned osteotomy and the pre-operative mandible model / *Man_{side}_accurate* as *entities* and press **apply**, see Figure B.6.A/B.
13. A intersection between the two parts will be end result B.6.C.
14. Rename this part to the following name: *PatientNumber_Man_{side}_Inter_Planned*. e.g. *PT001_Man_L_Inter_Planned*

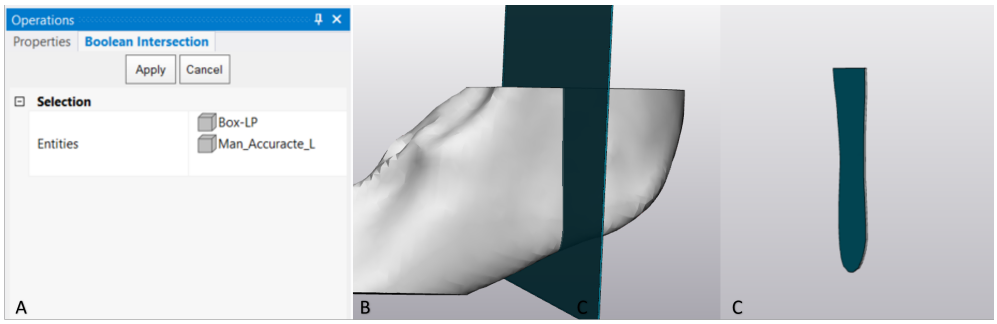

Figure B.6: Boolean intersection of the planned osteotomy with the mandible
A) The operations window with the box and the pre-operative mandible as entities. B) The preoperative mandible with the planned box. C) The created intersection

15. Repeat from step 11 onwards for that actual osteotomy.
16. Group the following objects into a group called *Intersection*
    - Boxes of the osteotomies (planned and actual)
    - Man_{side}_accurate (if applicable)
    - Intersections (planned and actual)
17. Add the *Intersection* group to the correct subgroup in the *Measurement* group.

B.2.3. Angular deviation

The angular deviation is determined by a change rotational change in the local coordinate systems (LCS) of the planned and actual osteotomies. Start with the coordinate system of the planned osteotomy. This coordinate system is defined based on the saw slot/flange of the PSC. The saw slot/flange is designed to guide the saw through the bone in one specific direction, identical to the planned osteotomy. The x-axis of the local coordinates system is presented by the height of the slot/flange. The y-axis of the local coordinate system is defined by the length of the PSC slot/flange. The z-axis points out the plane, and the right-hand rule determines the direction.

18. Start with defining the LCS of the planned osteotomy. This is done according to the slot/flange of the PSC.
19. Only **show** the the PSC.
20. Activate **Datum Plane** in the *Analytical* Tab from the *Design* menu toolbar.
21. Create a **Datum Plane** representing the cutting direction. The order of selecting the point will determine the direction of the x and y-axis. It is therefore important to precisely follow the order of instruction below:
    (a) Point one: This point is the origin of the plane/LCS and should be placed on the front side in the top corner of the PSC slot.

(b) Point two: This point will create the x-axis together with point one. Place this point right across point one; on the back side of the top corner of the PSC slot.

(c) Point three: This point will create the y-axis together with point one. Place this point right below point one; on the front side in the bottom corner of the PSC slot.

22. Press **apply**, see Figure B.7.
23. Rename the datum plane to *PatientNumber_Man_{side}_TM*_Planned*. e.g. *PT001_Man_L_TM_Planned*.
    *TM: Transformation Matrix.
24. Activate **Analytical to Mesh** to convert the created datum plane to a mesh object, see Figure B.7.B. Selected the datum plane *PatientNumber_Man_{side}_TM_Planned* as *Entity*.

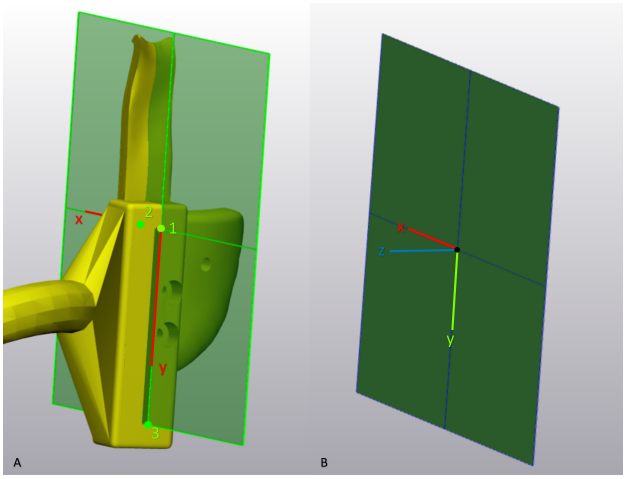

Figure B.7: Local coordinate system of the planned osteotomy
A) Create a datum plane by placing 3 points on the correct position of the cutting guide slot. B) convert the datum plane to a mesh object

The coordinate system of the actual osteotomy is roughly determined. The x and y axes will again be in plane while the z-axis is pointing outwards. The direction of the x and y axes should roughly align to the x and y axes of the planned plane but will later be positioned correctly by an automatic rotation around z-axis.

25. Show the box of the actual osteotomy; created in step 8, together with the PSC.
26. Create a **Datum Plane** by picking points that correspond to the LCS of the planned osteotomy the best, use the resection guide as orientation, see Figure B.8.A. The order of selecting the point will determine the direction of the x and y-axis. It is therefore important to precisely follow the order of instruction below:

    (a) Point one: This point is the origin of the plane/LCS. and should be placed on the ventral top corner of the box.

    (b) Point two: This point will create the x-axis together with point one. Place this point right across point one; on the dorsal side of the top corner of the box.

    (c) Point three: This point will create the y-axis together with point one. Place this point right below point one; on the ventral bottom corner of the box.

27. Make sure that all the points are either on the front side or the back side of the box and press apply to create the datum plane.
28. Rename the datum plane to *PatientNumber_Man_{side}_TM_Actual*. e.g. *PT001_Man_L_TM_Actual*.
29. Activate **Analytical to Mesh** to convert the created datum plane to a mesh object, see Figure B.8.B. Selected the datum plane *PatientNumber_Man_{side}_TM_Actual* as *Entity*.

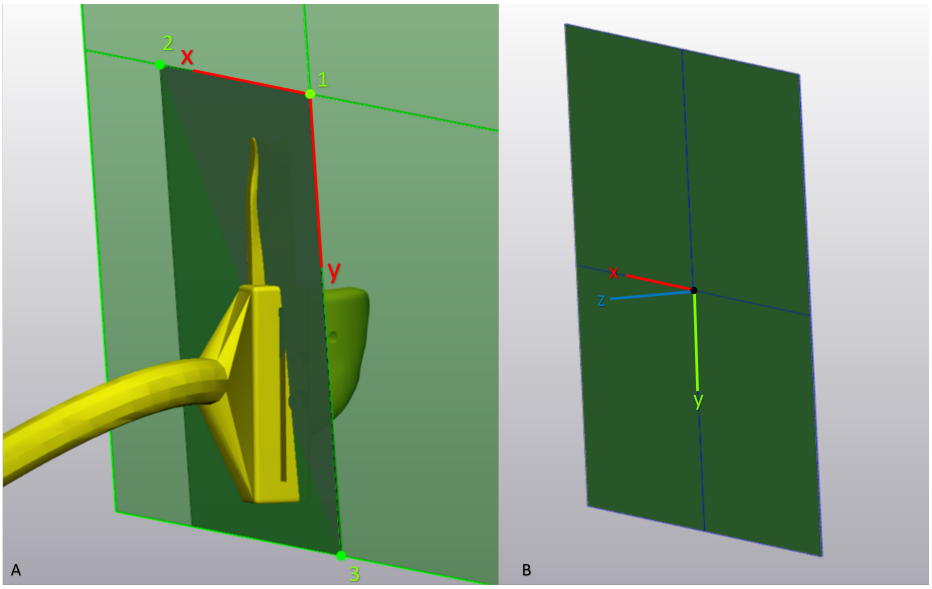

Figure B.8: Local coordinate system of the actual osteotomy
A) Create a datum plane by placing 3 points in the correct position of the actual box. B) convert the datum plane to a mesh object

30. Verify the orientation of the LCS of the planned and actual osteotomy by clicking on the plus sign in front of the mesh object in object three. Right-click on *Object coordinate system* and press **Show**. The x- (red) and y-axis (green) should be in plane and have roughly the same direction. The z-axis (blue) should be pointing in the same direction.
31. Group the following objects into a group called *LCS*
    - Created datum planes of the LCS (planned and actual)
    - Mesh objects of the datum planes (planned and actual)
32. Add the *LCS* group to the correct subgroup in the *Measurement* group.

Repeat all the steps above for both the left and the right resection osteotomies.

B.2.4. Reference point tumour

A reference point of the tumour is created to determine the direction of the displacement of the resection osteotomies.

33. **Show only** the pre-operative mandible and the two planned resection osteotomies.
34. Activate **Point** in the *Analytical* Tab from the *Design* menu toolbar.
35. Select **Coordinates** as method. Select a point on the pre-operative mandible in the middle of the resected part.
36. Convert the analytical to a mesh with the **Analytical to Mesh** function from the *Design* menu toolbar.
37. Rename the part to *{StudyNumber_Tumor}*.
38. Manually align the part to the centre or the resected part of the mandible.

B.2.5. Save results

All outcomes should be saved in a common location. The outcomes of this section are the intersections of resection osteotomies with the pre-operative mandible model and the actual and planned local coordinate systems of the resection osteotomies.

39. Start with saving the intersection by activating **export** from the *file* menu toolbar. Select **STL** as the export type.

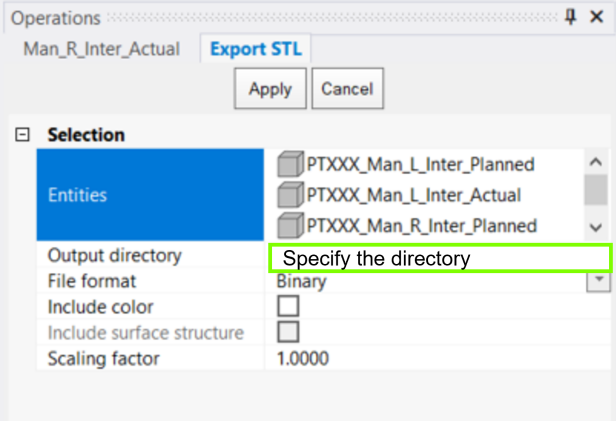

Figure B.9: Save intersection

40. Selected all created resection intersection and the reference point of the tumour as *Entities*. Change the *Output directory* to a common location. and press **Apply**, see Figure B.9.

To save the local coordinate systems a transformation matrix will be exported from from all local coordinate systems to the world coordinate system.

41. Start by defining the world coordinate system, see B.10.A/B. Do this by creating a new datum plane created by the following three points:
    (a) Point one: [0;0;0]
    (b) Point two: [1;0;0]
    (c) Point three: [0;1;0]
42. Rename the datum plane to *origin*.
43. Activate **Analytical to Mesh** to convert the created datum plane to a mesh object.
44. To export the transformation matrix, activate **export** from the *file* menu toolbar and select **Tranformation Matrix** as export type.
45. Select one of the LCS as the *Entity*, select the **origin** as the *Target Entity* and keep the output directory similar to step 40, see Figure B.10.C.

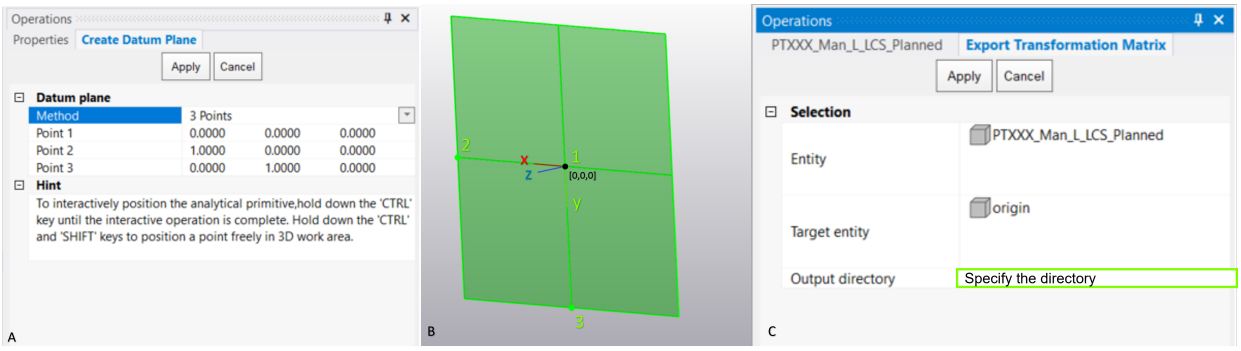

Figure B.10: Saving local coordinate system

B.3. Reconstruction osteotomies

In this section, you will create all the necessary parts to evaluate the reconstruction osteotomies. The models used as input are listed below and shown in Figure B.11

- Pre-operative fibula model
- Planned fibula segments
- Actual fibula segments
- Reconstructin PSC in reference to the pre-operative fibula.
- Planned and actual reconstruction osteotomies

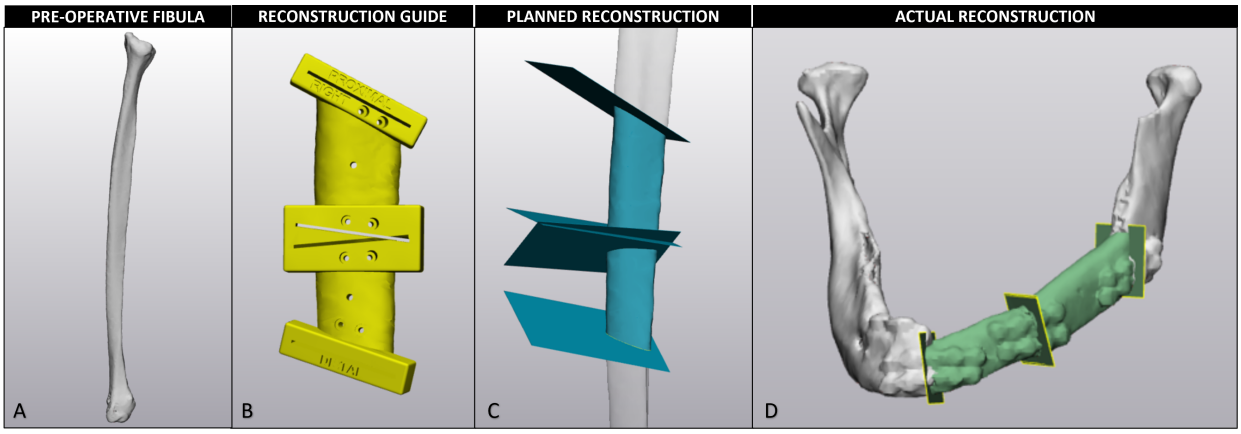

Figure B.11: Input models for the resection osteotomy analysis
A) The fibula before surgery. B) The PSC is used to create the planned reconstruction osteotomies. C) The planned reconstruction segments in blue with associated reconstruction osteotomies. D) The actual reconstruction segments in green with associated reconstruction osteotomies.

46. Verify if all needed models (listed above) are present in the opened file.

B.3.1. Registration

The first step is to align the actual osteotomy to the pre-operative fibula model to establish the proper baseline for the deviation measurements. The actual fibula segments will be aligned to the planned fibula segments moving along the actual osteotomies.

47. Start with one fibula segment with the two associated osteotomies.
48. Create a **duplicate** of the planned fibula segment, the actual fibula segment and the actual osteotomies (e.g. Fib_L_P, Fib_L_A, Fib_L_Osteo_L_A and Fib_L_Osteo_R_A).
49. Align the actual fibula segment to the planned fibula segment moving along the actual osteotomies. First, an initial alignment is performed, followed by an alignment using a surface registration.
    (a) Selected **Align** from the *Menu Toolbar* and activate **N Points Registration**. The planned fibula segment is the **Fixed entity**, the actual fibula segment is the **Moving entity** and the actual osteotomies are the **Moving along entities**, see Figure B.12.A.
    (b) Selected a minimum of three **triangle nodes** on each model. Make sure to pick specific landmarks that are easily recognised on both models and press **apply** to perform the transformation, see Figure B.12.B. Close the operation by pressing **Cancel**

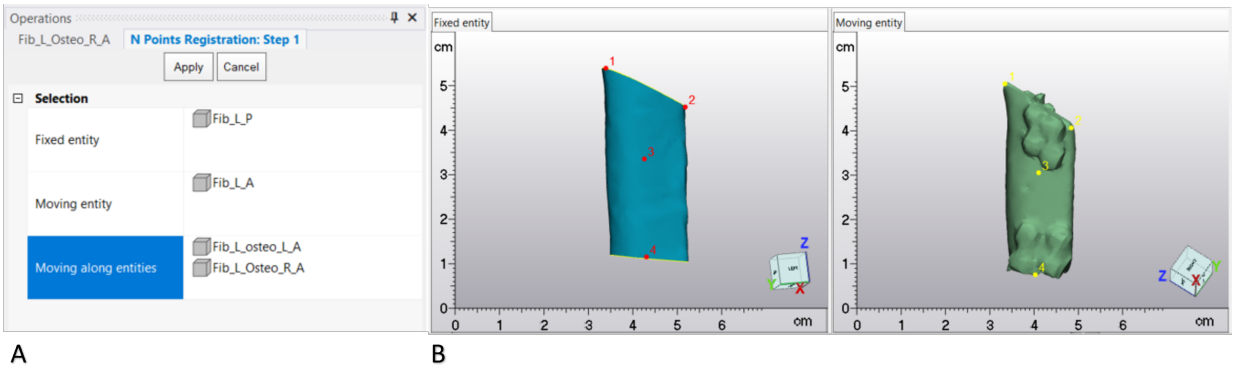

Figure B.12: Landmark registration
A) The operation window with the chosen entities. B) The landmarks on the planned fibula segment. C)The landmarks on the actual fibula segment mandible in the same position

(c) Activate the **Global Registration** from the **align** toolbar and selected similar **fixed**, **moving** and **Moving along** entities, see Figure B.13.A.

(d) The **distance threshold** parameter be set on automatic. The number of iterations should be set to min 1000.

(e) **Apply** the global registration and evaluate the *average distance error* in the *logger*. Press **apply** until you are satisfied with the results and the average distance error has stabilized, see Figure B.13.B/C.

(f) Verify the position of the segment and evaluate if the results are optimal. If needed, adjust the position of the actual segment **manually** by matching the bone surfaces of the segments.

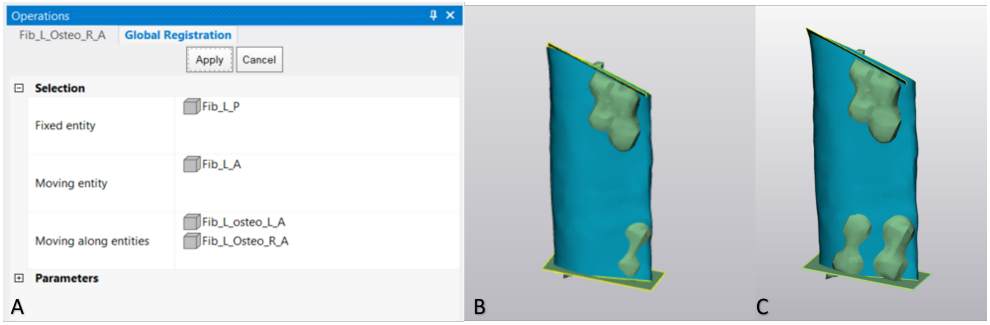

Figure B.13: Global registration
A) Shows the operation window with the chosen entities. B) Shows the starting position of the models. C) shows the end position of the models

(g) Create a new group called *Measurements*. With a subgroup named after the location of the evaluated segment (e.g. Fib_L). Group the aligned models in a new subgroup called *Aligned models*, and store this subgroup in the designated group. (Fib_L).

50. Add the planned osteotomies (e.g. Fib_L_Osteo_L_P & Fib_L_Osteo_R_P) to the newly created group of the *Aligned models*.

B.3.2. Distance deviation

51. Activate **Update OCS** of the *align* menu toolbar. Selected the planned osteotomies (e.g. Fib_L_Osteo_L_P & Fib_L_Osteo_R_P) as an entity and *inertia axis* as method and press **apply**. This function will update the coordinate system of the Fib_L_Osteo_L_P / Fib_L_Osteo_R_P to its inertia axes.
52. Selected **Mesh** form the *Design* menu toolbar, and activate **Box**. Create a box around the planned and actual osteotomies. The box should have a thickness of 0.2. The height and the weight should be

set so the box covers the whole cross-section of the pre-operative fibula model, see Figure B.14.A. Rename the box to the location of the osteotomy and osteotomy type(actual or planned) (e.g. Box_L_L_P, Box_L_R_P, Box_L_L_A and Box_L_R_A), see Figure B.14.B.

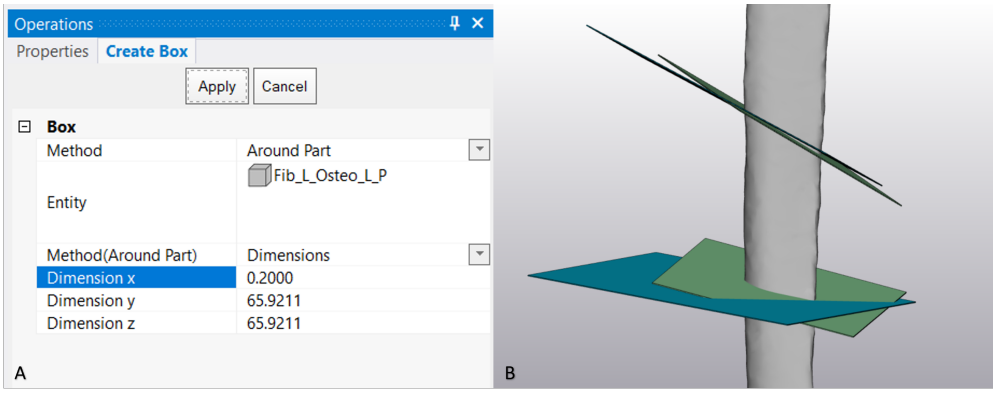

Figure B.14: Create a box
A)The operations window with the osteotomy as the entity; with the thickness of the box set to 0.2 mm. B) The created planned (blue) and actual(green) boxes in relation to the fibula model (grey)

53. Perform a **Boolean intersection** with the pre-operative fibula model and the 4 osteotomies.
    (a) Start with one of the planned osteotomies. Duplicate the box and the pre-operative mandible model and hide all other objects.
    (b) Activate **Boolean Intersect** from the *Design* menu toolbar. Selected the box of the planned osteotomy and the pre-operative fibula model as *entities* and press **Apply**, see Figure B.15.A/B.
    (c) An intersection between the two parts will be end result B.15.C.
    (d) Rename this part to the following name: *{Patient number}_Fib_{(side segment}_Inter_{side osteotomy}_Planned* (e.g. *PT001_Fib_L_Inter_L_Planned*).

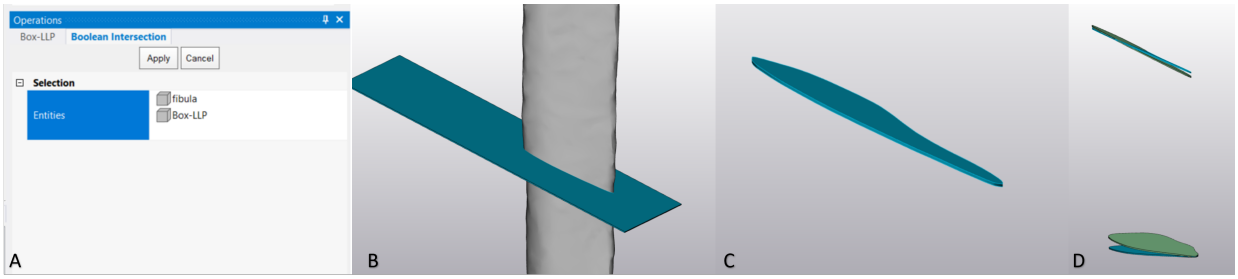

Figure B.15: Boolean intersection of the left planned osteotomy with the fibula
A) The operations window with the box and the pre-operative fibula as entities. B) The preoperative fibula with the planned box. C) The created intersection. D) Shows all the intersections related to one fibula segment (the two planned intersections (blue) and the two actual intersections (green)

54. Repeat from step 53 onwards to create the three other intersections; one more of the planned osteotomy and both the actual osteotomies, see Figure B.15.D.
55. Group the following objects into a group called *Intersection*
    - The four boxes of the osteotomies
    - Intersections
56. Add the *Intersection* group to the correct subgroup in the *Measurement* group.

B.3.3. Angular deviation

The angular deviation is determined by a change rotational change in the local coordinate systems (LCS) of the planned and actual osteotomies. Start with the coordinate system of the planned osteotomy. This

coordinate system is defined similar as the planned LCS of the resection osteotomies.

57. Start with defining the LCS of the planned osteotomy. This is done according to the slot/flange of the PSC.
58. Ensure that the fibula bone is correctly oriented, with the proximal end pointing upwards and the distal end pointing downwards, see Figure B.16.A.
59. Only **Show** the the reconstruction PSC, see Figure B.16B.
60. Activate **Datum Plane** in the *Analytical* Tab from the *Design* menu toolbar.
61. Create a **Datum Plane** representing the cutting direction. The order of selecting the point will determine the direction of the x and y axis. It is therefore important to precisely follow the order of instruction below:
    (a) Point one: This point is the origin of the plane/LCS. and should be placed on the front side in the top left corner of the PSC slot.
    (b) Point two: This point will create the x-axis together with point one. Place this point right across point one; on the back side of the top left corner of the PSC slot.
    (c) Point three: This point will create the y-axis together with point one. Place this point right to the side of point one; on the front side in the top right corner of the PSC slot.
62. Press **Apply**, see Figure B.16.C.
63. Rename the datum plane to *{Patient Number}_Fib_{side segment}_TM*_{side osteotomy}_Planned*. e.g. *PT001_Fib_L_TM_L_Planned*.
    *TM: Transformation Matrix.
64. Activate **Analytical to Mesh** to convert the created datum plane to a mesh object, see Figure B.16.D. Selected the datum plane *{Patient Number}_Fib_{side segment}_TM*_{side osteotomy}_Planned* as *Entity*.
65. Repeat for the other planned osteotomy.

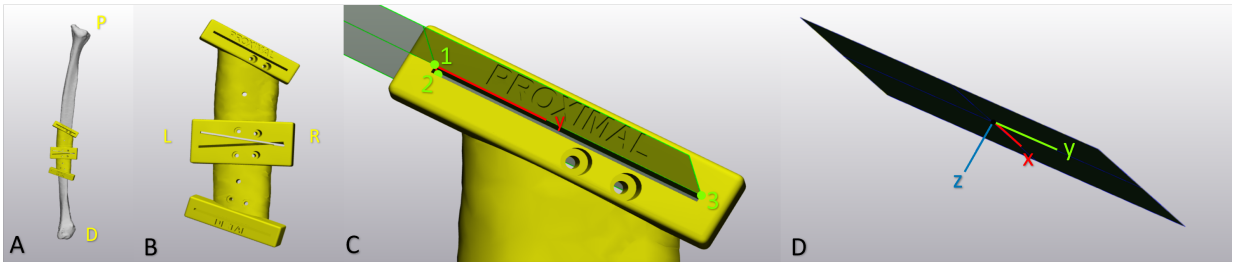

Figure B.16: Local coordinate system of the planned osteotomy
A) Verify the correct orientation of the fibula, with the proximal end pointing upwards and the distal end pointing downwards. B) Only show the resection PSC. C) Create a datum plane by placing 3 points in the correct position in the PSC slot. D) Convert the datum plane to a mesh object

The coordinate systems of the actual osteotomies are roughly determined. The x and y axes will again be in-plane while the z-axis is pointing outwards. The direction of the x and y axes should roughly align to the x and y of the planned plane but will later be positioned precisely by an automatic rotation around the z-axis.

66. Show the box of the actual osteotomy; created in step 52, together with the PSC.
67. Create a **Datum Plane** by picking points that correspond the most to the LCS of the planned osteotomy. Use the PSC as orientation, see Figure B.17.A. The order of selecting the point will determine the direction of the x and y axis. It is therefore important to precisely follow the order of instruction below:
    (a) Point one: This point is the origin of the plane/LCS and should be placed on the left top corner of the box.

(b) Point two: This point will create the x-axis together with point one. Place this point right across point one; on the back side of the top corner of the box.

(c) Point three: This point will create the y-axis together with point one. Place this point right below point one; on the ventral bottom corner of the box.

68. Make sure that all the points are either on the front side or the back side of the box and press apply to create the datum plane.
69. Rename the datum plane to *{Patient Number}_Fib_{side segment}_TM*_{side osteotomy}_Actual*. e.g. *PT001_Fib_L_TM_L_actual*.
70. Activate **Analytical to Mesh** to convert the created datum plane to a mesh object, see Figure B.17.B. Selected the datum plane *{Patient Number}_Fib_{side segment}_TM*_{side osteotomy}_Actual* as *Entity*.

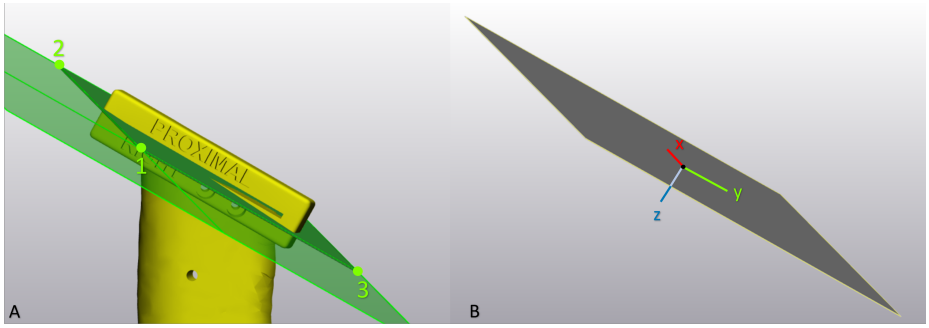

Figure B.17: Local coordinate system of the actual osteotomy
A) Create a datum plane by placing 3 points in the correct position on the actual box. B) Convert the datum plane to a mesh object

71. Verify the orientation of the LCS of the planned and actual osteotomy by clicking on the **plus sign** in front of the mesh object in the *object three*. Right-click on *Object coordinate system* and press **Show**. The x- (red) and y-axis (green) should be in plane and have roughly the same direction. The z-axis (blue) should be pointing in the same direction.
72. Group the objects listed below into a group called *LCS*
    - Datum Planes of the LCS (planned and actual)
    - Mesh objects of the datum planes (planned and actual)
73. Add the *LCS* group to the correct subgroup in the *Measurement* group.

Repeat all the steps above for all fibula segments.

B.3.4. Save results

All outcomes should be saved in a common location. The outcomes of this section are the intersections and the local coordinate system of reconstruction osteotomies.

74. Start with saving the intersection by activating **export** from the *file* menu toolbar. Select **STL** as the export type.
75. Selected all created reconstruction intersections as *Entities*. Change the *Output directory* to the common location and press **Apply**.

To save the local coordinate systems a transformation matrix will be exported from all local coordinate systems to the world coordinate system.

76. Use the plane (named origin) representing the world coordinate system, defined in step 41.
77. To export the transformation matrix, activate **export** from the *file* menu toolbar and select **Transformation Matrix** as export type.
78. Select one of the LCS as the *Entity*, select the *origin plane* as the *Target Entity* and save to the common output directory.

B.4. Abbreviations

Table B.1: Abbreviations

Models	Abbreviations (Planned)	Abbreviations (Actual)
Left remnant mandible	Man_L_P	Man_L_A
Right remnant mandible	Man_R_P	Man_R_A
Left side of left fibula segment	Fib_L_P	Fib_L_A
Right side of left fibula segment	Fib_L_P	Fib_L_A
Left side of right fibula segment	Fib_R_P	Fib_R_A
Right side of right fibula segment	Fib_R_P	Fib_R_A
Osteotomy		
Left resection osteotomy	Man_L_Osteo_P	Man_L_Osteo_A
Right resection osteotomy	Man_R_Osteo_P	Man_R_Osteo_A
Left resconstruction osteotomy of the left fibula segment	Fib_L_Osteo_L_P	Fib_L_Osteo_L_A
Right resconstruction osteotomy of the left fibula segment	Fib_L_Osteo_R_P	Fib_L_Osteo_R_A
Left resconstruction osteotomy of the right fibula segment	Fib_R_Osteo_L_P	Fib_R_Osteo_L_A
Left resconstruction osteotomy of the right fibula segment	Fib_R_Osteo_R_P	Fib_R_Osteo_R_A
Intersections		
Left resection Intersection	PTXXX_Man_L_Inter_Planned	PTXXX_Man_L_Inter_Actual
Right resection Intersection	PTXXX_Man_R_Inter_Planned	PTXXX_Man_R_Inter_Actual
Left resconstruction Intersection of the left fibula segment	PTXXX_Fib_L_Inter_L_Planned	PTXXX_Fib_L_Inter_L_Actual
Right resconstruction Intersection of the left fibula segment	PTXXX_Fib_L_Inter_R_Planned	PTXXX_Fib_L_Inter_R_Actual
Left resconstruction Intersection of the right fibula segment	PTXXX_Fib_R_Inter_L_Planned	PTXXX_Fib_R_Inter_L_Actual
Left resconstruction Intersection of the right fibula segment	PTXXX_Fib_R_Inter_R_Planned	PTXXX_Fib_R_Inter_R_Actual
Local coordinate system (LCS)		
Left resection LCS	PTXXX_Man_L_TM_Planned	PTXXX_Man_L_TM_Actual
Right resection LCS	PTXXX_Man_R_TM_Planned	PTXXX_Man_R_TM_Actual
Left resconstruction LCS of the left fibula segment	PTXXX_Fib_L_TM_L_Planned	PTXXX_Fib_L_TM_L_Actual
Right resconstruction LCS of the left fibula segment	PTXXX_Fib_L_TM_R_Planned	PTXXX_Fib_L_TM_R_Actual
Left resconstruction LCS of the right fibula segment	PTXXX_Fib_R_TM_L_Planned	PTXXX_Fib_R_TM_L_Actual
Left resconstruction LCS of the right fibula segment	PTXXX_Fib_R_TM_R_Planned	PTXXX_Fib_R_TM_R_Actual

C

User guide: Python script

When all the intersections and LCS of the osteotomies of all patients are created, the Python script can be run. This script calculates the distance and angular deviations and exports the results to an Excel sheet.

1. Start by opening the *Main.py* and *functions.py* files.
2. Change the *base_directory* to the location where the intersections and LCS are saved.
3. Change *patients* to all the included patients.
4. Run the script.
5. The results will be exported to an Excel file called *results.xlsx*. The Excel file will be saved in the same location, as where the the Python script is saved.
6. This Excel file will have three tabs:
    - Mandible Distance: contains the distance deviation (mm) of the resection osteotomies
    - Fibula length: contains the distance deviation (mm) of the reconstruction osteotomies
    - Rotation: contains the angular deviations (°) of the resection and reconstruction osteotomies.

D

User guide: Observer variability

A method has been developed to evaluate the accuracy of computer-assisted surgery in mandibular resection and reconstruction. This method consists of a combination of manual and automatic steps, each with its own variability risk. To assess the reproducibility of the developed method, a variability analysis is developed. The analysis will assess the intra- and inter-variability of the manual step, which is assumed to have the highest risk of introducing variability: post-operative osteotomy determination. This manual takes the observer through a step-by-step guide on localising post-operative osteotomies. The post-operative osteotomies will be localised three times:

- Initial localisation osteotomies (Primary observer)
- Intra-observer: Second localisation osteotomy (Primary observer)
- Inter-observer localisation osteotomies (Second observer)

The primary observer will execute the remaining steps of the designed method, and the disparities in the final outcomes will give valuable insights into the effect of the variability of the osteotomy localisation.

The osteotomy location is used to differentiate between osteotomies within one subject (see Figure D.1). These locations are abbreviated for user-friendliness, as shown in Table D.1.

In this manual, you will use Mimics [52] and 3-Matic [53] to view the pre-operative model and create the post-operative resection and reconstruction osteotomies. The analysis will be performed on five randomly selected subjects. The input and output for this analysis will be as follows for each subject:

Input
- Post-operative imaging
- Pre-operative models
  - Mandible
  - Remnant mandible (left and right)
  - Resection guide
- Post-operative models
  - Remnant mandible (left and right)
  - Fibula segments

Output
- Osteotomies
  - Points
  - Plane

Table D.1: Abbreviations

Osteotomy location	**Abbreviation**
Left remnant mandible	Man_L
Right remnant mandible	Man_R
Left side of left fibula segment	Fib_L_L
Right side of left fibula segment	Fib_L_R
Left side of right fibula segment	Fib_R_L
Right side of right fibula segment	Fib_R_R

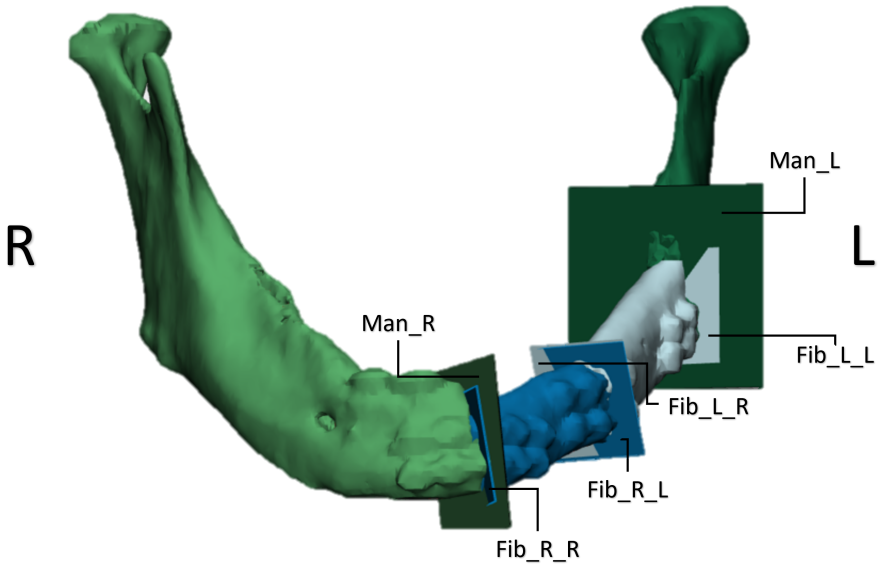

Figure D.1: Osteotomy locations

The manual will walk you through the following steps:

1. Loading files
2. Identification of the osteotomy
3. Point measurement
4. Fit plane
5. Saving results

Osteotomy localisation

Loading files

The materials required for the osteotomy localisation are located in a shared file. Each subject has a Mimics file, a 3-Matic file, and an empty folder for each osteotomy location.

1. Open one of the Mimics files called *Subx_osteotomy_mimics.mcs*.
2. In the Mimic file, the post-operative models can be seen in the group *models*, including the overall reconstruction and the individual segments (mandible and fibula).
3. Review the object in the 2D and 3D viewer to get a general idea about the anatomy of the different segments making up the reconstructed mandible.

Identification of the osteotomy

The next step is to localise the osteotomy made during the surgery. The osteotomies are located on the ends of the remnant mandible and fibula segments. The natural shape of the structure is disrupted here, which is seen as an abrupt and unexpected change in the contrast. The same protocol is used to localise the resection as the reconstruction osteotomies. However, prior to the determination of the resection osteotomies, an examination of the cutting guide design must be performed. The patient-specific cutting guide translates the planned osteotomy from the virtual environment to the operation room. The designed saw slot of the guide does not always cover the full cross-section of the mandible. Especially osteotomies, which cross the ramus or dentition. The distal part of these osteotomies requires high accuracy for the tumour margin and reconstruction. The proximal part can be done free-handed. It is important to review the cutting guide design and evaluate where the osteotomy is made according to the planning. If the osteotomy is partially guided by the cutting guide, the assessment of the actual osteotomy is only valid on the guided

part. Therefore, the cutting guide must be aligned with the post-operative imaging to consider where to assess the post-operative osteotomy properly. To register the cutting guide to the post-operative imaging, the planned remnant mandible of the evaluated side is aligned to the actual remnant model [D.2.c], taking along the resection cutting guide [D.2.d]. The translated cutting guide is subsequently imported to Mimics [52].

For the variability analysis, the resection-cutting guide has been assessed and aligned to make the process less time-consuming. The aligned resection guides are available in the subgroup *Man_L or Man_R* in group *Osteotomy*.

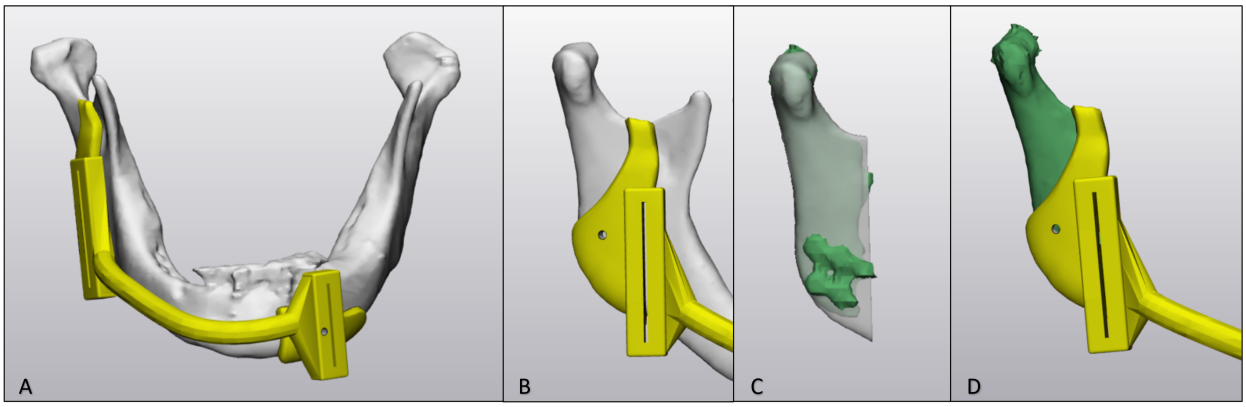

Figure D.2: Resection cutting guide
A) and B) Overview of models delineating the precision area for osteotomy, including the resection cutting guide and the pre-operative mandible. C) Registration of the planned remnant mandible to the actual remnant mandible. D) Cutting guide aligned with the actual remnant mandible.

Point measurement

The osteotomy is determined by systematically setting points at the end of the sawn bone segments. These will form a point cloud through which a plane can be fitted. A point cloud will be created for each osteotomy. The following steps will guide you through the point measurements:

4. Start with one osteotomy that you want to determine. In this example, the right mandible resection osteotomy will be analysed.
    - If you are analysing a resection osteotomy, you need to verify which part of the osteotomy is made according to the cutting guide.
    - Visualise the cutting guide in the 2D image viewer by making the object and its contours visible in the object tree [D.3].
    - Analyse the cutting slot of the guide and set the points within that range.

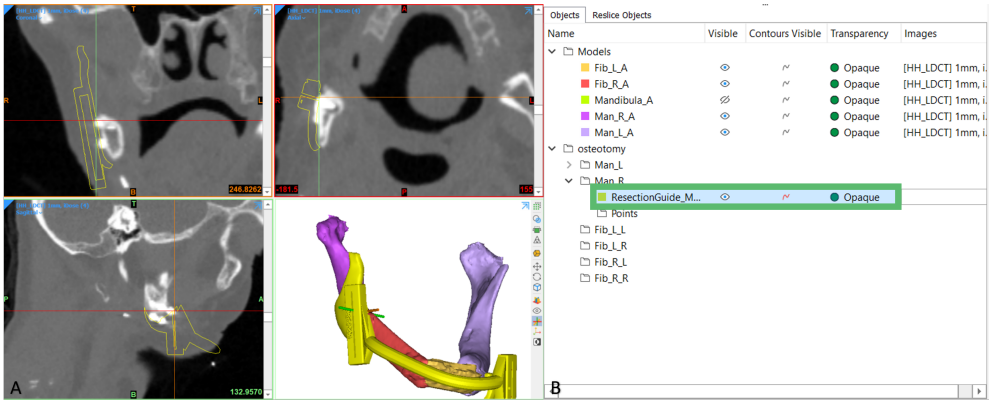

Figure D.3: A) The contour of the cutting guide on the post-operative imaging and the object on the post-operative mandible reconstruction. B) Visualizes the resection guide in the 2D and 3D viewer.

5. To create a point measurement activate **point** in the *analyze menu* Toolbar.
6. Scroll through the axial, sagittal, and coronal slices and identify in which view the bone cut is seen the most clearly.
7. Begin by positioning a point on one side of the bone cut. Progress through the slices towards the opposite side of the bone cut, marking two points on every couple of slices adjacent to the outermost edge of the bone segment. Ensure points are placed only in areas that are clearly visible. Be aware that certain regions are hard to assess due to artefacts from the fixation material. [D.4].
8. The mask of the segmented parts may be used for orientation but must be turned off when setting the points to prevent bias.

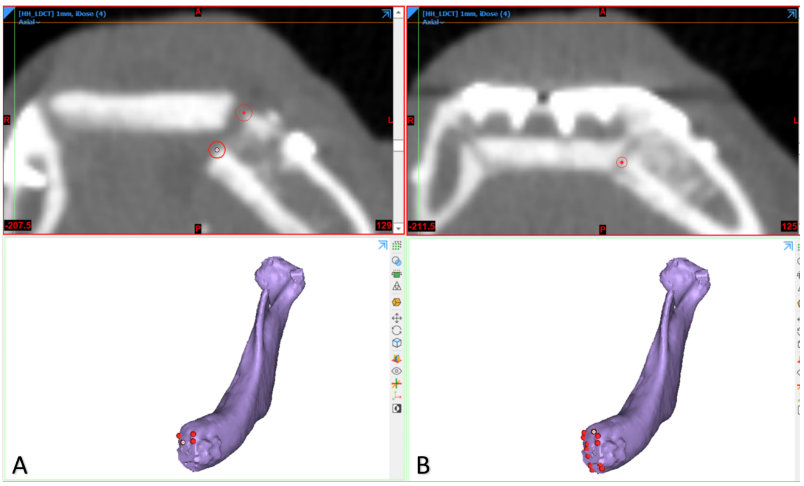

Figure D.4: Setting points
A) Two points on the outermost edge of the bone segment. B) Only one point is set due to a scattered view caused by artefacts from fixation material

9. Complete the points for one osteotomy.
10. Confirm the points on the three different views (axial, coronal, sagittal) and adjust if necessary.
11. The created points will together form a point cloud. Select all points and drag them to the group *points* of the assessed osteotomy.
12. Select all points again and export them as STL files by right-clicking and selecting **STL+** [D.5].
13. In the *STL+* window press **Add** to add the points to *Objects to be converted*. Change the output directory by selecting the **file icon**. Navigate to the subject that is analysed, select the folder named

after the assessed osteotomy and press **finish**.

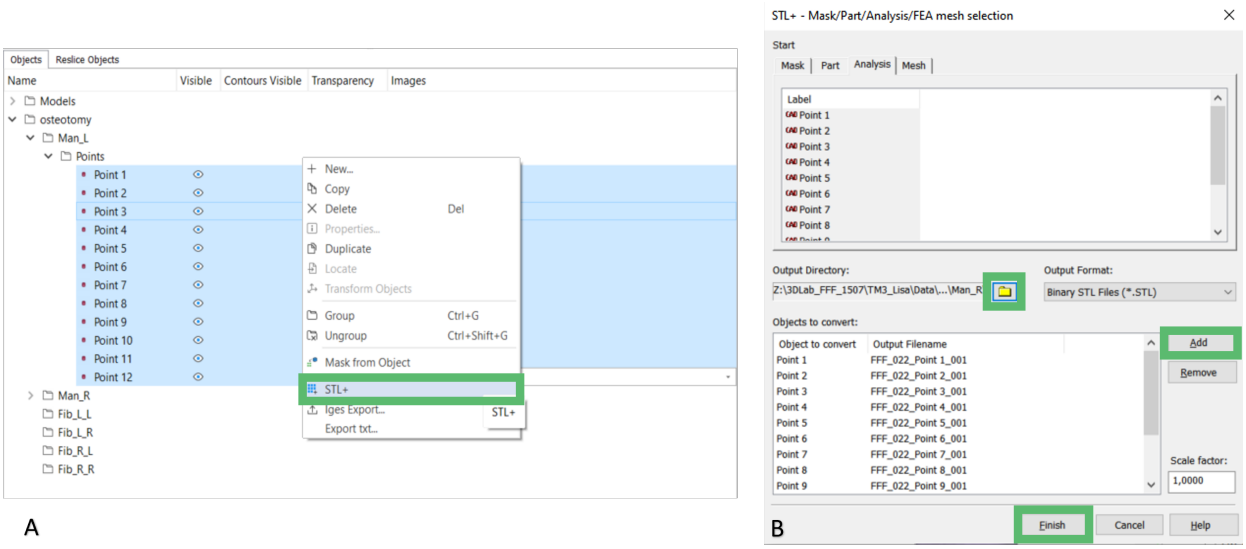

Figure D.5: Export point as STL

Fit plane

For the next step, the generated point cloud is imported into 3-Matic, and a datum plane is fitted through.

14. **Open** the 3-Matic file called *Subx_Measurement_3_matic.mcs*
15. Import the point cloud by clicking on **Import part** from the File menu toolbar and import all points.
16. Drag all points to the point group of the assessed osteotomy.
17. To fit a plane through the point cloud, navigate to the *design* Toolbar, select *Analytical* and choose **Datum plane**.
18. The *Create a Datum plane* tab will open in the *Operation* section. Selected **Fit plane** as *Method* and add the *points cloud* as *Fitting entities*. Press apply [D.6].

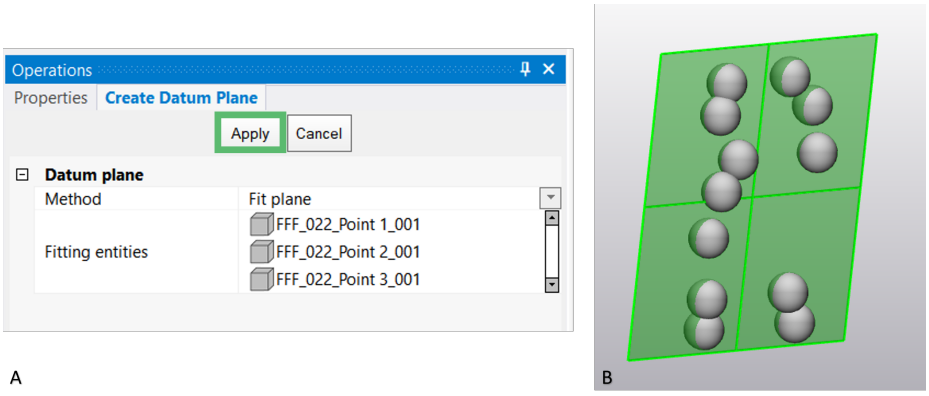

Figure D.6: A) Operational window *Create Datum Plane*. B) Fitted datum plane through points.

19. Create an STL model from the datum plane by pressing **analytical to part** in the *design* toolbar.
20. Rename the create plane; Sub*X* _ *OsteotomyLocation*_Osteotomy.
21. Transfer back to Mimics by **Copying** the plane in 3-Matic and **pasting** it in Mimics.

22. Verify the location of the created osteotomy on the imaging in the axial, coronal and sagittal view. If the osteotomy is positioned incorrectly, check the placed point and adjust where necessary [D.7]. Repeat steps 12 to 21 until you are satisfied with the result.

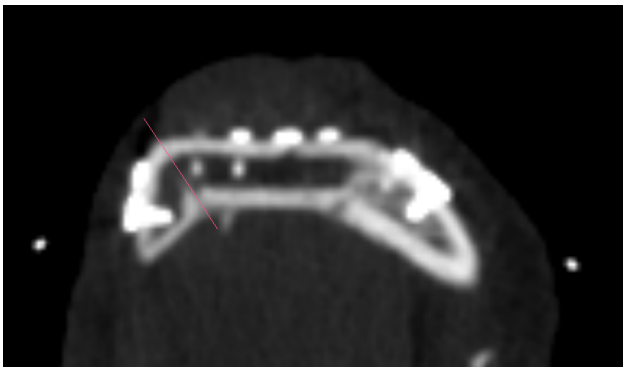

Figure D.7: Verification osteotomy post-operative imaging

23. Perform steps 4 to 21 for all the osteotomies.

Saving results

24. **Save** the Mimics and 3-Matic file on the original location.
25. Repeat the manual for all 5 subjects.

E

Results

E.1. Distance deviation resection osteotomies

Table E.1

Patient ID	Osteotomy Location	Center of Mass Distance	Maximum Distance
Pt001	Man_L	1,7	2,9
Pt001	Man_R	3,9	6,4
Pt002	Man_L	-0,4	-1,4
Pt002	Man_R	-0,8	-1,4
Pt003	Man_L	-1,2	-3,1
Pt003	Man_R	0,0	0,2
Pt004	Man_L	2,1	2,2
Pt004	Man_R	0,5	1,6
Pt005	Man_L	1,2	2,3
Pt006	Man_L	-1,7	-3,4
Pt006	Man_R	3,7	4,9
Pt007	Man_L	-1,4	-2,5
Pt007	Man_R	3,8	4,1
Pt008	Man_L	-0,8	-1,9
Pt008	Man_R	1,1	2,0
Pt009	Man_L	0,4	1,6
Pt009	Man_R	-1,5	-2,3
Pt010	Man_L	-0,9	-1,7
Pt010	Man_R	0,8	0,9
Pt011	Man_L	-8,3	-12,2
Pt011	Man_R	-0,8	-1,6
Pt012	Man_L	0,6	1,4
Pt012	Man_R	0,7	1,9
Pt013	Man_L	0,7	1,5
Pt013	Man_R	2,2	2,8
Pt014	Man_L	5,9	6,2
Pt014	Man_R	-4,9	-5,1
Pt015	Man_L	3,7	6,0
Pt015	Man_R	-3,1	-3,8
Pt016	Man_L	-2,2	-2,7
Pt016	Man_R	3,0	4,4
	Absolute Average	2,1	3,1
	Absolute STD	1,9	2,3
	Absulute Median	1,4	2,3

E.2. Distance deviation reconstruction osteotomies

Table E.2

Patient ID	Osteotomy Location	Fibula Segment Length Planned	Fibula Segment Length Actual	Fibula Segment Length Difference
Pt001	Fib_L	62,7	59,2	3,4
Pt001	Fib_R	35,8	31,3	4,5
Pt002	Fib_L	38,6	36,9	1,7
Pt002	Fib_R	29,8	31,9	-2,0
Pt003	Fib_L	52,4	40,4	12,0
Pt003	Fib_R	43,7	44,8	-1,1
Pt004	Fib_L	27,9	29,8	-1,9
Pt004	Fib_R	31,9	31,6	0,4
Pt004	Fib_M	69,3	67,9	1,4
Pt005	Fib_L	52,1	52,7	-0,7
Pt005	Fib_R	51,2	50,4	0,8
Pt006	Fib_L	29,4	26,9	2,4
Pt006	Fib_R	54,6	53,7	0,9
Pt007	Fib_L	65,2	65,6	-0,4
Pt007	Fib_R	32,8	34,6	-1,8
Pt008	Fib	53,3	54,1	-0,8
Pt009	Fib_L	63,5	67,0	-3,6
Pt009	Fib_R	29,5	31,9	-2,4
Pt009	Fib_M	32,5	42,1	-9,6
Pt010	Fib_L	28,5	26,8	1,7
Pt010	Fib_R	49,1	49,8	-0,7
Pt011	Fib_L	36,6	33,3	3,4
Pt011	Fib_R	33,5	30,7	2,8
Pt012	Fib	54,3	55,4	-1,1
Pt013	Fib_L	35,3	34,2	1,1
Pt013	Fib_R	30,3	27,5	2,8
Pt014	Fib_L	31,8	30,6	1,2
Pt014	Fib_R	46,3	44,2	2,1
Pt015	Fib	57,9	56,6	1,3
Pt016	Fib	66,4	64,8	1,6
	Absolute Average	44,2	43,5	2,4
	Absolute STD	13,4	13,5	2,5
	Absolute Median	41,1	41,2	1,7

E.3. Angular deviation resection osteotomies

Table E.3

Patient ID	Osteotomy Location	Rotation X axis	Rotation Y axis
Pt001	Man_L	4,8	6,4
Pt001	Man_R	17,5	0,8
Pt002	Man_L	4,9	3,8
Pt002	Man_R	2,3	2,2
Pt003	Man_L	3,7	13,0
Pt003	Man_R	0,1	2,9
Pt004	Man_L	0,9	3,8
Pt004	Man_R	4,6	0,9
Pt005	Man_L	3,0	6,6
Pt006	Man_L	0,5	11,5
Pt006	Man_R	5,8	0,3
Pt007	Man_L	3,4	5,9
Pt007	Man_R	3,0	4,3
Pt008	Man_L	5,3	1,8
Pt008	Man_R	0,8	12,8
Pt009	Man_L	2,2	13,0
Pt009	Man_R	4,9	3,3
Pt010	Man_L	3,2	1,4
Pt010	Man_R	0,2	0,8
Pt011	Man_L	4,4	24,5
Pt011	Man_R	1,3	5,4
Pt012	Man_L	1,6	5,9
Pt012	Man_R	2,2	19,0
Pt013	Man_L	4,0	1,0
Pt013	Man_R	2,1	4,4
Pt014	Man_L	3,9	4,0
Pt014	Man_R	0,8	0,9
Pt015	Man_L	9,6	1,4
Pt015	Man_R	3,8	2,8
Pt016	Man_L	0,9	1,8
Pt016	Man_R	7,5	10,3
	Average	3,7	5,7
	STD	3,4	5,8
	Median	3,2	3,8

E.4. Angular deviation reconstruction osteotomies

Table E.4

Patient ID	Osteotomy Location	Rotation X axis	Rotation Y axis
Pt001	Fib_L_L	6,7	4,5
Pt001	Fib_L_R	5,6	8,3
Pt001	Fib_R_L	5,6	1,2
Pt001	Fib_R_R	5,2	16,3
Pt002	Fib_L_L	3,6	3,0
Pt002	Fib_L_R	6,6	7,3
Pt002	Fib_R_L	6,8	14,1
Pt002	Fib_R_R	0,5	17,2
Pt003	Fib_L_L	11,9	8,3
Pt003	Fib_L_R	1,9	1,0
Pt003	Fib_R_L	8,8	30,1
Pt003	Fib_R_R	6,2	25,3
Pt004	Fib_L_L	4,2	0,8
Pt004	Fib_L_R	0,6	0,7
Pt004	Fib_R_L	3,0	2,6
Pt004	Fib_R_R	4,7	2,3
Pt004	Fib_M_L	0,6	2,4
Pt004	Fib_M_R	0,0	0,8
Pt005	Fib_L_L	4,8	7,9
Pt005	Fib_L_R	8,1	1,1
Pt005	Fib_R_L	8,2	5,2
Pt005	Fib_R_R	2,3	3,5
Pt006	Fib_L_L	2,3	5,6
Pt006	Fib_L_R	6,4	4,5
Pt006	Fib_R_L	2,5	10,4
Pt006	Fib_R_R	4,7	7,8
Pt007	Fib_L_L	1,3	3,6
Pt007	Fib_L_R	13,2	4,7
Pt007	Fib_R_L	7,7	2,2
Pt007	Fib_R_R	1,0	0,8
Pt008	Fib_L	0,6	2,3
Pt008	Fib_R	3,1	8,6
Pt009	Fib_L_L	38,2	5,5
Pt009	Fib_L_R	26,6	52,9
Pt009	Fib_R_L	7,0	0,6
Pt009	Fib_R_R	9,3	5,7
Pt009	Fib_M_L	25,7	9,9
Pt009	Fib_M_R	19,7	5,4
Pt010	Fib_L_L	6,7	42,8
Pt010	Fib_L_R	15,7	37,5
Pt010	Fib_R_L	6,7	43,0
Pt010	Fib_R_R	13,8	1,7
Pt011	Fib_L_L	2,9	4,7
Pt011	Fib_L_R	5,4	1,5
Pt011	Fib_R_L	2,1	3,9
Pt011	Fib_R_R	2,4	13,1
Pt012	Fib_L	16,2	8,6
Pt012	Fib_R	10,8	0,6
Pt013	Fib_L_L	0,1	4,1
Pt013	Fib_L_R	2,0	10,1
Pt013	Fib_R_L	0,7	10,7

Pt013	Fib_R_R		12,4	6,5
Pt014	Fib_L_L		1,7	1,7
Pt014	Fib_L_R		2,1	8,5
Pt014	Fib_R_L		10,5	4,5
Pt014	Fib_R_R		3,1	28,8
Pt015	Fib_L		1,3	4,6
Pt015	Fib_R		1,7	5,1
Pt016	Fib_L		3,7	4,5
Pt016	Fib_R		12,1	3,5
		Average	6,8	9,1
		STD	7,1	11,4
		Median	5,0	4,9